2014

Bio-based polymeric materials from vegetable oils

Ruqi Chen
Iowa State University

Bio-based polymeric materials from vegetable oils

by

Ruqi Chen

A dissertation submitted to the graduate faculty

in partial fulfillment of the requirements for the degree of

DOCTOR OF PHILOSOPHY

Major: Materials Science and Engineering

Program of Study Committee:
Michael R. Kessler, Major Professor
Jason Chen
Kaitlin Bratlie
Xiaoli Tan
Samy Madbouly

Iowa State University
Ames, Iowa
2014

TABLE OF CONTENTS

ACKNOWLEDGMENT

First, I would thank my major professor Dr. Michael R. Kessler and my co-advisor Dr. Jason Chen for their support, guidance, patience and tolerance all through my Ph.D. career. Also, I'll thank Dr. Xiaoli Tan, Dr. Kaitlin Bratlie and Dr. Samy Madbouly for being my Ph.D. advisory committee members and for providing valuable advice and suggestions in my prelim exam. I acknowledge the financial support from Kumho Petrochemical Co. Ltd. which makes my Ph.D. journey in United States come true.

Then, I would like to show my gratitude to my current and former colleagues in Polymer Composites Research Group for their assistance, discussions and suggestions – Dr. Ying Xia, Dr. Rafael Quirino, Dr. Tom Garrison, Dr. Mahendra Thunga, Dr. Hongyu Cui, Dr. Peter Hondred, Dr. Eliseo De León, Danny Vennerberg, Yuzhan Li, Chaoqun Zhang, Hongchao Wu, Rui Ding, Kunwei Liu, Hong Lu, Shengzhe Yang, and Harris Handoko. I would also like to thank Michael Zenner (Chemistry Department) for his generosity in providing chemicals that were used in my research work. Additionally, I would appreciate Tracey Pepper (Genetics, Development & Cell Biology, Iowa State University) for her assistance in TEM measurement, Dr. Steve Veysey (Department of Chemistry, Iowa State University) for his assistance in FTIR measurement.

At last, I would like to thank my beloved parents and my mother-in-law for their ever-lasting love and encouragement. Especially, I would like to thank my wife,

Xiaoying Zhang, for her understandings even though we have been parted for the past five years. I am looking forward to getting united with her after my graduation.

Finally, I want to appreciate Bayer Material Science for offering me a job as an Innovative Manager located in Shanghai. The responsibilities of this job are comprised of research and development, customer service and business opportunity seeking. The job is challenging for a fresh Ph.D., but it is a good start for my industrial career in long term view.

ABSTRACT

Vegetable oils have been utilized in developing various types of bio-based materials in my research work.

Bio-based polyhydroxy fatty acids have been subject to ring-opening epoxidized soybean oil with alkaline catalyst DBU to generate polyols with varying OH numbers. Polyurethane films were obtained using these polyols polymerized with isophrone diisocyanates. The polyhydroxy fatty acids were also used as internal emulsifiers in anionic polyurethane dispersion synthesis due to the presence of carboxylic acid groups in their structures. In addition, acrylated epoxidized soybean oil was involved in another project. 2-methyl aziridine was added to acrylic groups via Michael addition mechanism under mild conditions. The resulting aziridine-containing compound could be polymerized with bio-based polyacids rapidly at room temperature. Plus, thermal polymerization of soybean oil has been studied. The heat-bodied soybean oils were subject to ozonolysis followed by reduction in order to produce polyols with primary hydroxyls, which are relatively reactive.

The principle of the research is to develop products with considerably high bio-content. The soaring price of petroleum has become a global issue so that industry and academia have been seeking bio-renewable substitutions which can be potentially converted to versatile products that have comparable properties to petroleum-based merchandise.

CHAPTER 1: GENERAL INTRODUCTION

1.1 Introduction

Requirements for sustainability, cost reductions, concerns for environmental issues, and competitive properties are the bases for the development of new bio-based materials. Starch [1-5], cellulose [6-11], protein [12-16], flax [17-19] have been exploited for various applications. Besides, vegetable oil has attracted increasing attention as one of the most promising options because of its ready availability, relatively low cost, environmental sustainability, and low eco-toxicity. Biological vegetable oils are outstanding renewable raw materials for developing new monomers and polymers. Generally, most vegetable oils are triglycerides with some exceptions (cashew nut oil), see Figure 1-1. Their structures are basically esters of glycerin and fatty acids. In Table 1-1, common fatty acids are listed. Vegetable oils are considered non-reactive raw materials and in order to make them reactive, functional groups have to be introduced. Considering the listed fatty acids' structures, there are several potential sites in the triglyceride molecule suitable for the chemical modifications: double bonds, ester bonds and bis-allylic positions. As seen in Table 1-2, different vegetable oils are composed of different contents of various fatty acids. It is worth mentioning that the values are statistically averaged results.

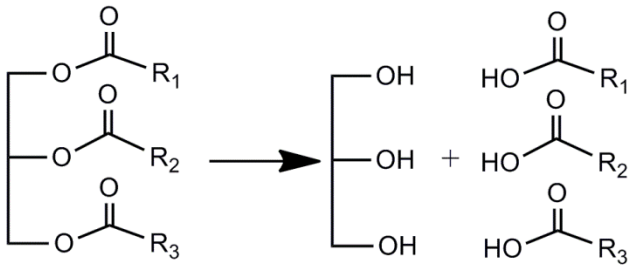

Figure 1-1 Structure of triglyceride

Table 1-1 List of common fatty acids

Acid	Structure
Caprylic	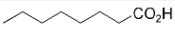
Capric	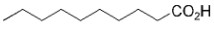
Lauric	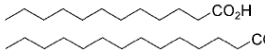
Myristic	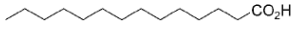
Palmitic	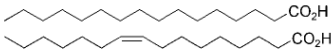
Palmitoleic	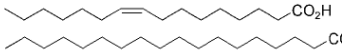
Stearic	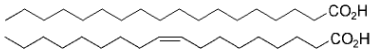
Oleic	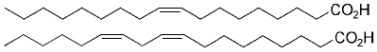
Linoleic	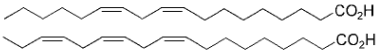
Linolenic	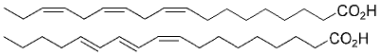
α-Eleostearic	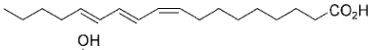
Ricinoleic	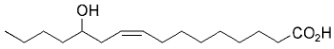
Vernolic	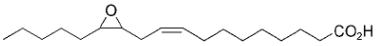
Licanic	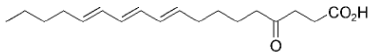

Table 1-2 List of common vegetable oils

Natural oil	Average annual production [10^6 tons]	Fatty acids [%] palmitic	stearic	oleic	linoleic	linolenic	Double bonds[a]	Iodine value [mg/100 g]
Soybean	26.52	11.0	4.0	23.4	53.3	7.8	4.6	117–143
Palm	23.53	42.8	4.2	40.5	10.1	–	1.7	44–58
Rapeseed/Canola	15.29	4/4.1	2/1.8	56/60.9	26/21.0	10/8.8	3.8/3.9	94–120/110–126
Sunflower	15.29	5.2	2.7	37.2	53.8	1.0	4.7	110–143
Tallow	8.24	27	7	48	2	–	–	35–48
Lard	6.75	26	11	44	11	–	–	45–75
Butterfat	6.26	26	11	28	2	–	–	29–41
Groundnut	5.03	11.4	2.4	48.3	31.9	–	3.4	80–106
Cottonseed	4.49	21.6	2.6	18.6	54.4	0.7	3.9	90–119
Coconut	3.74	9.8	3.0	6.9	2.2	–	–	6–11
Palm kernel	2.95	8.8	2.4	13.6	1.1	–	–	14–24
Olive	2.52	13.7	2.5	71.1	10.0	0.6	2.8	75–94
Corn	2.30	10.9	2.0	25.4	59.6	1.2	4.5	102–130
Fish	1.13	10–22	–	11-25	–	–	–	104–110
Linseed	0.83	5.5	3.5	19.1	15.3	56.6	6.6	168–204
Sesame	0.76	9	6	41	43	1.0	3.9	103–116
Castor	0.56	1.5	0.5	5.0	4.0	0.5	2.7	82–88

Vegetable oils can be subject to a number of chemical modifications/reactions for different purposes. Herein, four reported methods using vegetable oils have been summarized.

1) Polymerized vegetable oil

Polymerization of vegetable oils (soybean, linseed) was first reported being conducted via thermal method [20]. Bisallylic structure may convert into conjugated intermediate at elevated temperature with or without catalyst, which facilitates Diels-Alder addition. However, thermal polymerization of vegetable oils inevitably reaches the decomposition temperature of oils and has been claimed to result in relatively high loss of material and generate residuals of small fragments. Ionescu *et al.* have developed a cationic polymerization of soybean and linseed oil at low temperature, without weight loss [21]. The cyclization reaction temperature was significantly lowered by the presence of superacids. The degree of polymerization is dependent on the unsaturation of oils and time of reaction. Bodied soybean oil has been used in ink industry [20].

2) Biofuel

Vegetable oils and their derivatives, especially methyl/ethyl esters, are commonly referred as biodiesel. In order to obtain methyl/ethyl esters, transesterification reaction is necessary, which actually involves the saponification reaction and methanol/ethanol esterification. The reaction can be catalyzed by alkalis , acids or enzymes [22]. Vegetable oil fuels are not competitive with respect to petroleum fuels at the moment due to the high cost in transesterification and 20% less heat value (HV) generation than gasoline.

However, with increasing price of petroleum, there is an growing interest in using vegetable oils and their derivatives in diesel engines.

3) Polyol

Vegetable oil is one of the most promising options for polyol synthesis due to its readily availability, relatively low cost, environmental sustainability and low eco-toxicity. Vegetable oils are mainly triglycerides, constituted by glycerol with three fatty acid chains. There are a variety of fatty acids: palmitic (C16:0), stearic (C18:0), oleic (C18:1), linoleic (C18:2), linolenic (C18:3), ricinoleic (C16:1), etc. The unsaturated bonds and hydroxyl groups present in the fatty acids open the opportunities for various chemical modifications to promote the reactivity of vegetable oil molecules. Figure 1-2 illustrates the well-developed methods to incorporate hydroxyl groups onto vegetable oils. Hydroformylation, though proceeded under harsh conditions, yields reactive primary hydroxyl groups in two steps. Aldehydes are produced in the first step in the presence of CO and H_2 along with catalysts, and then reduced into hydroxyl groups. Ozonolysis has also been reported as an effective technique to give primary hydroxyl groups at double bond sites [23-25]. Transesterification/Transamidation were claimed to be an effective route to yield polyols [26, 27]. But the main drawback of this method is obvious as the fatty acid arm would be present in the polymer network as dangling chain, acting as plastisizers which could have negative impact on thermal and mechanical properties of the polymer. Epoxidation of carbon-carbon double bonds followed by ring-opening is one of the most common routes to generate hydroxyl groups. Alcohols [28, 29], amines [30, 31], carboxylic acids [32], halogenated acids [33, 34], etc. are typically used in ring-opening step.

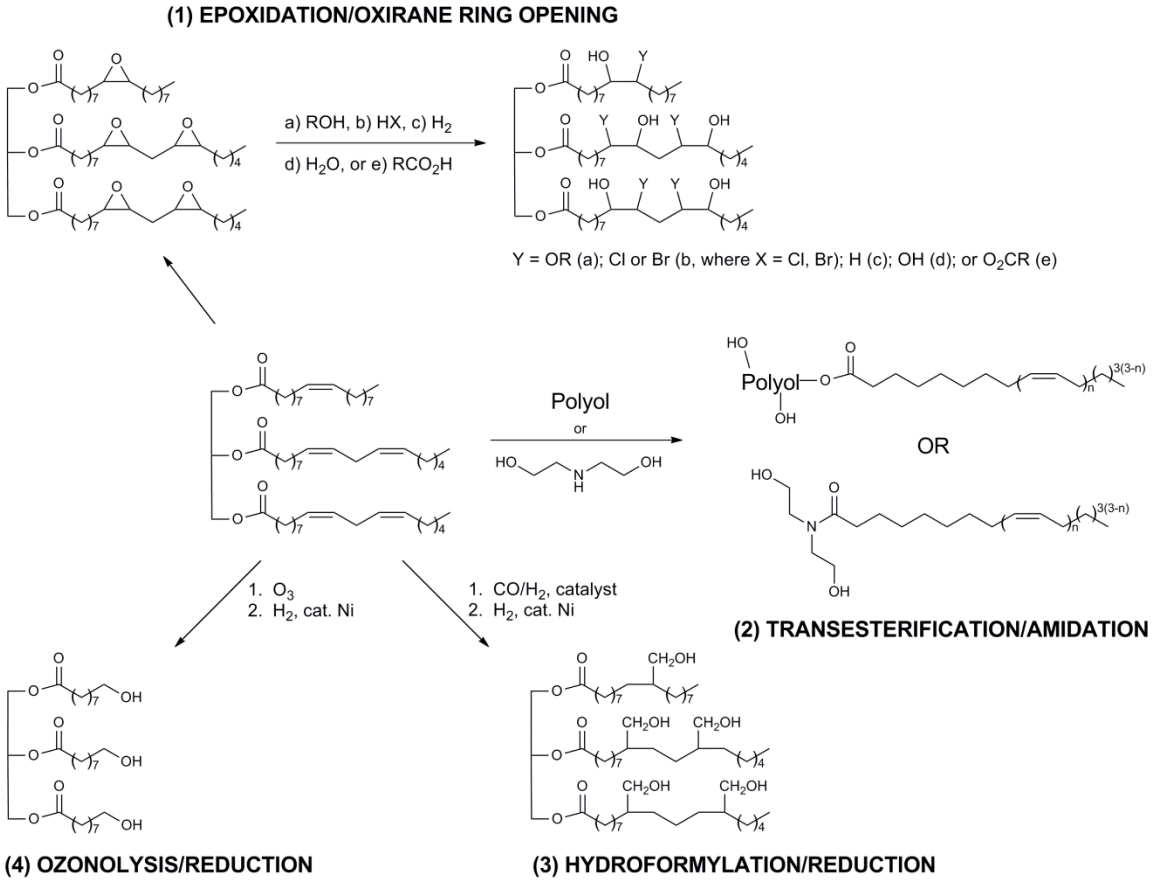

Figure 1-2 Various modifications of vegetable oils to polyols

Polyol is a key component in routine polyurethane synethsis. The other indispensable component is polyisocyanates, such as methylene diphenyl diisocyanate (MDI), isophorone diisocyanate (IPDI), toluene diisocyanate (TDI), hexamethylene diisocyanate (HDI), etc., see Figure 1-3. Given that there are limited types of polyisocyanates commercially available in the market, the properties of polyurethane products are largely dependent on the selection of polyol or blending of multiple polyols.

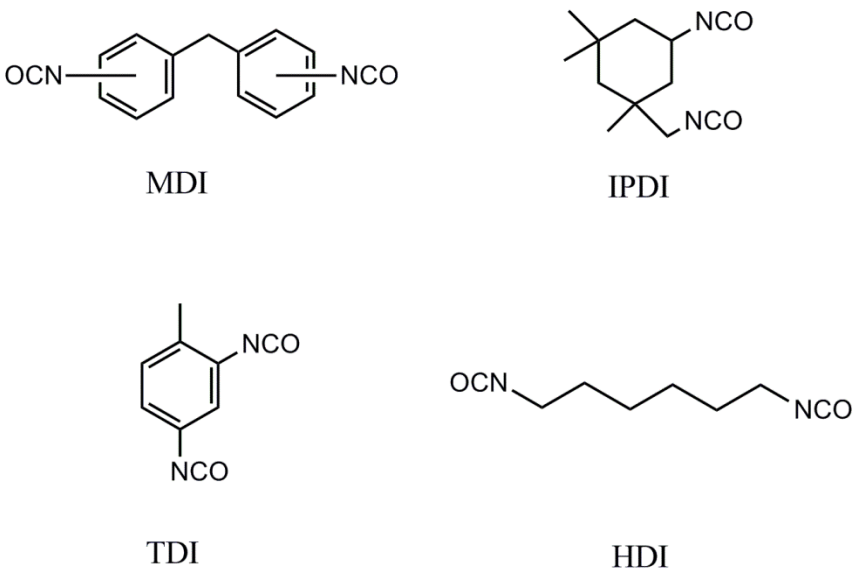

Figure 1-3 Illustration of commercial isocyanates

Polyurethanes (PUs), which contain recurring urethane linkages in the main chain, have been widely developed into a variety of applications, such as coatings, adhesives, sealants, foams, elastomers, etc. Conventionally, polyurethane is synthesized via isocyanate route, which is essentially a reaction between a polyol and an isocyanate. Both components involved in industrial manufacturing are typically derived from petroleum-based products. However, the depletion of crude oil and the accompanied environment issues have triggered global awareness of the importance of bio-renewable alternatives in future polyurethane industry. Recent studies on bio-based isocyanates have been focusing on developing non-phosgene route. The basic design is pertaining to the thermal degradation of acyl azide on bio-based carrier which would yield isocyanate via Curtius rearrangement [35-37]. On the other hand, bio-based polyols have been extensively investigated in the past few decades and subject to partial substitution of petroleum-based starting materials in industrial productions [38].

4) Acrylated Vegetable Oil

Acrylation is also a common method to modify vegetable oil into useful and reactive starting material. Acrylated-epoxidized soybean oil (AESO) is now being mass produced and marketed. Traditionally, the production involves two steps from soybean oil. The first step is the epoxidation of soybean oil. After, this epoxy intermediate is reacted with acrylic acid [39] in presence of an acid as catalyst. The level of acrylatation plays an important role in determining the mechanical properties of derivatove products of AESO [40]. AESO is fascinating due to the high reactivity of the acrylic groups pertaining to easy polymerization/copolymerization via free radicals reaction [41-44].

1.2 Dissertation organization

The content of this thesis has covered various topics of the modifications and utilizations of vegetable oils - mainly soybean oil.

In chapter 2, epoxidized soybean oil and epoxidized linseed oil were used as the starting materials for being ring-opened by methanol and glycol, followed by saponification. Subsequently, by keeping molar ratio of carboxylic acid in fatty acid to epoxy group in epoxidized soybean oil as 0.5:1, polyols were produced via a reported solvent-free method. The stated ratio was proved to be optimized from the result of GPC as there was least remaining unreacted epoxidized soybean oil and fatty acid. PU films prepared from these polyols exhibit significant difference in thermal and mechanical properties of their PU films. The resulting PUs exhibit properties from rigid and brittle plastic to soft and ductile elastomer in accordance with the variation of OH number. PU

properties for specific applications can be willingly tailored with respect to OH number of polyols developed via this route.

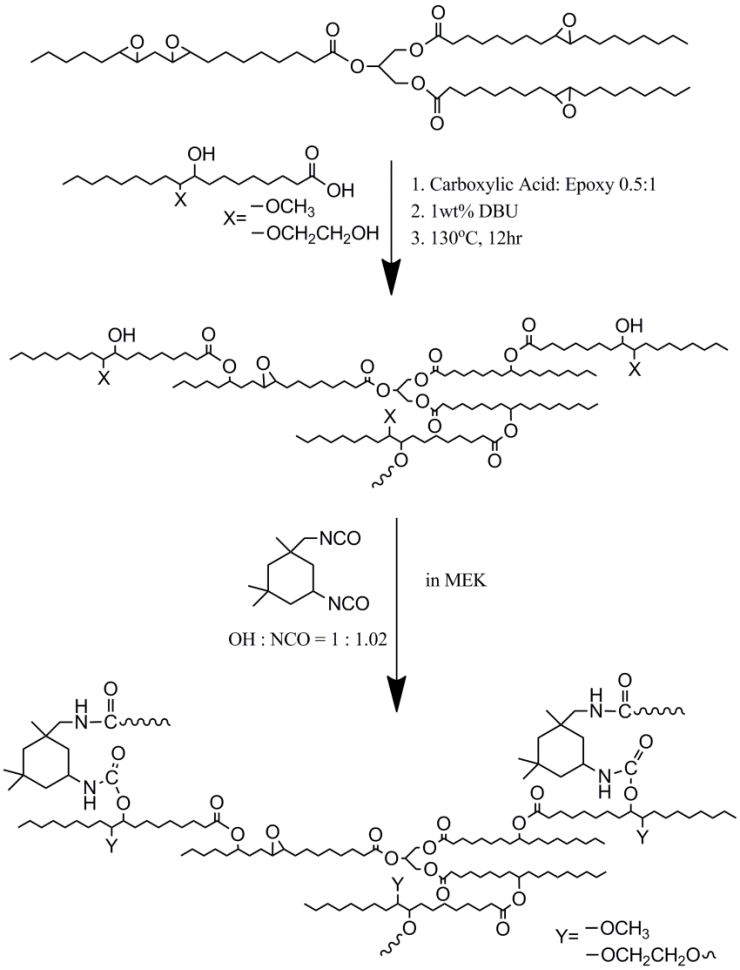

Figure 1-4 Illustration of process for chapter 2

In Chapter 3, epoxidized linseed oil (ELO) was ring-opened by glycol and HCl followed by saponification into polyhydroxyl fatty acid (FA). The obtained FA has an average functionality of OH as 4.8, which ensures the formation of crosslinking structure of PU at polymerization step. Besides, the high acid number of 139.3 mg KOH/g is the key factor in this work since the carboxylic group would be neutralized into ionic form which stabilizes the dispersions in water phase. Herein, two novel types of DMPA-free

waterborne PUDs have been developed. CasFAD was obtained from castor oil, FA and IPDI while FAD was prepared from FA and IPDI. Both PUDs are stable and have particle size as 35.11 nm and 56.11 nm, respectively. The thermal and mechanical properties of the resulting PUD films were characterized and compared with previously developed CasPAD, which was obtained from castor oil, DMPA and IPDI.

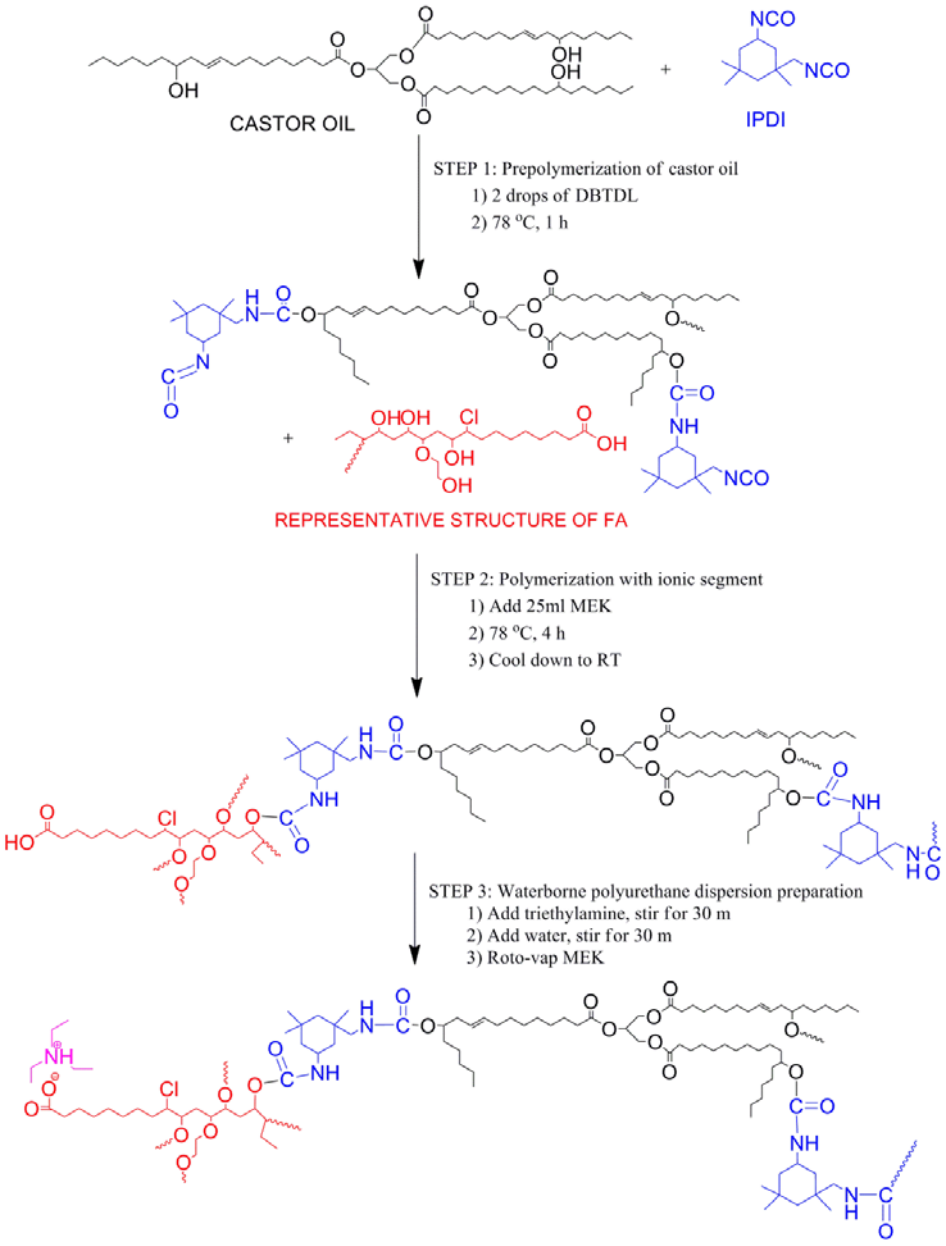

Figure 1-5 Illustration of process for chapter 3

In chapter 4, 2-methylaziridine was grafted onto acrylated epoxidized soybean oil (AESO) via Michael addition under mild conditions. The obtained aziridine-containing compound was subject to rapid room-temperature polymerization with succinic acid, citric acid and isosorbide-based di-acid, all of which are bio-based materials. The resulting polymeric products possess significantly high bio-content. The concept of this work conforms to the global awareness of the importance of bio-renewable materials. The fast polymerization rate could also trigger the interest of industry to develop the valuable applications of this novel polymerization system.

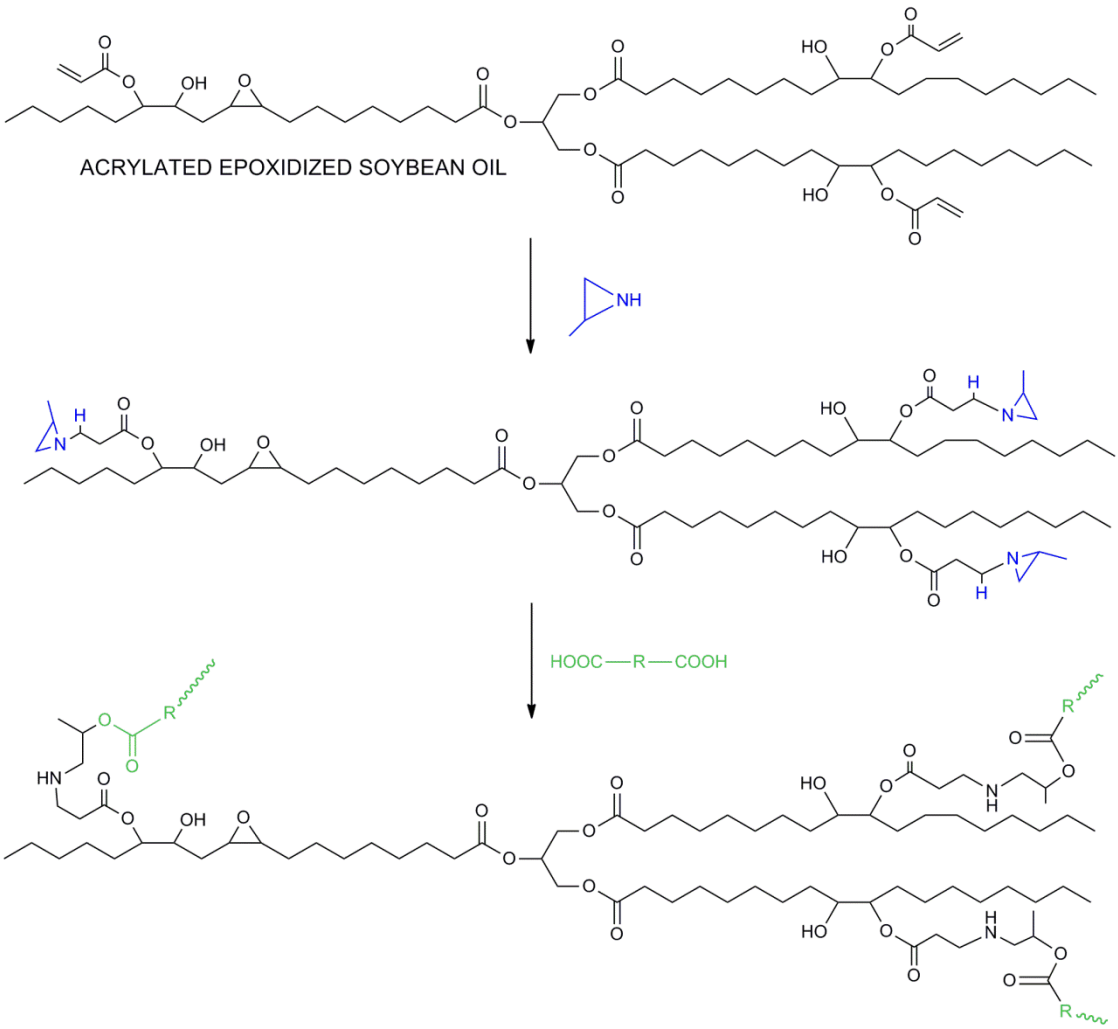

Figure 1-6 Illustration of process for chapter 4

In chapter 5, polyols with high functionality were acquired by coupling heat-bodying and ozonolysis techniques. Soybean oil was polymerized via thermal heating for various lengths of time. The remaining double bonds were then oxidized, cleaved and reduced into hydroxyl groups. The obtained polyols possess primary hydroxyl groups which are more reactive than secondary hydroxyls. Thermal and mechanical properties of PU films from these bio-based polyols were systematically studied with respect to the characteristics of the polyols.

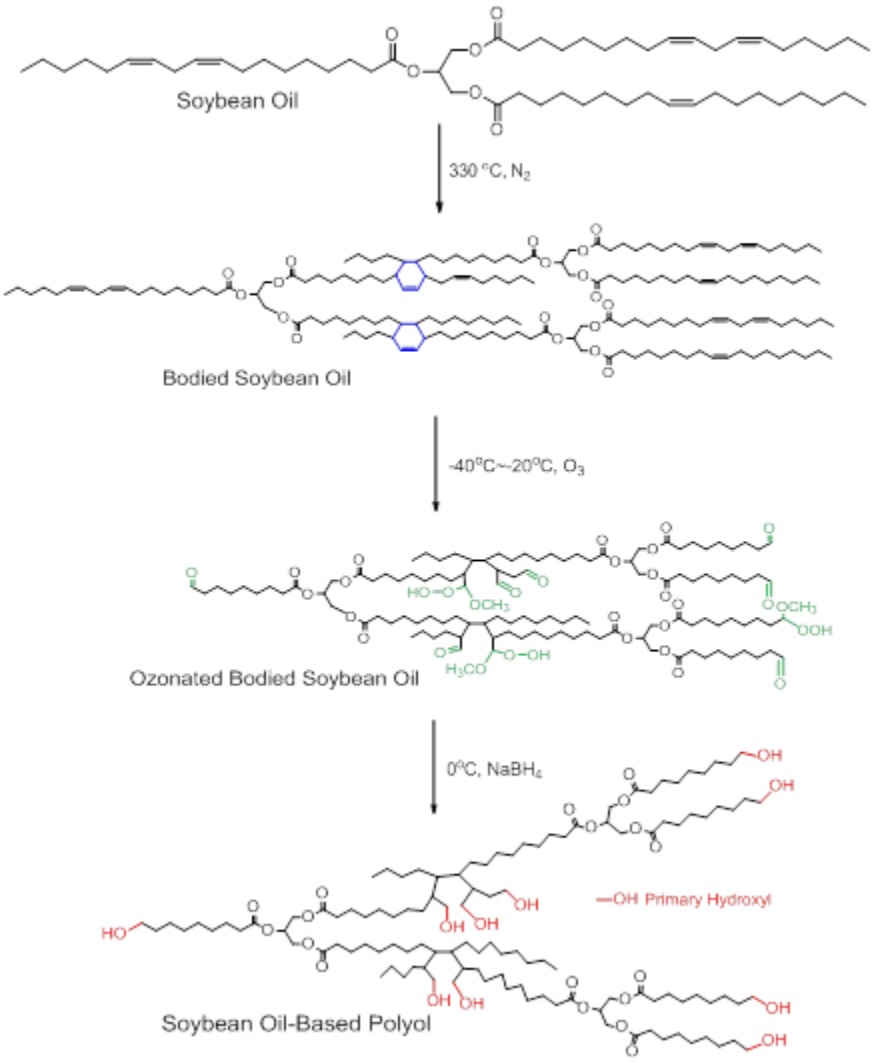

Figure 1-7 Illustration of process for chapter 5

The goal of this dissertation is to illustrate various viable modifications of vegetable oils for different purposes. The research could be critical, since industry and academia are calling for bio-renewable materials in replacement of petroleum-based resource in concern of the deficiency of crude oil. Vegetable oils, known for their abundance and low costs, could partially or fully substitute petroleum-based monomers in a wide range of polymer applications if they are properly engineered.

1.3 References

1. Uhlmann F: **Starch as a Renewable Resource for Industry**. *Landbauforsch Volk* 1985, **35**(4):163-173.

2. Shaabani A, Rahmati A, Badri Z: **Sulfonated cellulose and starch: New biodegradable and renewable solid acid catalysts for efficient synthesis of quinolines**. *Catal Commun* 2008, **9**(1):13-16.

3. Li SH, Zhuang XW, Wang CP, Chu FX: **Renewable Resource-Based Composites of Thermoplastic Acorn Starch and Polycaprolactone: Preparation and FTIR Spectrum Analysis**. *Spectrosc Spect Anal* 2011, **31**(4):992-996.

4. Lu YS, Tighzert L, Berzin F, Rondot S: **Innovative plasticized. starch films modified with waterborne polyurethane from renewable resources**. *Carbohyd Polym* 2005, **61**(2):174-182.

5. Lu YS, Tighzert L, Dole P, Erre D: **Preparation and properties of starch thermoplastics modified with waterborne polyurethane from renewable resources**. *Polymer* 2005, **46**(23):9863-9870.

6. Gotze T, Kreyenschulte H, Stockelhuber KW, Heinrich G, Marsche M, Richter S: **Cellulose: a renewable and reinforcing filler for elastomers. Spherical and fibrous cellulose types in comparison to conventional fillers**. *Kgk-Kaut Gummi Kunst* 2013, **66**(4):20-29.

7. Zhang JJ, Liu ZH, Kong QS, Zhang CJ, Pang SP, Yue LP, Wang XJ, Yao JH, Cui GL: **Renewable and Superior Thermal-Resistant Cellulose-Based Composite Nonwoven as Lithium-Ion Battery Separator**. *Acs Appl Mater Inter* 2013, **5**(1):128-134.

8. Figueiredo JA, Ismael MI, Anjo CMS, Duarte AP: **Cellulose and Derivatives from Wood and Fibers as Renewable Sources of Raw-Materials**. *Top Curr Chem* 2010, **294**:117-128.

9. Black H: **Materials - Bacterial cellulose strengthens renewable polymer composites**. *Chem Ind-London* 2008(14):11-11.

10. Lee SH, Lee SY, Cho MS, Nam JD, Choi HR, Koo JC, Lee Y: **Renewable resource using cellulose derivatives by melt process**. *Key Eng Mat* 2006, **326-328**:847-850.

11. Argyropoulos DS: **Cellulose and renewable materials division: a renewed outlook for the future**. *Cellulose* 2002, **9**(2):103-104.

12. Wang WS, Guo YL, Otaigbe JU: **Synthesis, characterization and degradation of biodegradable thermoplastic elastomers from poly(ester urethane)s and renewable soy protein isolate biopolymer**. *Polymer* 2010, **51**(23):5448-5455.

13. Withey GD, Kim JH, Xu J: **DNA-programmable multiplexing for scalable, renewable redox protein bio-nanoelectronics**. *Bioelectrochemistry* 2008, **74**(1):111-117.

14. Papanikolaou S, Chevalot I, Galiotou-Panayotou M, Komaitis M, Marc I, Aggelis G: **Industrial derivative of tallow: a promising renewable substrate for microbial lipid, single-cell protein and lipase production by Yarrowia lipolytica**. *Electron J Biotechn* 2007, **10**(3):425-435.

15. Zacco E, Pividori MI, Llopis X, del Valle M, Alegret S: **Renewable Protein A modified graphite-epoxy composite for electrochemical immunosensing**. *J Immunol Methods* 2004, **286**(1-2):35-46.

16. Humphrey AE, Gaden EL: **Single Cell Protein from Renewable and Nonrenewable Resources - Proceedings of Symposium on Single Cell Protein Substrates Presented at 1st Chemical Congress of North-American Continent, Mexico-City, Mexico, November 30 December 5, 1975 - Preface**. *Biotechnol Bioeng* 1977, **7**:R3-R3.

17. Vismara E, Gastaldi G, Valerio A, Bertini S, Cosentino C, Eisle G: **Alpha cellulose from industrial and agricultural renewable sources like short flax fibres, ears of corn and wheat-straw and its transformation into cellulose acetates**. *J Mater Chem* 2009, **19**(45):8678-8686.

18. Liu ZS, Erhan SZ, Akin DE, Barton FE: **"Green" composites from renewable resources: Preparation of epoxidized soybean oil and flax fiber composites**. *J Agr Food Chem* 2006, **54**(6):2134-2137.

19. Folster T, Michaeli W: **Flax - a Renewable Source of Reinforcing Fiber for Plastics**. *Kunstst-Ger Plast+* 1993, **83**(9):687-691.

20. Erhan SZ, Bagby MO: **Polymerization of Vegetable-Oils and Their Uses in Printing Inks**. *J Am Oil Chem Soc* 1994, **71**(11):1223-1226.

21. Ionescu M: **Polymerization of Soybean Oil with Superacids**.

22. Demirbas A: **Relationships derived from physical properties of vegetable oil and biodiesel fuels**. *Fuel* 2008, **87**(8-9):1743-1748.

23. Petrovic ZS, Zhang W, Javni I: **Structure and properties of polyurethanes prepared from triglyceride polyols by ozonolysis**. *Biomacromolecules* 2005, **6**(2):713-719.

24. Petrovic ZS, Milic J, Xu YJ, Cvetkovic I: **A Chemical Route to High Molecular Weight Vegetable Oil-Based Polyhydroxyalkanoate**. *Macromolecules* 2010, **43**(9):4120-4125.

25. Cvetkovic I, Milic J, Ionescu M, Petrovic ZS: **Preparation of 9-Hydroxynonanoic Acid Methyl Ester by Ozonolysis of Vegetable Oils and Its Polycondensation**. *Hem Ind* 2008, **62**(6):319-328.

26. Deka H, Karak N: **Bio-based hyperbranched polyurethanes for surface coating applications**. *Prog Org Coat* 2009, **66**(3):192-198.

27. Dutta S, Karak N: **Effect of the NCO/OH ratio on the properties of Mesua Ferrea L. seed oil-modified polyurethane resins**. *Polym Int* 2006, **55**(1):49-56.

28. Wang CS, Yang LT, Ni BL, Shi G: **Polyurethane Networks from Different Soy-Based Polyols by the Ring Opening of Epoxidized Soybean Oil with Methanol, Glycol, and 1,2-Propanediol**. *J Appl Polym Sci* 2009, **114**(1):125-131.

29. Dai HH, Yang LT, Lin B, Wang CS, Shi G: **Synthesis and Characterization of the Different Soy-Based Polyols by Ring Opening of Epoxidized Soybean Oil with Methanol, 1,2-Ethanediol and 1,2-Propanediol**. *J Am Oil Chem Soc* 2009, **86**(3):261-267.

30. Yang LT, Zhao CS, Dai CL, Fu LY, Lin SQ: **Thermal and Mechanical Properties of Polyurethane Rigid Foam Based on Epoxidized Soybean Oil**. *J Polym Environ* 2012, **20**(1):230-236.

31. Biswas A, Adhvaryu A, Gordon SH, Erhan SZ, Willett JL: **Synthesis of diethylamine-functionalized soybean oil**. *J Agr Food Chem* 2005, **53**(24):9485-9490.

32. Zhang CQ, Xia Y, Chen RQ, Huh S, Johnston PA, Kessler MR: **Soy-castor oil based polyols prepared using a solvent-free and catalyst-free method and polyurethanes therefrom**. *Green Chem* 2013, **15**(6):1477-1484.

33. Guo A, Cho YJ, Petrovic ZS: **Structure and properties of halogenated and nonhalogenated soy-based polyols *multiple melting for polyols**. *J Polym Sci Pol Chem* 2000, **38**(21):3900-3910.

34. Miao SD, Zhang SP, Su ZG, Wang P: **Synthesis of bio-based polyurethanes from epoxidized soybean oil and isopropanolamine**. *J Appl Polym Sci* 2013, **127**(3):1929-1936.

35. Hojabri L, Kong XH, Narine SS: **Novel Long Chain Unsaturated Diisocyanate from Fatty Acid: Synthesis, Characterization, and Application in Bio-Based Polyurethane**. *J Polym Sci Pol Chem* 2010, **48**(15):3302-3310.

36. More AS, Lebarbe T, Maisonneuve L, Gadenne B, Alfos C, Cramail H: **Novel fatty acid based di-isocyanates towards the synthesis of thermoplastic polyurethanes**. *Eur Polym J* 2013, **49**(4):823-833.

37. Zenner MD, Xia Y, Chen JS, Kessler MR: **Polyurethanes from Isosorbide-Based Diisocyanates**. *Chemsuschem* 2013, **6**(7):1182-1185.

38. Shen L, Haufe J, Patel MK: **Product Overview and Market Projection of Emerging Bio-based Plastics**. 2009.

39. Khot SN, Lascala JJ, Can E, Morye SS, Williams GI, Palmese GR, Kusefoglu SH, Wool RP: **Development and application of triglyceride-based polymers and composites**. *J Appl Polym Sci* 2001, **82**(3):703-723.

40. La Scala J, Wool RP: **Property analysis of triglyceride-based thermosets**. *Polymer* 2005, **46**(1):61-69.

41. Cayli G, Kusefoglu S: **Polymerization of Acrylated Epoxidized Soybean Oil with Phenol Furfural Resins via Repeated Forward and Retro Diets-Alder Reactions**. *J Appl Polym Sci* 2011, **120**(3):1707-1712.

42. Grishchuk S, Karger-Kocsis J: **Hybrid thermosets from vinyl ester resin and acrylated epoxidized soybean oil (AESO)**. *Express Polym Lett* 2011, **5**(1):2-11.

43. Sen S, Cayli G: **Synthesis of bio-based polymeric nanocomposites from acrylated epoxidized soybean oil and montmorillonite clay in the presence of a bio-based intercalant**. *Polym Int* 2010, **59**(8):1122-1129.

44. Wu SP, Rong MZ, Zhang MQ, Hu J, Czigany T: **Plastic foam based on acrylated epoxidized soybean oil**. *J Biobased Mater Bio* 2007, **1**(3):417-426.

CHAPTER 2: POLYOLS AND POLYUREHTANES PREPARED FROM EPOXIDIZED SOYBEAN OIL RING-OPENED BY POLYHYDROXY FATTY ACIDS WITH VARYING OH NUMBERS

A paper submitted to *Journal of Applied Polymer Science*

2.1 Abstract

Bio-based polyols from epoxidized soybean oil and different fatty acids were successfully prepared using a solvent-free method in order to investigate the effect of the polyols' OH numbers on the thermal and mechanical properties of the polyurethanes prepared using them. Epoxidized soybean oil/epoxidized linseed oil was ring-opened by methanol/glycol followed by saponification to prepare fatty acids. These fatty acids and epoxidized soybean oil were then used for further ring-opening reactions with DBU as catalyst. Gel permeation chromatography revealed that a molar ratio of carboxylic acid and epoxy group of 0.5:1 resulted in optimized polyols containing the smallest amounts of residual starting materials. The obtained polyols had OH numbers ranging from 150.4 mg KOH/g to 215.3 mg KOH/g. Polymerization was carried out between the polyols and IPDI at a ratio of OH : NCO of 1: 1.02, and the resulting polyurethane films were characterized by differential scanning calorimetry (DSC), dynamic mechanical analysis (DMA), ethanol absorption and uptake, thermogravimetric analysis (TGA), and tensile stress-strain tests. With increasing OH number of the polyols the PUs displayed an increase in crosslinking density, glass transition temperature (T_g), tensile strength and

Young's modulus, and a decrease in elongation and toughness. This work provides supplementary information on the effect of OH number of polyols obtained via a solvent-free ring-opening method on the mechanical and thermal properties of polyurethanes, of particular interest when designing PU products for specific purposes.

2.2 Introduction

Polyurethanes (PUs), commercially available first in 1954, have been employed in a wide range of applications, such as coatings, adhesives, sealants, foams, elastomers, and others [1]. Polyurethane is known for its recurring urethane linkages in the main chain and is commonly synthesized by mixing two components: one hydroxyl-bearing monomer and a monomer with isocyanate groups. As the available choices of poly-functional isocyanates are relatively limited, significant research and development effort has been spent on polyols for the preparation of polyurethane with desired properties. The soaring price of crude oil and increasing environmental concerns spurred the exploration of bio-renewable alternatives for future plastic development in both academia and industry. Considering the fact that polyol contributes the majority of the weight of polyurethane, makes the full or partial substitution of polyols from bio-renewable resources in order to increase the bio-content of PUs a promising approach.

Vegetable oil has attracted increasing attention as one of the most promising options because of its ready availability, relatively low cost, environmental sustainability, and low eco-toxicity. Vegetable oils, mainly triglycerides constituted by glycerol and three fatty acid chains, typically contain unsaturated carbon-carbon double bonds that are available for modification to form more reactive functional groups. Epoxidation of

double bonds followed by oxirane ring opening is commonly employed to graft attempted functional groups onto the vegetable oil molecules. Epoxidation is easily realized by *in-situ* oxidation with peracids formed by a reaction of hydrogen peroxide with formic or acetic acid and catalysts with yields of 75%–90% [2]. Alcohols [3, 4], amines [5, 6], carboxylic acids [7], halogenated acids [8], and others have been reported as effective agents in the subsequent ring-opening step. Miao *et al*. [9] successfully obtained polyols by ring-opening epoxidized soybean oil with isopropanol amine and hydrochloride. The effect of reaction time and temperature on the structure of the obtained polyols was studied thoroughly. Wang *et al*. [3] prepared polyols by using methanol, glycol and 1,2-propanediol to ring open epoxidized soybean oil and studied the impact of their OH number on polyurethane properties. The reaction protocol was used for the preparation of fatty acids in the study presented here. Recently, a solvent-free method for the preparation of polyol from castor oil based fatty acid (COFA) and epoxidized soybean oil was published [7]. This novel, green method is worth further systematic investigation, in particular the effect of fatty acids with different OH numbers on the properties of polyols and the resulting polyurethanes.

In this work, epoxidized soybean oil and epoxidized linseed oil were used as the starting materials and ring-opened by methanol and glycol. The OH numbers of the obtained fatty acids varied between 167.1 mg/KOH and 245.2 mg KOH/g while the fatty acids had similar acid numbers. Subsequently, the different fatty acids were used to produce polyols utilizing the solvent-free method reported in [7], where the molar ratio of carboxylic acid in fatty acid to epoxy group in epoxidized soybean oil was kept at 0.5:1. This molar ratio was determined as optimum by GPC, because it resulted in the least

amount of residual unreacted epoxidized soybean oil and fatty acid. In addition, the OH numbers of the obtained polyols increased with the OH numbers of the fatty acids. Fatty acids and polyols were characterized by proton nuclear magnetic resonance (^{1}H NMR), Fourier transform infrared spectroscopy (FTIR), gel permeation chromatography (GPC) and rheometry to determine their fundamental properties. Subsequently, the polyols were used to produce polyurethanes and the mechanical and thermal properties of their respective cast films were studied by differential scanning calorimetry (DSC), dynamic mechanical analysis (DMA), ethanol absorption and uptake, thermogravimetric analysis (TGA), and tensile tests. It was concluded that the crosslinking densities increased with increasing OH numbers of the polyols, which contributed to an increase in Young's modulus, tensile strength, and glass transition temperature (T_g).

2.3 Experimental

2.3.1 Materials

Epoxidized soybean oil (ESBO) was purchased from Scientific Polymer Inc., New York, NY. Epoxidized linseed oil (ELO) was kindly provided by American Chemical Service Inc., Griffith, IN. Magnesium sulfate ($MgSO_4$), potassium hydroxide (KOH), methanol, ethylene glycol, hydrochloric acid (HCl), and methyl ethyl ketone (MEK) were purchased from Fisher Scientific Company (Fair Lawn, NJ). Tetrafluoroboric acid solution (48 % in H_2O), isophorone diisocyanate (IPDI), and dibutyltin dilaurate (DBTDL) were obtained from Sigma-Aldrich (Milwaukee, WI). Ethanol was purchased from Decon Laboratories Inc., King of Prussia, PA. All materials were used as received without further purification.

2.3.2 Preparation of Fatty Acids

The initial step was the preparation of four different fatty acids from epoxidized soybean oil ring opened by (1) methanol and (2) glycol, and epoxidized linseed oil ring opened by (3) methanol and (4) glycol [3]. The ring-opened epoxidized oils were then saponified into fatty acids for later use.

(a) *Methanol route.* 100 g of epoxidized oil was dissolved in methanol (molar ratio of epoxy group of oil to hydroxyl group of methanol was 1:10) in the presence of 0.1 wt% tetrafluoroboric acid. The reaction was carried out in a two-necked round-bottom flask equipped with a condenser and mechanical stirrer at 65 °C for 2 h.

(b) *Glycol route*. The reaction setup was identical to the methanol route; however, the reaction temperature was 98 °C.

After being cooled down to room temperature, the reacting mixtures were extracted by ethyl acetate and washed with saturated sodium chloride solution three times. Organic solvent was then removed at 70 °C under reduced pressure. The obtained fatty alcohol was then saponified by KOH in a mixture of ethanol and water (50/50 v/v) at 73 °C for 4 h, and then neutralized using HCl. Fatty acid precipitated out of the uniform solution and was subsequently extracted by ethyl acetate. The organic layer was washed three times and dried over $MgSO_4$. Pure fatty acid was obtained upon removal of the organic solvent by roto-evaporation. Figure 2-1 shows the representative synthesis route.

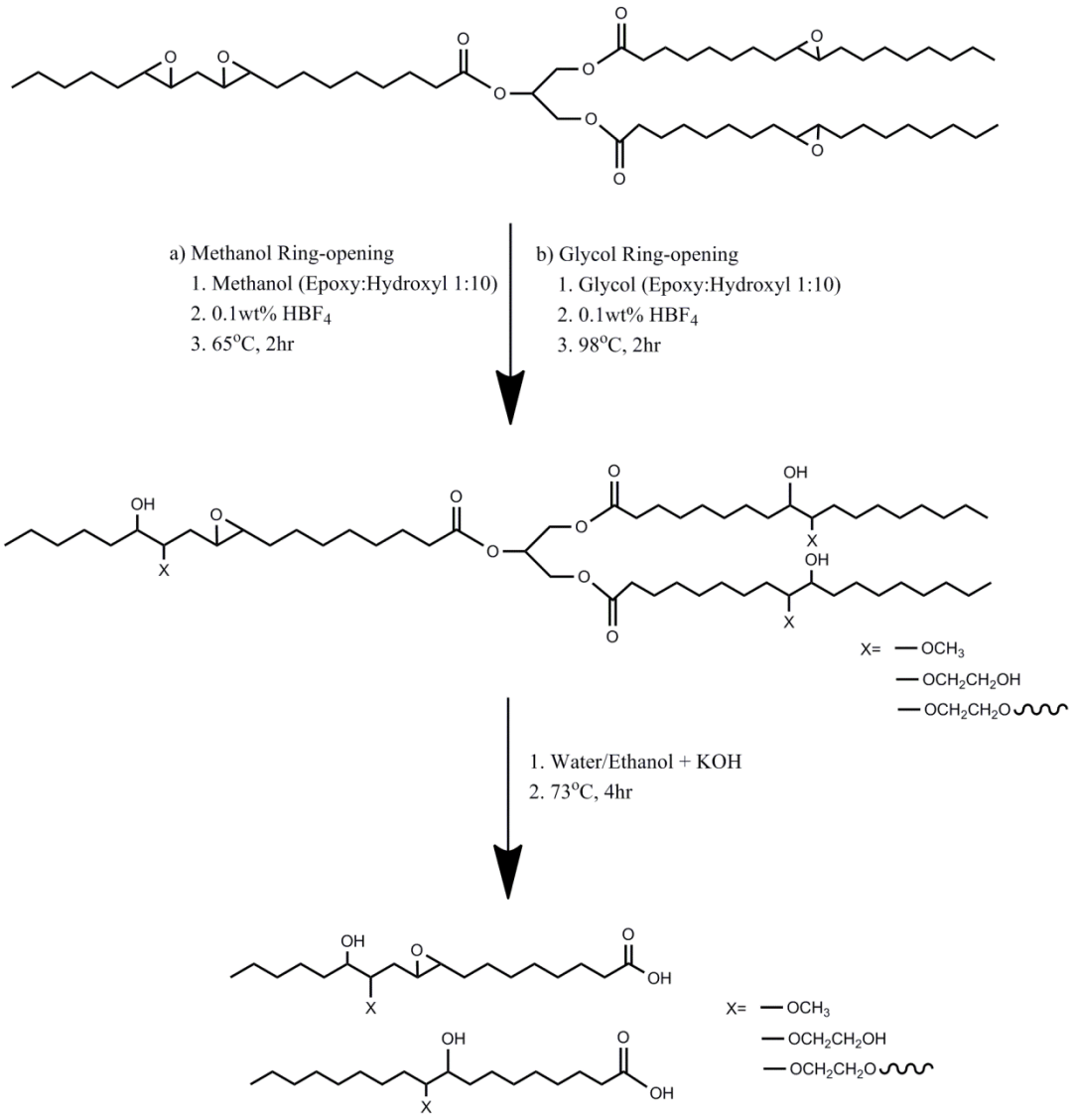

Figure 2-1 Preparation of fatty acids

2.3.3 Preparation of polyols from epoxidized soybean oil ring-opened by fatty acids with DBU catalyzer

Polyols were prepared by mixing fatty acids with epoxidized soybean oil in a flask under magnetic stirring at 130 °C in the presence of DBU as catalyst. The weight ratio of fatty acid to epoxidized soybean oil was determined by an initial molar ratio of carboxylic acid group to epoxy group of 0.5:1 [7]. The reaction proceeded for 6 h and the

obtained polyols were dark brown, viscous liquids. uijThe four polyols were identified as SMS, SGS, LMS and LGS, where the first letter “S” stands for ESBO and “L” stands for ELO, the second letter “M” represents ring-opened by methanol and “G” means ring-opened by glycol, and the last letter “S” refers to ESBO ring-opened by fatty acids. Figure 2-2 depicts the synthesis of polyols.

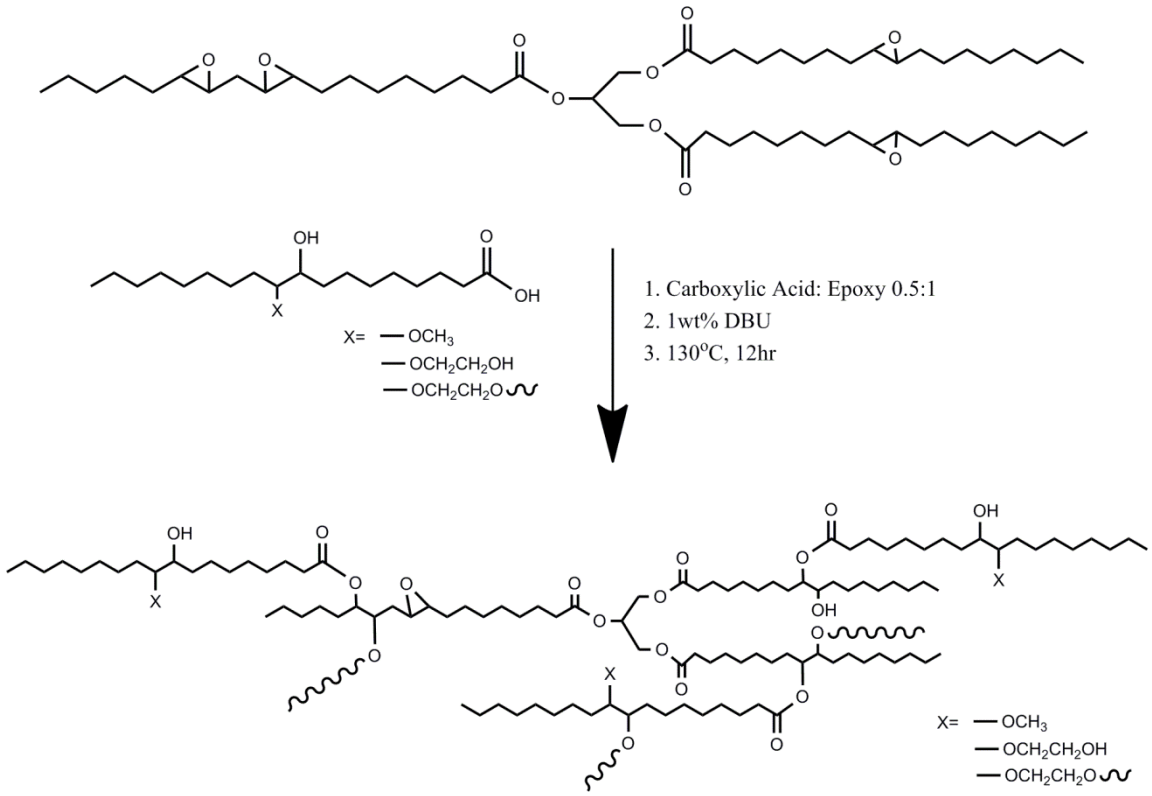

Figure 2-2 Preparation of representative polyols

2.3.4 Preparation of polyurethanes using polyols

Figure 2-3 shows the polymerization reaction creating polyurethanes, which was carried out in MEK as solvent at 60 °C for 3 h by mixing polyol, IPDI (molar ratio of OH and NCO was 1 : 1.02) and one drop of DBTDL. The solution was then poured into an 80

× 80 mm Teflon mold to produce thin films, which were post-cured and dried overnight at 80 °C. The obtained PU films were sliced into specific dimension for tests.

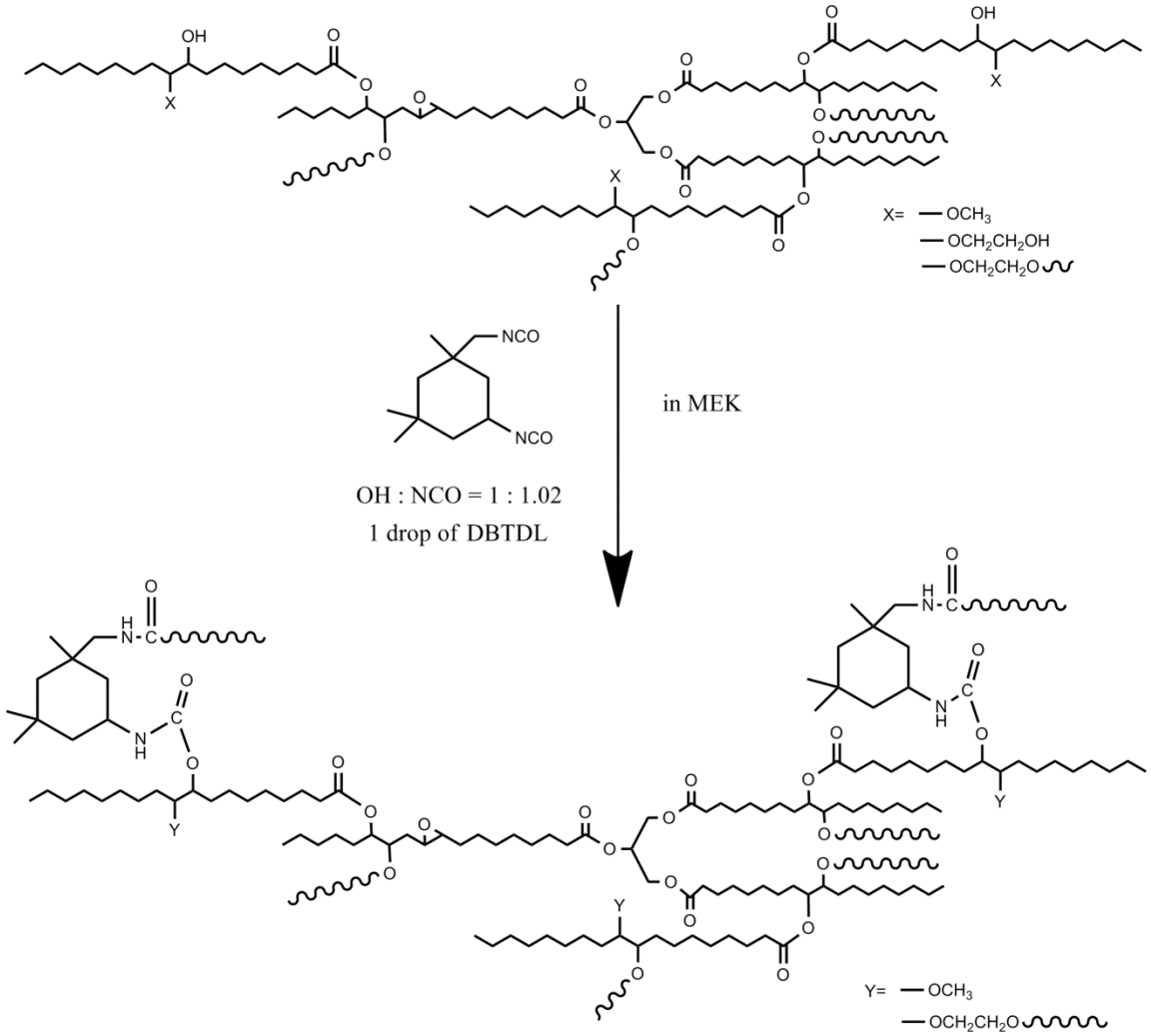

Figure 2-3 Illustration of polymerization reaction

2.3.5 Characterizations

^{1}H NMR spectra of the polyols were recorded on a Varian spectrometer (Palo Alto, CA) at 300 MHz in chloroform-*d*. A Bruker IFS66V FT-IR spectrometer was used to characterize both fatty acids and polyols. The scanning resolution was 4 cm^{-1} and the scanning range covered 4000 cm^{-1} to 400 cm^{-1}. The hydroxyl numbers and the acid

numbers of the fatty acids and polyols were determined using the Unilever method and the AOCS Official Method Te 1a-64, respectively. The average molecular weight was measured by a Thermo Scientific Dionex Ultimate 3000 GPC (Sunnyvale, CA) equipped with a Shodex Refractive Index (RI). The eluent solvent used was tetrahydrofuran with two Agilent PLgel 3μm 100 Å 300 × 7.5 mm (p/n PL1110-6320) and one Mesopore 300 × 7.5 mm (p/n PL1113-6325). The flow rate of THF was 1.0 mL/min and the measurement proceeded at room temperature. Rheological tests were performed using an AR2000 (TA Instrument). The rheological behavior of fatty acids and polyols was investigated by varying the shear rate from 10 s^{-1} to 1000 s^{-1} at designated temperatures.

Ethanol uptake and ethanol absorption tests were performed following reported methods [10]. W_0 was defined as the original weight of dry PU films with dimensions of 2 cm × 2 cm. Subsequently, the films were immersed in ethanol for 48 h, then towel-dried and their weight was recorded as W_1. Then, the samples were re-conditioned in an oven at 70 °C for 24 h and their weight was recorded as W_2. The percentage of ethanol absorption (W_a) and the percentage of weight loss (W_d) are calculated as:

$$W_a = \frac{W_1 - W_2}{W_2} \times 100\%$$

$$W_d = \frac{W_0 - W_2}{W_0} \times 100\%$$

Dynamic mechanical analysis (DMA) of the polyurethane films was carried out on a TA Instruments DMA Q800 dynamic mechanical analyzer using a film-tension mode of 1 Hz. Rectangular samples with a length of 15 mm and width of 10 mm were used for the analysis. The samples were cooled and held isothermally for 3 min at –80 °C

before raising the temperature to 120 °C at a rate of 3 °C/min. The glass transition temperatures (T_gs) of the samples were obtained from the peaks of the tan δ curves.

Thermogravimetric analysis (TGA) of the films was performed on a TA Instrument Q50 (New Castle, DE). The samples were heated from room temperature to 650 °C at a rate of 20 °C min^{-1} in air. The air flow rate was 60 mL/min. The remaining weight percentage was recorded as a function of temperature.

Differential scanning calorimetry (DSC) was conducted on a TA Instrument Q20. Samples with a weight of approximately 10 mg were heated to 120 °C to eliminate their heat history. The samples was cooled down to –50 °C by manually adding liquid nitrogen to the chamber and then heated to 120 °C at a programmed rate of 10 °C/min. The second heating ramp was recorded and the glass transition temperature was determined by the midpoint inflection method.

The tensile properties of the PU films were determined using an Instron universal testing machine (model 4502) with a crosshead speed of 100 mm/min. Samples were prepared in rectangular shape of 50 mm ×10 mm (length × width). At least three replicates were tested for each PU sample. The stress-strain curve was plotted and toughness, representing the ability of a material to absorb energy without fracturing, was calculated as the area beneath the curve.

2.4 Results and discussion

2.4.1 Preparations of Fatty Acis

The preparation of fatty acids involved the ring-opening of epoxidized vegetable oils followed by saponification. Neither methanol nor glycol were able to ring open all epoxy groups, which is in accordance with reported results [2, 11]. Additionally, in terms of the glycol ring-opening system, the presence of primary hydroxyl group exhibited high reactivity towards further ring-opening which caused oligomerization. The resulting oligomerized oil molecules caused high molecular weights in the obtained fatty acids. The GPC results confirmed this observation, as ESBO-methanol-FA and ELO-methanol-FA showed lower M_n and M_w than ESBO-glycol-FA and ELO-glycol-FA, see Table 2-1. In addition, oligomerization caused higher polymeric dispersion indices in the respective glycol ring-opened oils, and the viscosities at 40 °C of ESBO-Glycol-FA and ELO-Glycol-FA (1.15 Pa·s and 2.21 Pa·s, respectively) were higher than those of fatty acids derived by methanol ring-opening. Figure 2-4 shows FTIR spectra of the obtained fatty acids, with ESBO and ELO as references. All fatty acids exhibited a new broad trough between 3600 cm^{-1} to 2500 cm^{-1}, which was assigned to overlapped signal from the –OH stretching of the hydroxyl and the carboxylic groups [12]. The peak at 823 cm^{-1} was no longer observed for the fatty acids because most of the epoxy groups were reacted during the ring-opening step [13]. These two changes confirmed the success of the preparation of fatty acids.

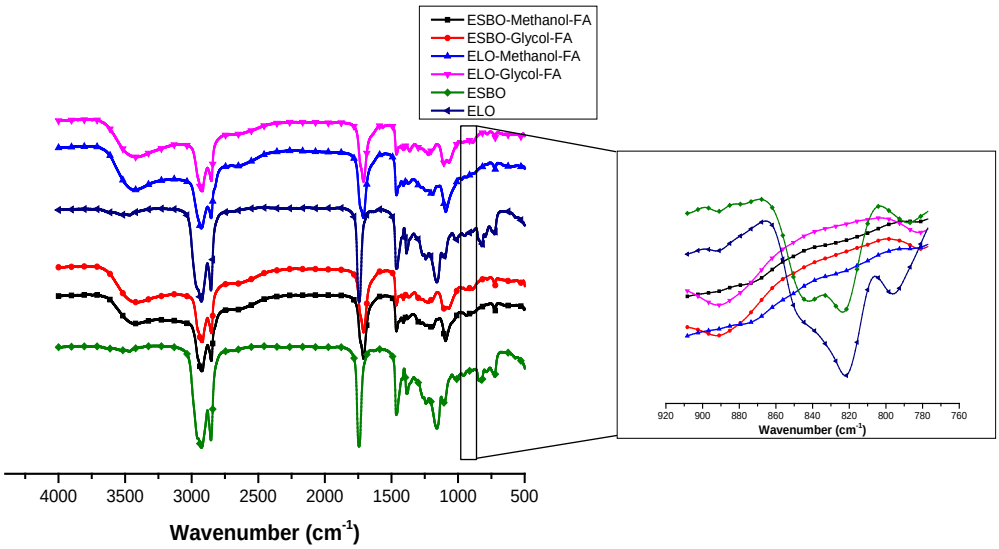

Figure 2-4 FTIR spectra of FA compared with ESBO and ELO

Table 2-1 Properties of fatty acids

Fatty Acid	OH number (mg KOH/g)	Acid number (mg KOH/g)	Viscosity at 40 ^{o}C (Pa·s)	M_n	M_w	PDI
ESBO-Methanol-FA	167.1	160.7	0.28	568	664	1.17
ESBO-Glycol-FA	186.0	151.4	1.15	889	1402	1.58
ELO-Methanol-FA	202.4	145.5	0.71	705	955	1.36
ELO-Glycol-FA	225.2	142.8	2.11	944	1476	1.56

2.4.2 Preparation and properties of polyols

The polyols were prepared in a one-pot process, requiring neither solvent nor washing. Trace amounts of DBU as catalyst not only lowered both reaction temperature and time, but also promoted the reactivity of the carboxylic acid group towards ring-opening in competence with that of the hydroxyl group [7].

The effect of the molar ratio between the carboxylic acid groups from fatty acid and the epoxy groups from epoxidized soybean oil was investigated by GPC. ESBO-methanol-FA with the lowest OH number and ELO-glycol-FA with the highest OH number were intentionally chosen as representatives. With increasing molar ration (from 0.3:1 to 0.7:1) both systems showed similar GPC patterns. . A low molar ratio of 0.3:1 did not provide the sufficient number of active functional groups to initiate ring-opening. Consequently, the spectra showed a shoulder in the ESBO position, indicating the presence of remaining ESBO that was not ring opened, see Figure 2-5 (a), As the ratio increased to 0.7:1, the shoulder in the ESBO position was suppressed as increasing numbers of epoxy groups were ring-opened, resulting in a prominent peak at the position of the corresponding fatty acids, indicating the presence of remaining fatty acids. As a conclusion, a molar ratio of 0.5:1 was determined as the optimized ratio with the lowest levels of unreacted fatty acid and ESBO. Same molar ratio was used for the polyol syntheses from ESBO-glycol-FA and ELO-methanol-FA.

^{1}H-NMR spectra of the polyols and ESBO are shown in Figure 2-6. A representative structure of the polyol is embedded to illustrate the assignments of the peaks. The appearance of Peak 1, corresponding to –COO–CH, confirmed that carboxylic acid ring-opening had occurred and an ester group anchored on the fatty acid chains was formed. Broad peaks between 3.2 ppm and 4.0 ppm were assigned to ether linkages formed by epoxy groups ring-opened by hydroxyl groups. The polyols did not show a noticeable Peak 4, which is assigned to the epoxy group, indicating that almost all epoxy groups were ring-opened.

FTIR spectra of the polyols are shown in Figure 2-7. Each ring opening of an epoxy group created one hydroxyl group. Together with the hydroxyl groups intrinsically present in fatty acids, the polyols contain a considerable number of hydroxyl groups that contribute to the broad peak between 3600 cm^{-1} and 3200 cm^{-1}. In the vicinity of 823 cm^{-1}, the polyol curves are wavy but show lower absorbance than the curve of ESBO, which matches the result from ^{1}H-NMR.

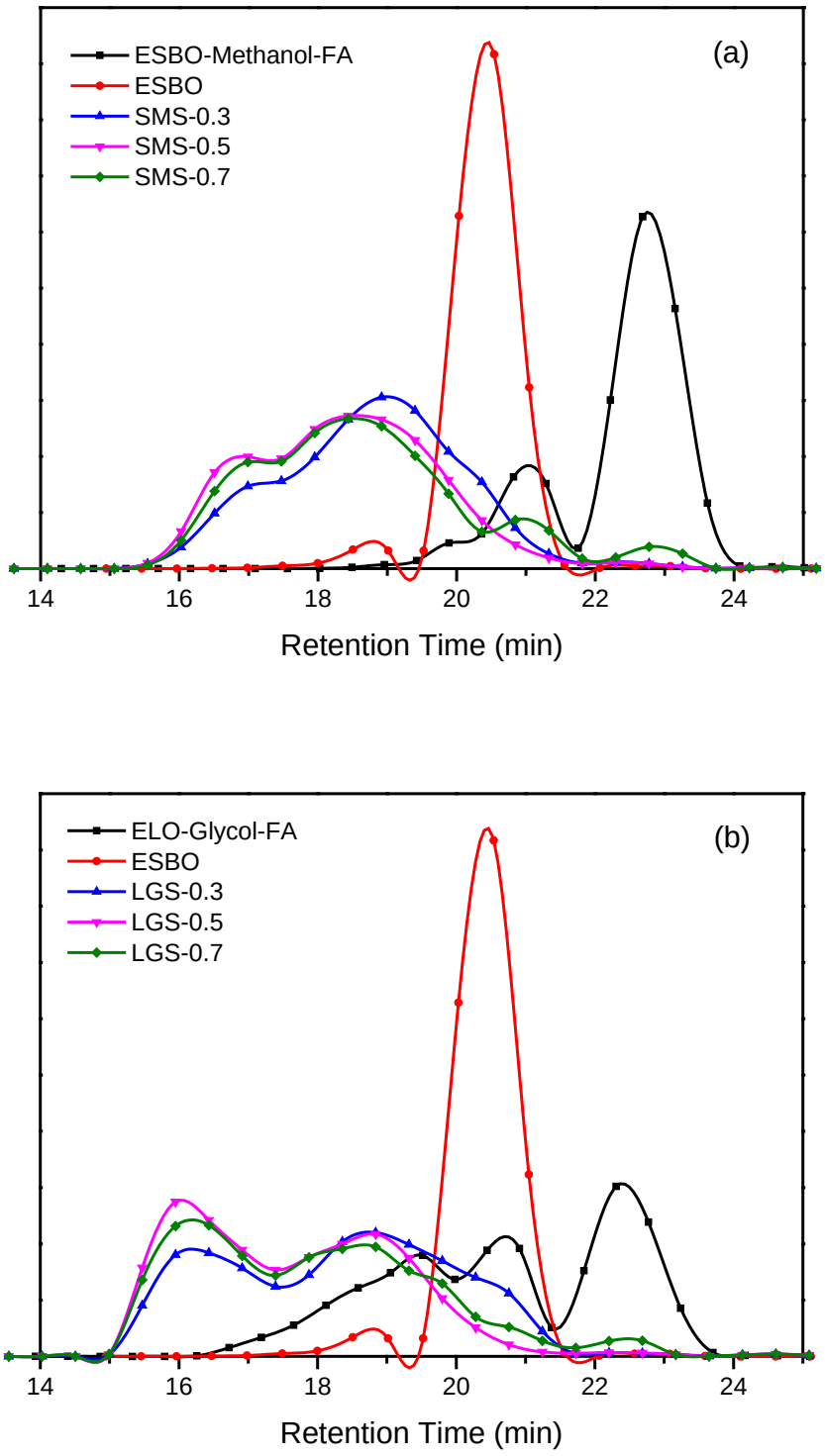

Figure 2-5 Effect of ratio between carboxylic acid and epoxy groups on GPC curves for (a) SMS and (b) LGS

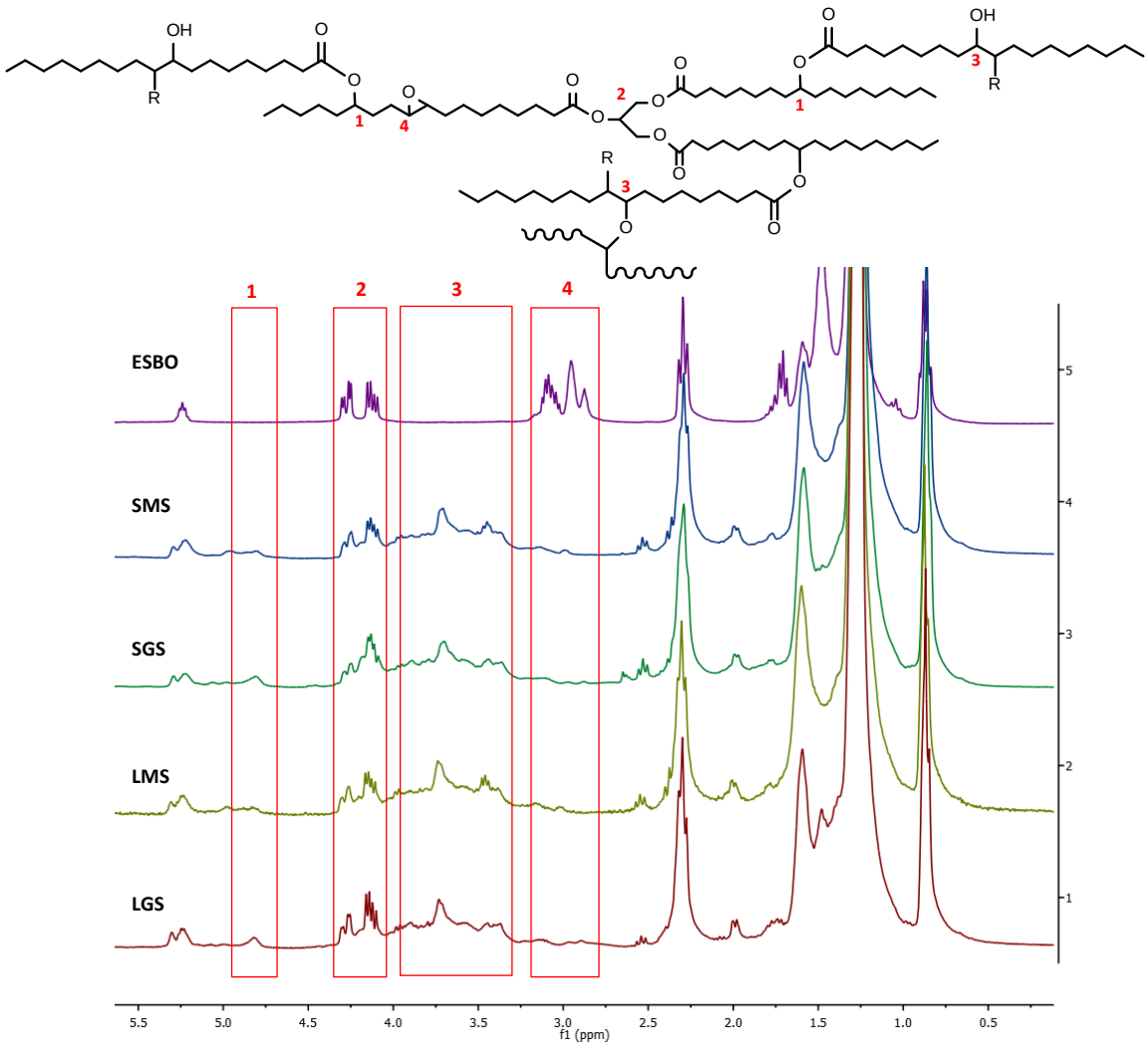

Figure 2-6 ^{1}HNMR spectra of polyols and ESBO

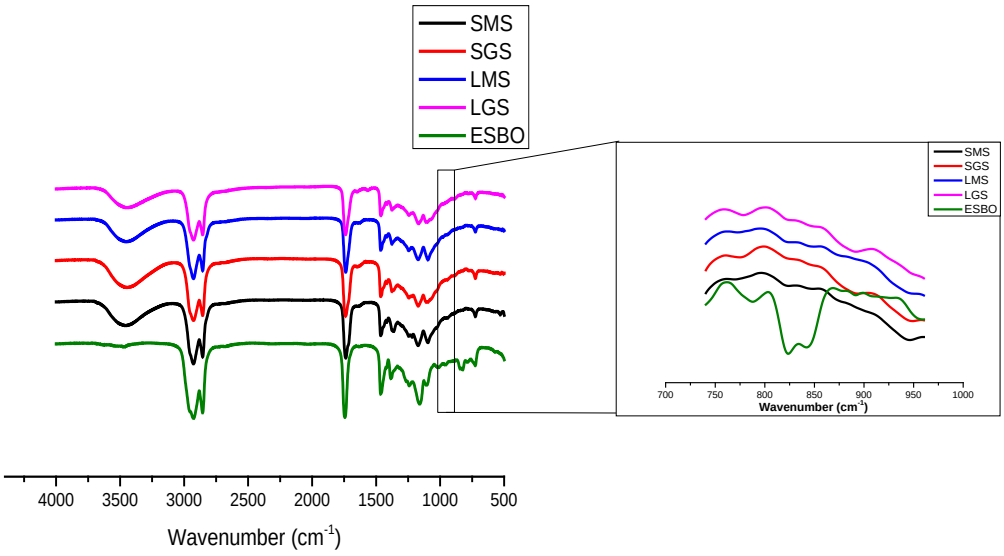

Figure 2-7 FTIR spectra of polyols and ESBO

Hydroxyl number, acid number, viscosity and molecular weight of the polyols are summarized in Table 2-2. The acid numbers of the polyols indicated the presence of small amounts of fatty acids in the mixture. The viscosity of the polyols mirrored that of the fatty acids; those obtained from glycol ring-opening were more viscous because of oligomerization. The OH numbers of the polyols were lower than those of the fatty acids. This was explained by the fact that when a carboxylic acid group ring opened an epoxy, one net hydroxyl was generated, whereas when a hydroxyl group ring opened an epoxy, there was no net effect on the functionality. Because the molecular weight was increased significantly by the coupling of fatty acid and ESBO, and because the carboxylic acid involved had only half the number of epoxy groups, it is theoretically possible for the obtained polyols to have OH number lower than the fatty acids. Moreover, the OH number of the polyols increased with an increase in OH numbers of the fatty acids, which offers an important pathway for the preparation of polyols with tailored OH numbers.

Table 2-2 Properties of the polyols

Fatty Acid	OH number (mg KOH/g)	Acid number (mg KOH/g)	Viscosity at 60°C (Pa·s)	M_n	M_w	PDI
SMS	150.4	1.2	1.17	2487	3389	1.36
SGS	168.5	0.8	3.72	2782	4434	1.59
LMS	190.8	0.7	1.77	2474	3402	1.37
LGS	211.3	1.5	5.54	3114	4715	1.51

2.4.3 Polyurethane properties

Differential scanning calorimetry (DSC) thermograms of the polyurethane films are shown in Figure 2-8. Each sample exhibited only one T_g and no melting or crystalizing peak, indicating that the samples had a homogenous, amorphous structure. With an increase in polyol OH number from 150.4 mg KOH/g to 215.3 mg KOH/g, the T_g increased from 19.0 °C to 56.3 °C. The increase in T_gs was attributed to an increasing content of hard segments, higher crosslinking density, and less plasticizing effect of dangling chains [14]. In order to compensate for the higher OH number of the polyols while maintaining a constant ratio between OH and NCO, higher levels of segment IPDI were used during polymerization. As summarized in Table 2-3, the hard segment content increased from 22.9% to 29.9% with increasing polyol OH numbers. The OH number of the polyols also significantly influenced the crosslinking density of the PU network, which was formed by intermolecular urethane linkages between soft segments and hard segments. Higher polyol OH number, indicating higher functionality, led to more fatty acid chains being crosslinked and incorporated into the PU network. As a result, fewer free fatty acid arms, acting as plasticizers, were present in the material.

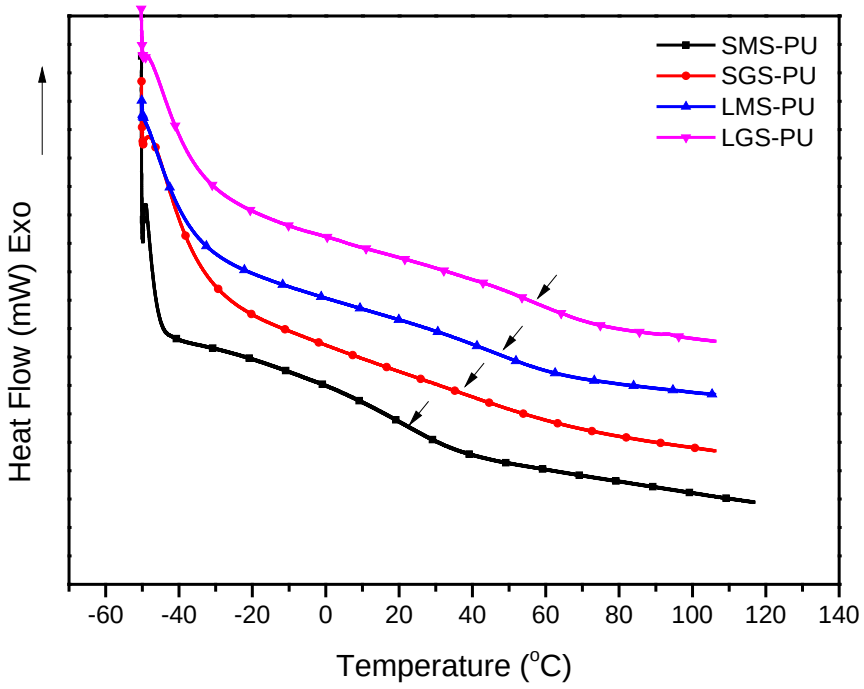

Figure 2-8 DSC scans of PU films

DMA was employed to study the temperature dependence of the storage modulus (E') and the loss factor (tan δ) of the PU films, see Figure 6. Below room temperature, all PU films were in a glassy state so that the storage modulus decreased slightly. As the temperature passed through the glass transition temperature, which is defined by the peak of tan δ, the storage moduli of the samples dropped by approx. 3 orders of magnitude. Subsequently, all samples entered into the rubbery state and E' exhibited less dependence on temperature. The observed rubbery plateau was evidence of the presence of a crosslinked network in the PU films; the storage modulus in the rubbery state increased with the polyol OH number and determined the crosslinking density of the network structure [11]. According to the kinetic theory of rubber elasticity [15], crosslinking density (ν_e) can be quantitatively determined using the following equation:

$$E' = 3v_e RT$$

where E' is the rubbery storage modulus, typically at T_g + 50 °C, R is the universal gas constant, and T is the absolute temperature. The calculated crosslinking density of the PUs ranged from 37.4 mol/m^3 to 911.9 mol/m^3 with increasing polyol OH numbers, see Table 2-3. The positive correlation between crosslinking density and polyol OH number revealed that an increasing fraction of fatty acid arms were incorporated into the network via urethane bonds as the OH number of the polyols increased. It is worth noting that the difference in T_g values obtained by DSC and DMA was mainly caused by the different nature of the two measurements. DSC measured the heat capacity change from frozen to unfrozen chains, while DMA measured the change in mechanical response of the polymer chains to heating [16]. Only one tan δ was observed for each material, indicating the homogeneous nature of all investigated PU samples. The height of tan δ decreased with increasing crosslinking density, matching reported properties of similar systems [7, 10]. With increasing OH numbers of the polyols, T_g increased from 39.3 °C to 80.5 °C, which was explained by the fact that polymer chain motion was more restricted in a network with higher crosslinking density. Also, because the stoichiometric ratio of OH to NCO of 1:1.02 was strictly controlled during the polymerization step, higher content of hard segment IPDI was contained in PUs from polyol with correspondingly higher OH numbers, contributing to the stiffness of the material.

The Fox-Losheak equation relates the crosslinking density and T_g [11, 17] :

$$T_g = T_{g\infty} + \frac{K}{M_c} = T_{g\infty} + kv$$

Where $T_{g\infty}$ is the glass-transition temperature of the linear polymer of the same structure, v is the number of cross-links per unit of volume (density/M_c), and K and k are consants for a given system. It was reported previously that v is linearly proportional to the OH number of the polyol, assuming the monomer conversion is complete [11, 18]. The linear fit of the data points in Figure 2-10 shows the dependence of the T_g of the PU films on the OH number of the corresponding polyol, documented by R^2 values of 0.968 and 0.982 for DSC and DMA measurements, respectively.

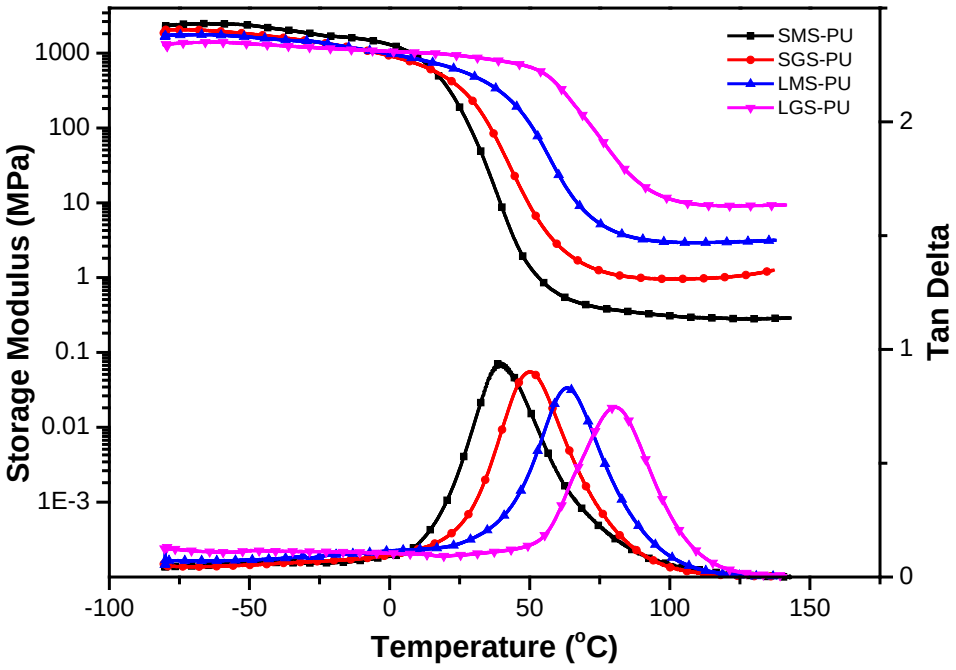

Figure 2-9 Storage modulus and loss factor of PU films as functions of temperature

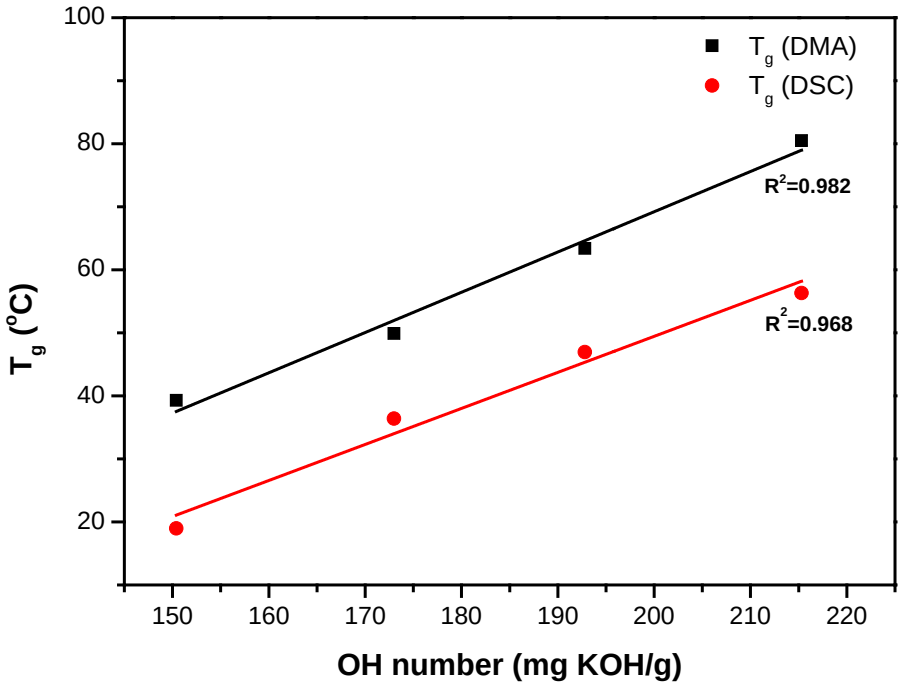

Figure 2-10 Dependence of glass transition temperature on OH number of polyols

Ethanol uptake and absorption experiments were performed to examine the degree of crosslinking for each PU film. As discussed with the DMA results, the OH numbers of the polyols were linearly related to the crosslinking density of the PU network. Figure 2-11 shows that after immersion the amount of absorbed ethanol and the weight loss of the PUs decreased from 133.1% to 61.4% and from 11.8% to 4.7%, respectively, while the OH number of the polyols increased from 150.4 mg KOH/g to 215.3 mg KOH/g. This indicated that ethanol absorption and uptake were reduced as the degree of crosslinking increased [10, 19].

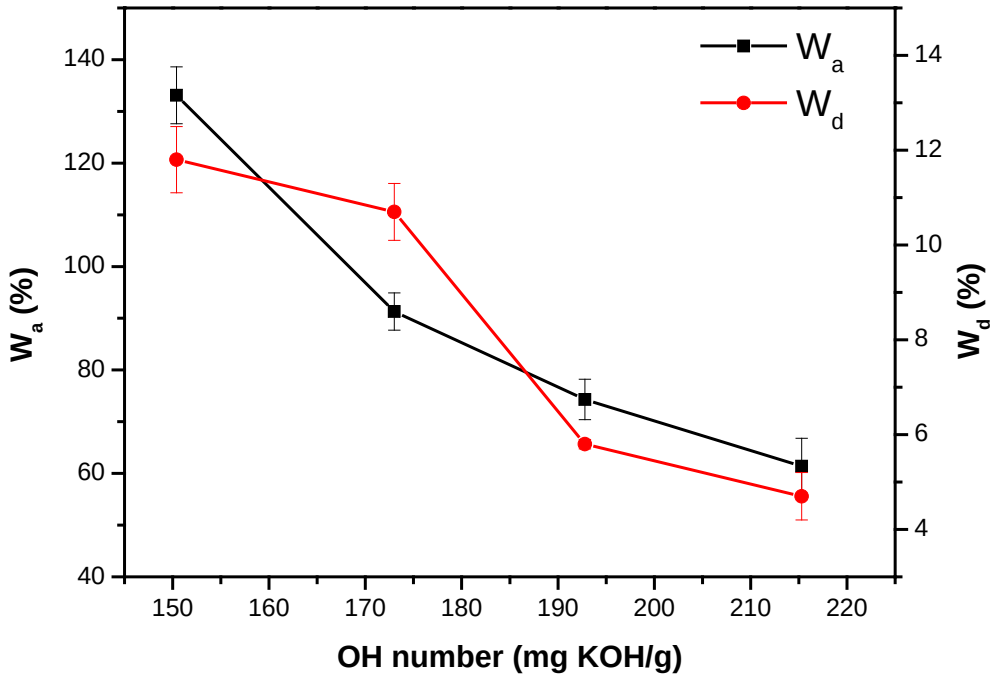

Figure 2-11 Dependence of ethanol absorption and uptake on OH number of polyols

TGA was conducted to investigate the thermal resistance of the PU films, see Figure 2-12. In general, PUs exhibit three stages of thermal decomposition in air atmosphere [3]. The first weight loss domain observed in the range from 200 °C to 300 °C is assigned to the dissociation of the labile urethane bonds. The dissociation of urethanes to isocyanates and alcohols, the formation of primary amines and olefins, and the formation of secondary amines were reported as three possible mechanisms [3]. The second thermal degradation stage between 300 °C and 450 °C is the result of chain scission in the soybean oil structure. The last stage, above 450 °C, is attributed to further thermo-oxidation of the PUs in air. The content of urethane bonds within each sample increased when the OH number of the corresponding polyol increased from 150.4 mg KOH/g to 215.3 mg KOH/g, given a constant molar ratio of OH and NCO. Higher

contents of labile urethane bonds caused the shift of T_{10} (temperature of 10 % weight loss) and T_{50} (temperature of 50% weight loss) from 305.2 °C to 298.9 °C and 383.5 °C to 370.9 °C, respectively. Similar results regarding the effect of increasing fractions of urethane bonds were reported by Lu *et al.* [11].

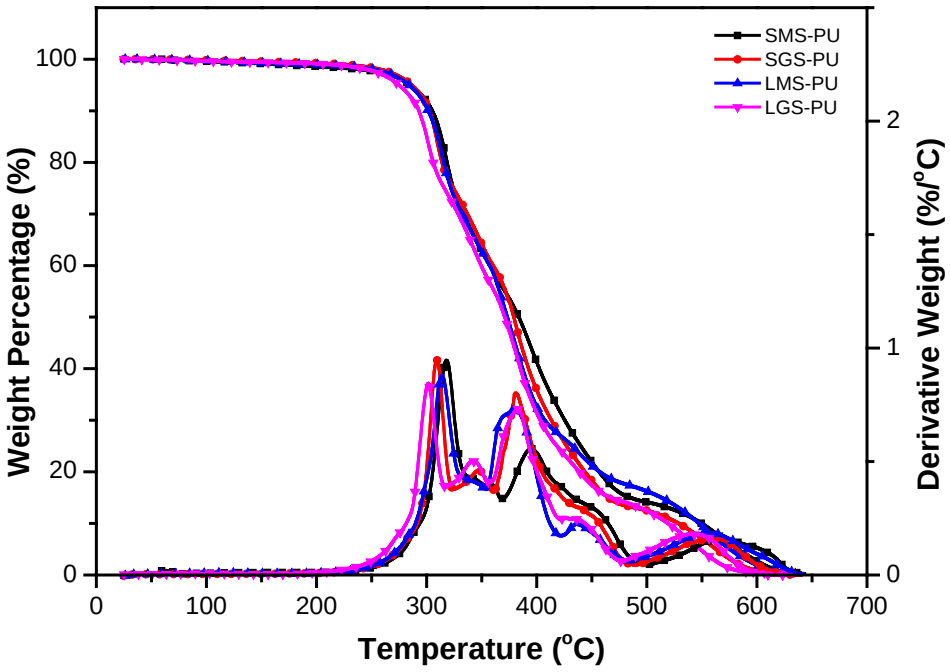

Figure 2-12 TGA curves and their derivative curves for PU films

Table 2-3 Physical and thermal properties of the polyurethanes

	Hard segment content (%)	Gel Content (%)	T_g (^oC) DSC	T_g (^oC) DMA	ν_e (mol/m^3)	T_{10} (^oC)	T_{50} (^oC)
SMS-PU	22.9	88.2	19.0	39.3	37.4	305.2	383.5
SGS-PU	25.5	89.3	36.4	49.9	103.4	302.5	379.1
LMS-PU	27.6	94.2	46.9	63.4	305.7	301.3	376.6
LGS-PU	29.9	95.3	56.3	80.5	911.9	298.9	370.9

Tensile properties of all PUs were measured and the stress-strain curves are plotted in Figure 10. Young's moduli, tensile strength at break, elongation at break and toughness are summarized in Table 2-4. In general, tensile strength and Young's modulus increased, while elongation decreased with increasing crosslinking density. The PU films with higher crosslinking densities had incorporated higher contents of hard segment IPDI, which contributed to their stiffness. At the same time, ductility dropped from 210.4% to 19.1% with increasing crosslinking density. The deformation profiles of the samples differed. For example, SMS-PU and SGS-PU deformed elastically before reaching their yielding point; then they exhibited strain hardening and finally broke at maximum strain. LMS-PU and LGS-PU exhibited strain softening in the plastic deformation domain, which occurred after yielding. Toughness was calculated by integrating the area below the stress-strain curve. SGS-PU exhibited the highest toughness (13.5 MPa), while LGS-PU, which had the highest tensile strength, was the least tough material among the examined PU films. Generally, brittle materials exhibit low toughness, while ductile materials are tough [10].

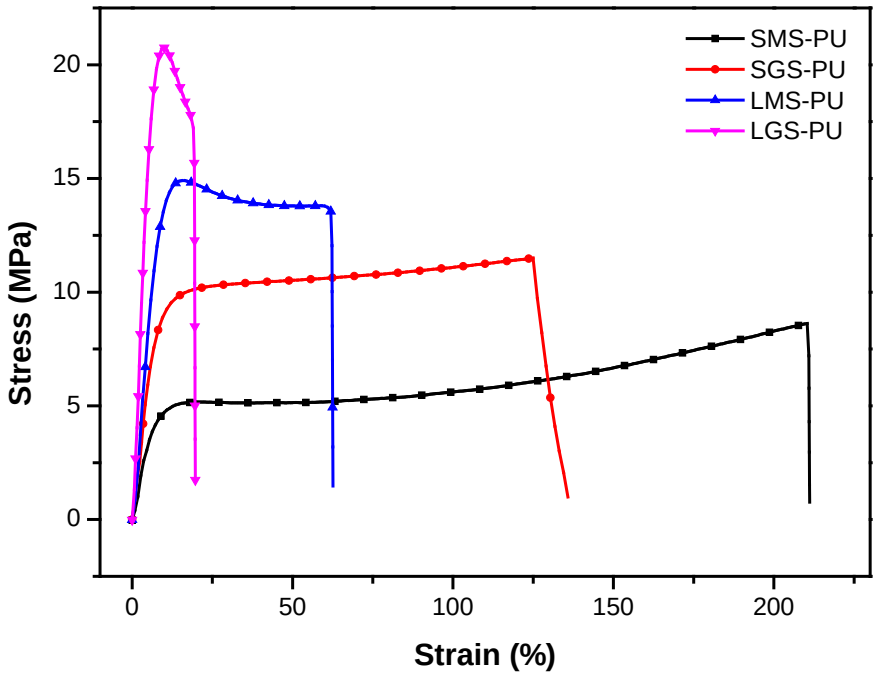

Figure 2-13 Stress-strain curves for PU films

Table 2-4 Mechanical properties of the polyurethanes

	E (MPa)	σ_b (MPa)	ε_b (%)	Toughness (MPa)
SMS-PU	67.2	8.6	210.4	12.7
SGS-PU	123.4	11.5	124.9	13.5
LMS-PU	166.6	13.5	61.9	8.2
LGS-PU	315.0	17.2	19.1	3.2

2.5 Conclusion

A series of fatty acids obtained from ESBO/ELO ring-opened by methanol/glycol were used to produce polyols using a solvent-free method. The fatty acids were reacted with ESBO at a ratio of carboxylic acid to epoxy groups of 0.5:1. The resulting polyols exhibited increasing OH numbers with increasing OH numbers of the fatty acids. PU films prepared from these polyols exhibited significant differences in thermal and mechanical properties. With increasing OH number, crosslinking density was significantly increased, resulting in PU networks with fewer free-motion available to the chains. This allowed for the tailoring of the properties of the resulting PUs, ranging from rigid and brittle to soft and ductile. The choice of epoxidized vegetable oil as starting material clearly determined the OH number of the resulting polyols because of the different functionalities of the respective epoxy groups. Being able to use the OH number of the polyol to influence the properties of PUs provides a pathway for the design of materials with desired thermo-mechanical properties.

2.6 References

1. Shen L, Haufe J, Patel MK: **Product Overview and Market Projection of Emerging Bio-based Plastic**s. Biofuels, Bioproducts and Biorefining, 2010, 4(1), 25-40.

2. Xia Y, Larock RC: **Vegetable oil-based polymeric materials: synthesis, properties, and applications**. *Green Chem* 2010, **12**(11):1893-1909.

3. Wang CS, Yang LT, Ni BL, Shi G: **Polyurethane Networks from Different Soy-Based Polyols by the Ring Opening of Epoxidized Soybean Oil with Methanol, Glycol, and 1,2-Propanediol**. *J Appl Polym Sci* 2009, **114**(1):125-131.

4. Dai HH, Yang LT, Lin B, Wang CS, Shi G: **Synthesis and Characterization of the Different Soy-Based Polyols by Ring Opening of Epoxidized Soybean Oil with Methanol, 1,2-Ethanediol and 1,2-Propanediol**. *J Am Oil Chem Soc* 2009, **86**(3):261-267.

5. Yang LT, Zhao CS, Dai CL, Fu LY, Lin SQ: **Thermal and Mechanical Properties of Polyurethane Rigid Foam Based on Epoxidized Soybean Oil**. *J Polym Environ* 2012, **20**(1):230-236.

6. Biswas A, Adhvaryu A, Gordon SH, Erhan SZ, Willett JL: **Synthesis of diethylamine-functionalized soybean oil**. *J Agr Food Chem* 2005, **53**(24):9485-9490.

7. Zhang CQ, Xia Y, Chen RQ, Huh S, Johnston PA, Kessler MR: **Soy-castor oil based polyols prepared using a solvent-free and catalyst-free method and polyurethanes therefrom**. *Green Chem* 2013, **15**(6):1477-1484.

8. Guo A, Cho YJ, Petrovic ZS: **Structure and properties of halogenated and nonhalogenated soy-based polyols *multiple melting for polyols**. *J Polym Sci Pol Chem* 2000, **38**(21):3900-3910.

9. Miao SD, Zhang SP, Su ZG, Wang P: **Synthesis of bio-based polyurethanes from epoxidized soybean oil and isopropanolamine**. *J Appl Polym Sci* 2013, **127**(3):1929-1936.

10. Xia Y, Larock RC: **Castor-Oil-Based Waterborne Polyurethane Dispersions Cured with an Aziridine-Based Crosslinker**. *Macromol Mater Eng* 2011, **296**(8):703-709.

11. Lu YS, Larock RC: **Soybean-Oil-Based Waterborne Polyurethane Dispersions: Effects of Polyol Functionality and Hard Segment Content on Properties**. *Biomacromolecules* 2008, **9**(11):3332-3340.

12. Marechal Y: **Ir-Spectra of Carboxylic-Acids in the Gas-Phase - a Quantitative Reinvestigation**. *J Chem Phys* 1987, **87**(11):6344-6353.

13. Adhvaryu A, Erhan SZ: **Epoxidized soybean oil as a potential source of high-temperature lubricants**. *Ind Crop Prod* 2002, **15**(3):247-254.

14. Zlatanic A, Petrovic ZS, Dusek K: **Structure and properties of triolein-based polyurethane networks**. *Biomacromolecules* 2002, **3**(5):1048-1056.

15. Andjelkovic DD, Valverde M, Henna P, Li FK, Larock RC: **Novel thermosets prepared by cationic copolymerization of various vegetable oils - synthesis and their structure-property relationships**. *Polymer* 2005, **46**(23):9674-9685.

16. Lu YS, Larock RC: **New hybrid latexes from a soybean oil-based waterborne polyurethane and acrylics via emulsion polymerization**. *Biomacromolecules* 2007, **8**(10):3108-3114.

17. Fox TG, Loshaek S: **Influence of Molecular Weight and Degree of Crosslinking on the Specific Volume and Glass Temperature of Polymers**. *J Polym Sci* 1955, **15**(80):371-390.

18. La Scala J, Wool RP: **Property analysis of triglyceride-based thermosets**. *Polymer* 2005, **46**(1):61-69.

19. Lai JZ, Ling HJ, Chen GN, Yeh JT, Chen KN: **Polymer hybrids from self-emulsified PU anionomer and water-reducible acrylate copolymer via a postcuring reaction**. *J Appl Polym Sci* 2003, **90**(13):3578-3587.

CHAPTER 3: ANIONIC WATERBORNE POLYURETHANE DISPERSION FROM BIO-BASED IONIC SEGMENT

A paper submitted to *Green Chemistry*

3.1 Abstract

In preparation of anionic waterborne polyurethane dispersion, bio-based polyhydroxy fatty acid (FA) was prepared by ring-opening epoxidized linseed oil with glycol and HCl followed by saponification and subsequently used as an ionic segment to replace 2,2-bis(hydroxymethyl)propionic acid (DMPA). With an OH functionality of 4.8, FA can crosslink, and its carboxylic group is able to provide surface charge for the stabilization of the resulting polymer in the water phase. Two novel anionic waterborne polyurethane dispersions, CasFAD (castor oil, FA, IPDI) and FAD (FA, IPDI), were successfully prepared and compared to a conventional control sample of CasPAD (castor oil, DMPA, IPDI). CasPAD, CasFAD, and FAD exhibited particle sizes of 29.92 nm, 35.15 nm, and 56.11 nm, respectively. PUD films were obtained by casting the dispersions into molds and subsequently characterized by differential scanning calorimetry (DSC), dynamic mechanical analysis (DMA), ethanol absorption and uptake, thermogravimetric analysis (TGA), and tensile stress-strain tests. CasFAD displayed a decrease in glass transition temperature (T_g), tensile strength, and Young's modulus, but an increase in elongation compared to CasPAD caused by its lower hard segment content. FAD behaved like a brittle, glassy material with higher Young's modulus and lower

ductility than CasFAD because of its relatively higher crosslinking density. This work proves the viability of incorporating vegetable-oil based polyhydroxy fatty acids as ionic segments into anionic waterborne polyurethane dispersions.

3.2 Introduction

Over the past decades, polyurethanes (PUs) have been employed in various applications, such as coatings, adhesives, sealants, foams, elastomers, and others [1]. Environmental concerns regarding conventional, solvent-based PUs have led to the development of waterborne, anionic and cationic polyurethane dispersions (PUDs) because of their environmentally-friendly nature and low content of volatile organic chemicals (VOCs) and hazardous air pollutants (HAPs) [2]. The basic chemical components of waterborne PUDs are commonly known building blocks, including polyols, isocyanates, catalysts, additives, and others [3]. A general awareness of the finite crude oil reserves has triggered extensive studies focused on using bio-based resources for the manufacture of polyols rather than petroleum-based materials. Vegetable oil is one of the most promising options because of its ready availability, relatively low cost, environmental sustainability, and low eco-toxicity. This work has led to the successful development of anionic PUDs from methoxylated soybean oil polyols [4]. Castor oil, which contains approx. 2.4 hydroxyl groups per molecule, is one of the vegetable oils suitable to produce polyols for PUD preparation [5].

The distinct feature of waterborne PUDs is the presence of external or internal emulsifiers that provide stability to the hydrophobic polyurethane dispersed in the water phase. Internal emulsifiers, which are incorporated into the polymer network structure,

are favored because the particle sizes in the resulting PUDs are smaller, leading to better stability. For anionic PUDs, dimethylol propionic acid (DMPA) is typically used as an internal emulsifier. DMPA serves as a chain extender in reaction with isocyanates, and its carboxylic acid group in ionic form provides surface charge to PU particles, stabilizing PUDs in the water phase [5]. However, DMPA is not derived from bio-renewable resources so that the bio-content of the waterborne PUD system is limited.

Vegetable oils are potential starting materials to replace DMPA because they are triglycerides constituted of glycerol and three fatty acid chains, typically containing unsaturated carbon-carbon double bonds that are available for modifications. Hydroformylation [6, 7], epoxidation followed by ring-opening [8-10], ozonolysis [11] and other methods can be employed to convert the double bonds into hydroxyl groups, which react with isocyanates to form urethane bonds. In addition, vegetable oil-based polyols can be saponified into polyhydroxy fatty acids [12] which exhibit similar properties as DMPA as long as the average functionality of the hydroxyl is exceeds 2.

In this work, epoxidized linseed oil (ELO) was ring-opened by glycol and HCl, followed by saponification into polyhydroxy fatty acid (FA). Oligomerization during the glycol ring-opening step created FAs with a number average molecular weight of 1147 g/mol. The calculated average functionality of the hydroxyl group was 4.8 providing the FA with sufficient functionality to serve as a crosslinking agent. The presence of a carboxylic acid group also allowed the FA to be employed as an ionic segment. Two novel types of DMPA-free, waterborne PUDs were developed: CasFAD was obtained from castor oil, FA and isophorone diisocyanate (IPDI), while FAD was prepared from FA and IPDI. Both PUDs were stable and had particle sizes of 35.2 nm and 56.1 nm,

respectively. The thermal and mechanical properties of the resulting PUD films were characterized and compared to those of CasPAD, which was obtained from castor oil, DMPA and IPDI. Literature research indicates that this is the first report on the substitution of DMPA by an internal emulsifier/ionic segment based on bio-renewable resources [13-19]. This work proves the feasibility of using vegetable oil-based polyhydroxy fatty acids to create stable, anionic waterborne PUDs.

3.3 Experimental

3.3.1 Materials

Epoxidized linseed oil (ELO) (approximately 5.5 oxirane rings per triglyceride) was kindly provided by American Chemical Service Inc., Griffith, IN. Magnesium sulfate ($MgSO_4$), potassium hydroxide (KOH), ethylene glycol, hydrochloric acid (HCl), and methyl ethyl ketone (MEK) were purchased from Fisher Scientific Company (Fair Lawn, NJ). Tetrafluoroboric acid solution (48% in H_2O), 2,2-bis(hydroxymethyl)propionic acid (DMPA), isophorone diisocyanate (IPDI), dibutyltin dilaurate (DBTDL), sodium bicarbonate ($NaHCO_3$), triethyleneamine (TEA), and castor oil were obtained from Sigma-Aldrich (Milwaukee, WI). Ethanol was purchased from Decon Laboratories Inc., King of Prussia, PA. All materials were used as received without further purification.

3.3.2 Preparation of highly branched fatty acid

The preparation of highly branched fatty acids followed three steps:

(1) Ring-opening of ELO with glycol

100 g of epoxidized linseed oil was mixed with 200 g of glycol in a 500 mL round-bottom flask (molar ratio of epoxy:OH was approximately 1:11). After the addition of 0.1 wt% HBF_4, the mixture was allowed to react at 98 °C for 2 h under constant stirring; the product was extracted using acetone, and then washed with saturated NaCl solution, and the organic layer was used in the next step.

(2) Ring-opening of unreacted epoxide ring with HCl

50 g of HCl was added to the acetone solution obtained in previous step and reacted at 40 °C for 1 h. Ethyl acetate was used to extract the polyol. Sodium bicarbonate and sodium chloride solution were used sequentially to wash the product until it was neutral. The organic layer was dried over $MgSO_4$ and the solvent was removed subsequently. The effectiveness of the additional ring-opening reaction by HCl was reflected in the increase in OH numbers from 221.9 mg KOH/g to 229.2 mg KOH/g.

(3) Saponification of the polyol

The polyol was dissolved in ethanol and potassium hydroxide was added to trigger saponification at 73 °C. The reaction proceeded for 4 h followed by the addition of HCl to neutralize the reactants until phase separation was observed. The fatty acid was extracted by ethyl acetate and washed three times with saturated NaCl solution. After drying over $MgSO_4$, polyhydroxy fatty acid (FA) with dark brown color was obtained after removal of organic solvent by roto-evaporation. OH number titration, acid number titration, and rheological and GPC tests were performed to characterize the physical properties of the obtained FA and the results are summarized in Table 1. The preparation route for FA is illustrated in Fig 3-1.

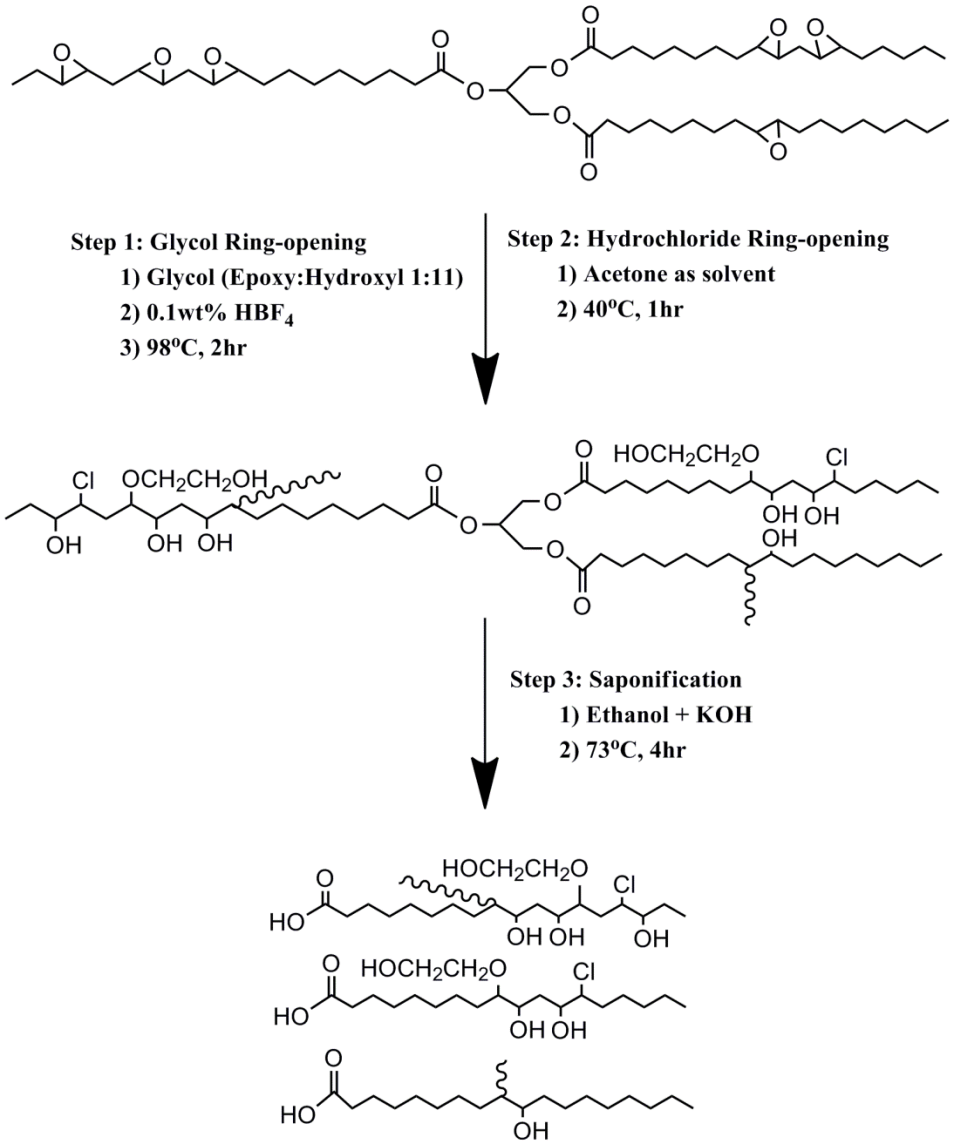

Figure 3-1 Preparation of FA

3.3.3 Preparation of anionic waterborne polyurethane dispersions (PUDs)

Unsuccessful approaches to prepare PUDs from FA may provide insight into the nature of the PUD synthesis. Xia [1] reported in his work that castor oil, DMPA, IPDI were first subjected to polymerization without solvent for 1 h. In our original approach, DMPA was replaced by FA to synthesize CasFAD. The complex composition and high reactivity of FA caused rapid gelation of the mixture within less than 30 s. In order to

solve the gelation problem, polymerization was initiated in solvent solution in order to effectively lower the reaction rate. However, the obtained PUD precipitated after removal of the organic solvent, which may have been caused by the significant difference in reactivity between castor oil and FA. Castor oil consists of triglycerides composed of roughly 85% ricinoleic acid with a secondary hydroxyl group at the C12 site, while FA contains primary hydroxyl groups derived from ELO ring-opened by glycol. The fact that the primary hydroxyl group exhibited relatively higher reactivity towards isocyanate than the secondary hydroxyl group resulted in a faster incorporation of FA into the crosslinked network [2]. Consequently, the core of the PUD particles was more likely composed of FA, while the shell was mainly made of castor oil. Because FA was the component bearing carboxylic acids, which are critical for the stabilization of the PUD particles in the water phase, insufficient FA content in the outer shell led to weak interactions of the PUD particles with the water molecules, creating an unstable waterborne PUD system. In addition, the fact that the simultaneous polymerization of castor oil, DMPA and IPDI resulted in stable dispersions is not in conflict with this explanation, because DMPA is insoluble in castor oil and IPDI. Therefore, DMPA went through a retarded heterogeneous polymerization, possibly resulting in the higher DMPA content in the outer shell of the PUD particles.

A modified synthesis route was therefore chosen and three different types of PUDs were synthesized and determined to be stable after no precipitate was detected within one week of sitting still.

1) Castor oil - fatty acid PUD (CasFAD)

Castor oil (5.05 g) and IPDI (3.12 g) were introduced into a two-neck flask equipped with a mechanical stirrer. The flask was placed in an oil bath set at 78 °C and the mixture was stirred for 5 min to ensure homogeneity. Then, 2 drops of DBTDL were added to trigger polymerization. After 1 h, FA (3.30 g) in 25 mL MEK was poured into the pre-polymer and allowed to polymerize for another 4 h. Once the reaction was terminated the reactants were cooled to room temperature and TEA (2 equiv. per mole of COOH from FA) was added under vigorous stirring for 30 min. Finally, 150 mL water was used for the phase reversal and the organic solvent was removed under reduced pressure. The molar ratio of OH of castor oil to OH of FA to NCO of IPDI was 1:1:2. The synthesis route of CasFAD is shown in Figure 3-2.

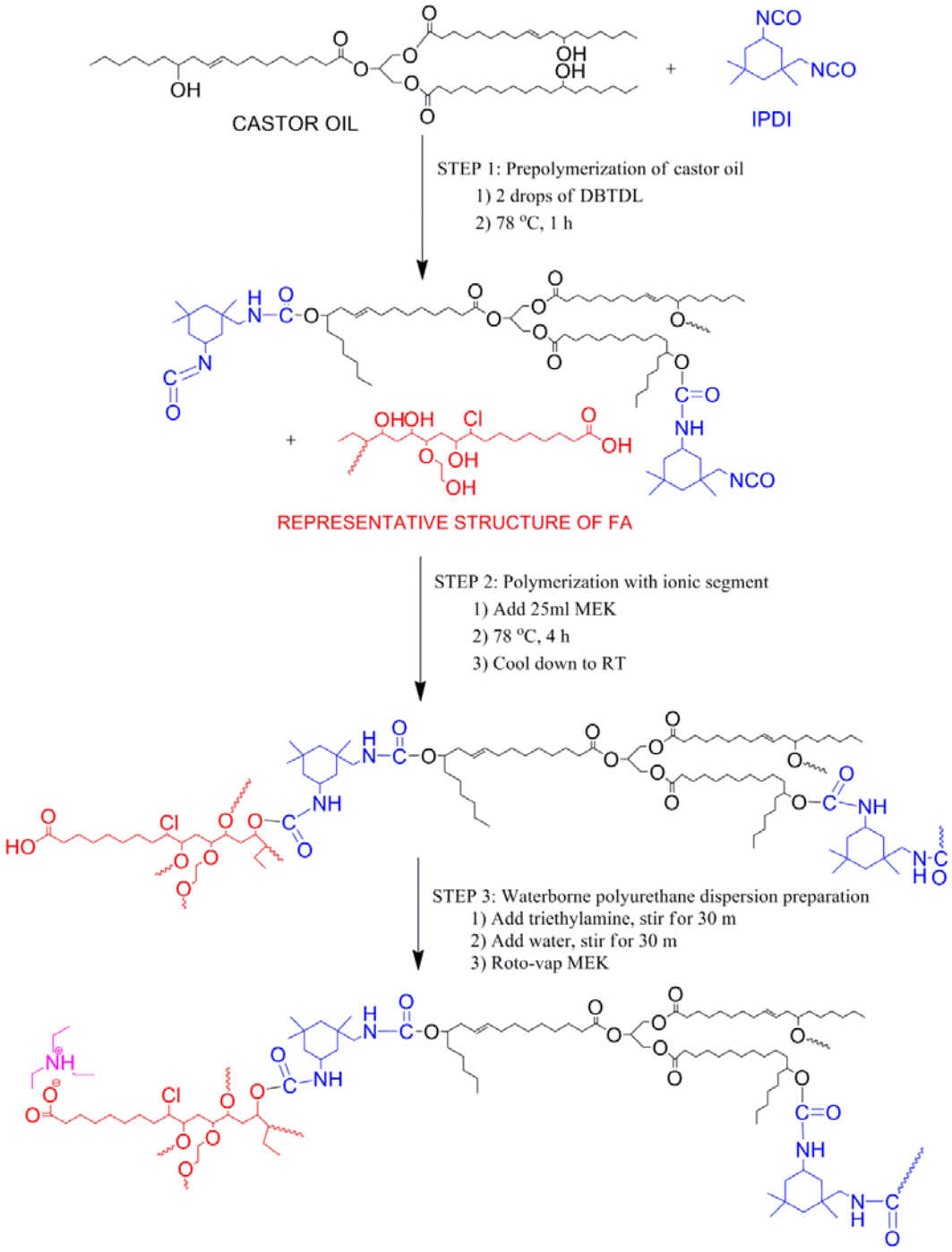

Figure 3-2 Preparation of CasFAD

2) Fatty acid PUD (FAD)

The preparation process started with the solution polymerization of FA (8.71 g), IPDI (4.05 g) and DBTDL in 25 mL MEK for 4 h. The mixture gelled rapidly without solvent, which was attributed to the high reactivity and complicated composition of the FA. The subsequent procedural steps were identical to those taken in the preparation of CasFAD.

3) Castor oil - DMPA PUD (CasPAD)

The preparation method was similar to the one used to prepare CasFAD; however, DMPA was used instead of FA. It is worth mentioning that DMPA is not soluble in MEK so that DMPA was added in its powder form along with MEK.

Figure 3-3 shows the visual appearance of the obtained PUDs. With the increasing FA content, which had a dark brown color, the resulting PUDs turned darker. Polyurethane films were obtained by casting the PUD into a Teflon mold and allowing it to dry out at ambient temperature. Heat-drying was performed in a conventional oven at 80 °C overnight. The obtained PU films were cut into desired dimensions for specific characterizations.

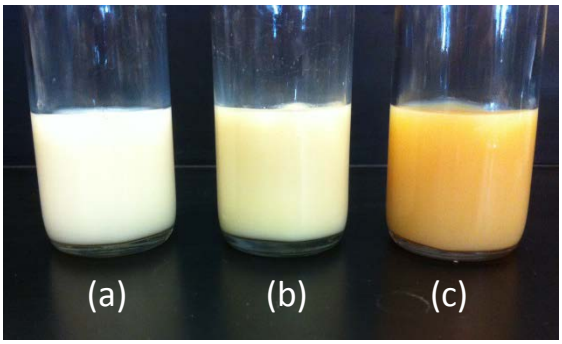

Figure 3-3 Visual appearance of (a) CasPAD, (b) CasFAD, and (c) FAD

3.3.4 Characterizations

^{1}H NMR spectra were recorded on a Varian spectrometer (Palo Alto, CA) at 300 MHz for FA and ELO in chloroform-*d*. A Bruker IFS66V FT-IR spectrometer was employed to record infrared spectra of FA and ELO. The scanning resolution was 4 cm^{-1} and the scanning range covered 4000 cm^{-1} to 400 cm^{-1}. The hydroxyl and acid numbers of the fatty acids and polyols were determined using Unilever method and AOCS Official Method Te 1a-64, respectively. The average molecular weight was measured by a Thermo Scientific Dionex Ultimate 3000 GPC (Sunnyvale, CA) equipped with a Shodex Refractive Index (RI). The eluent solvent used was tetrahydrofuran with two Agilent PLgel 3 μm 100 Å 300 × 7.5 mm (p/n PL1110-6320) and one Mesopore 300 × 7.5 mm (p/n PL1113-6325). The flow rate of THF was 1.0 mL/min and the measurement was conducted at room temperature. The rheological test was performed at 40 °C using an AR2000 (TA Instrument). The rheological behavior of FA was investigated by varying the shear rate from 10 s^{-1} to 1000 s^{-1}. A JEOL scanning and transmission electron microscope (Japan Electron Optic Laboratories, Peabody, MA) was used to observe the morphology of the PUD particles. Diluted PUD (2 μl with approx. 0.1 wt% solid content) was placed on 200-mesh carbon film grid. After drying, the grid was exposed to RuO_4 for 10 min before observation. The size distribution of the PUDs was determined by NanoZS90 Zeta-sizer (Worcestershire, UK) at room temperature.

Dynamic mechanical analysis (DMA) of the polyurethane films was carried out on a TA Instruments DMA Q800 dynamic mechanical analyzer using a film-tension mode of 1 Hz. Rectangular samples with a length of 15 mm and a width of 10 mm were used for the analysis. The samples were cooled and held isothermally for 3 min at –60 °C

before raising temperature to 100 °C at a rate of 3 °C/min. The glass transition temperatures (T_gs) of the samples were determined by the peaks of the loss modulus curve.

Thermogravimetric analysis (TGA) of the films was conducted on a TA Instrument Q50 (New Castle, DE). The samples were heated from room temperature to 650 °C at a rate of 20 °C min^{-1} in air with a flow rate of 60 mL/min. The remaining weight was recorded as a function of temperature and plotted.

Differential scanning calorimetry (DSC) was performed on a TA Instrument Q20. The samples were weighed and placed in Tzero Hermetic pans and subsequently heated to 80 °C to eliminate their heat history. The samples were then cooled to -80 °C by manually adding liquid nitrogen to the chamber and re-heated to 80 °C at a programmed rate of 10 °C/min. The second heating ramp was recorded and glass transition temperature was determined by the midpoint inflection method.

The tensile properties of the PU films were determined with an Instron universal testing machine (model 4502) with a crosshead speed of 100 mm/min. Rectangular samples with the dimensions 50 mm ×10 mm (length × width) were prepared. At least three replicates were tested for each PU sample. The stress-strain curve was plotted and toughness, representing the ability of a material to absorb energy before fracture, was calculated as the integrated area beneath the curve.

3.4 Results and discussion

3.4.1 Preparation and properties of FA

The preparation of FA started with the ring-opening of ELO by glycol and HCl, followed by saponification into fatty acid chains. Glycol, which is an effective ring-opening agent [20], inevitably causes oligomerization among oil molecules [2]. Consequently, multiple oil molecules can be coupled via ether linkages so that the obtained fatty acids exhibit higher than predicted molecular weights. The GPC data collected (Table 3-1) confirmed that the number average molecular weight reached 1147 g/mole, which indicated that on average approximately three fatty acid chains were coupled. Noticeably, FA's polymeric dispersion index (PDI) of 1.8 indicated a broad molecular weight distribution, also indicative of oligomerization. The functionality of OH was estimated by:

$$f_n = \frac{\text{OH } number \times \overline{M_n}}{1000 \times M_{KOH}}$$

FA exhibited an average functionality of 4.8, ensuring the formation of a crosslinking structure in PU. In addition, its high acid number of 139.3 mg KOH/g was a key factor in this work, because the carboxylic group was neutralized into an ionic form, stabilizing the dispersion in the water phase. The presence of hydroxyl groups and carboxylic groups ensured high intermolecular hydrogen bonding, so that the prepared FAs exhibited a viscosity as high as 4.6 Pa·s at 40 °C.

Table. 3-1 Summary of FA properties

OH number (mg KOH/g)	f_n	Acid number (mg KOH/g)	Viscosity (Pa·s) at 40 °C	M_n	M_w	PDI
235.1	4.8	139.3	4.6	1147	2068	1.8

Figure 3-4 shows FTIR spectra of FA and ELO. For FA, a new broad trough between 3600 cm^{-1} to 2500 cm^{-1} emerged, which was attributed to the overlapped signal from –OH stretching of the hydroxyl and carboxylic groups, confirming the presence of the desired functional groups [21]. The peak at 823 cm^{-1}, assigned to the epoxy group, disappeared for FA because of the ring-opening reactions [22]. These two changes in the FTIR spectra confirmed the completion of oxirane ring reduction and saponification.

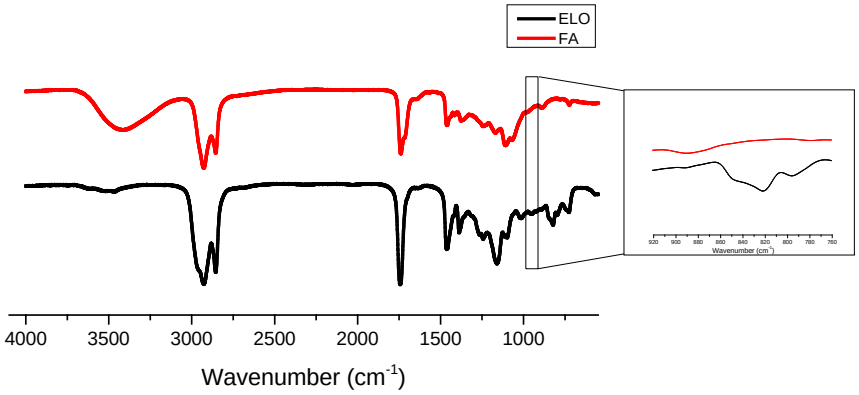

Figure 3-4 FTIR spectra of ELO and FA from ELO

^{1}H-NMR spectra of FA and ELO are shown in Figure 3-5. Signal 1 (5.25 ppm) and signal 2 (4.0 ppm–4.4 ppm), which are attributed to the backbone glyceride structure, were not prominent for FA [23]. This confirmed the cleavage of the triglyceride structure

into fatty acid chains during the saponification step. Signal 3 (2.8 ppm–3.2 ppm) for ELO was attributed to epoxy groups, and e1 (2.9 ppm) in particular was attributed to the epoxy group anchored to the fatty acid arm with only one derivative group [9]. The presence of e1 in FA indicated that a trace amount of the epoxy groups was not reduced. In addition, signal 4 (3.2 ppm–4.0 ppm) was mainly created by multiple forms of ether linkages in FA, indicating the complex nature of the ring-opened product. Also, signal 5 (2.3 ppm), assigned to the methylene group adjacent to the carboxyl group $–CH_2–COO–$, did not significantly shift when ELO was converted to FA [24].

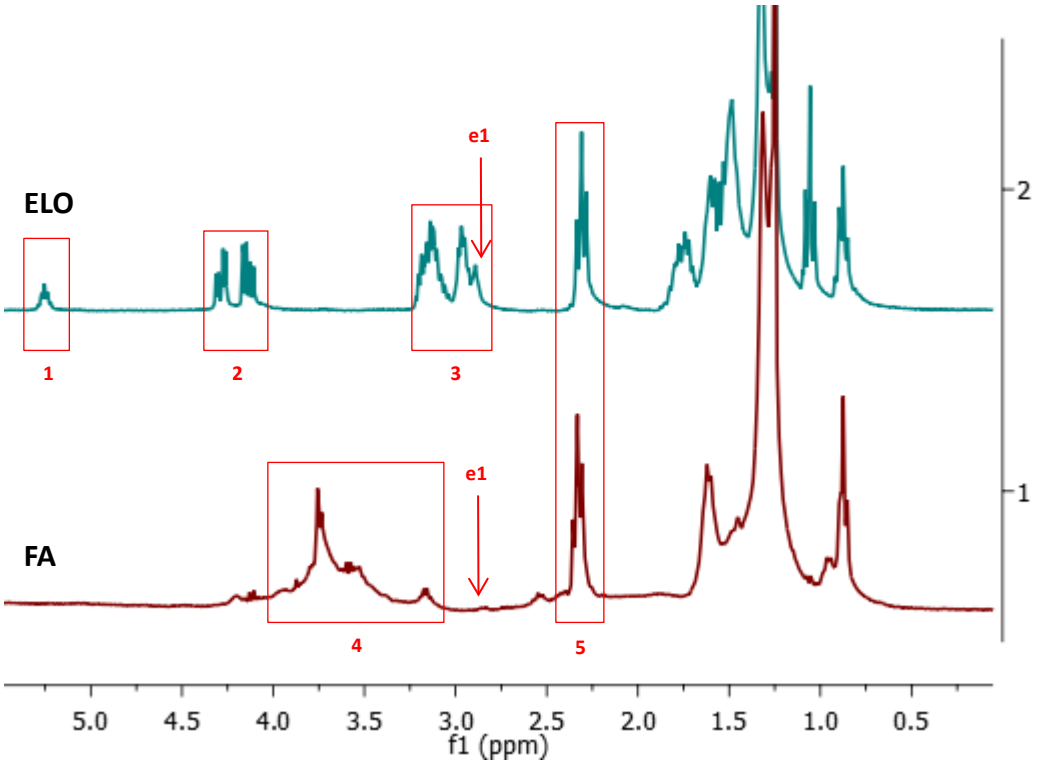

Figure 3-5 FTIR spectra of FA and ELO

3.4.2 Preparation and properties of PUDs

The TEM images of the different PUDs are shown in Figure 3-6, while their size distributions are presented in Figure 3-7. Statistical data regarding average particle

diameters and polydispersity indeces (PDI) were determined using Dispersion Technology Software (Malvern Instruments Ltd.) and are summarized in Table 3-2. CasPAD and CasFAD exhibited average particle sizes of 30.0 nm and 35.2 nm, respectively. The significant difference was attributed to the fact that the ionic segment FA (M_n = 1147 g/mol) was substantially larger than DMPA (M_n = 134 g/mol), based on their molecular weights. However, both exhibited similar PDIs, as both PUD systems started with a pre-polymerization reaction between castor oil (PDI = 1.02) and excess IPDI, which yielded uniform core seeds. Compared to CasFAD, FAD exhibited larger average particle sizes (56.1 nm) and a higher PDI (0.274), resulting from the difference in synthesis route. The preparation of CasFAD started from a castor oil/IPDI pre-polymer with uniform structure, while FAD preparation directly started with a solution polymerization reaction between IPDI and FA with its complicated composition. The particle sizes of the obtained PUDs may also have been affected by other factors such as hydrophilicity, pre-polymer viscosity, ionic group position, and others [4, 25, 26]. However, the PUD particle size had no direct impact on the physical properties of the resulting PU films [4].

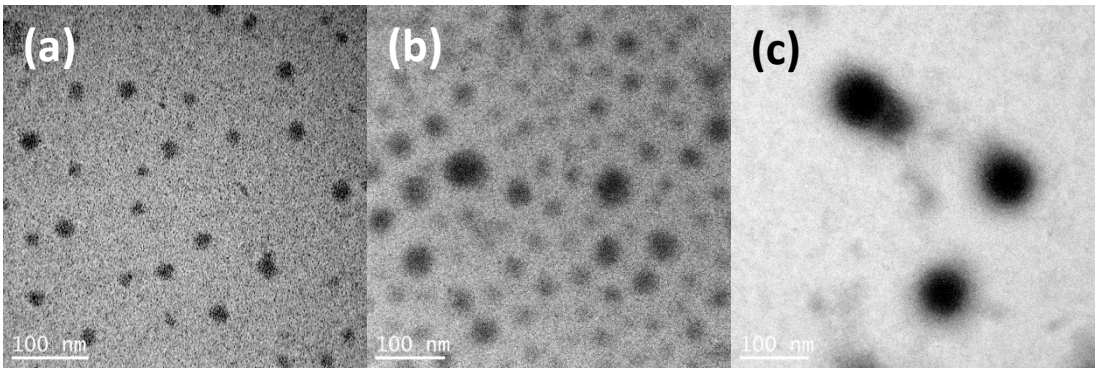

Figure 3-6 TEM images of PUD particles of (a) CasPAD, (b) CasFAD and (c) FAD

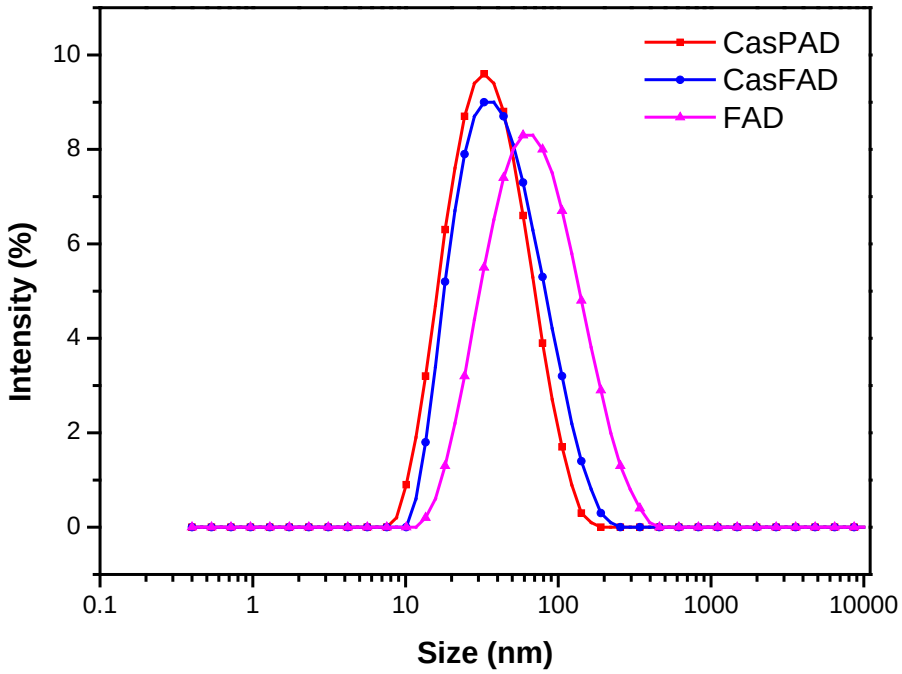

Figure 3-7 Particle size distribution for PUDs

Table 3-2 Size distribution of PUDs

PUD	Z-Average Size (nm)	PDI
CasPAD	30.0	0.232
CasFAD	35.2	0.221
FAD	56.1	0.274

3.4.3 Polyurethane films properties

Differential scanning calorimetry (DSC) thermograms of the obtained PUD films are shown in Figure 3-8. Each PUD exhibited only one T_g and no melting or crystallizing peak, indicating that all PUs had homogenous, amorphous structure. CasPAD had a T_g of 12.9 °C, which matched reported data [5]. When DMPA was replaced by FA, the hard segment content dropped from 52.1% to 36.4%. As a result, the chain mobility was less

restricted in CasFAD so that it exhibited a lower T_g of 5.9 °C. On the other hand, FAD had a significantly higher T_g (17.6 °C) than CasFAD. Although castor oil and FA have the same number of hydroxyl groups, the OH number of CasFAD was estimated to be 187.9 mg KOH/g, while the OH number of the FAD system was 235.1 mg KOH/g. The substantial difference in OH number led to different crosslinking densities, which directly influenced the respective T_gs [4]. In addition, the hard segment content of FAD was higher than that of CasFAD, which also influenced the T_g [27].

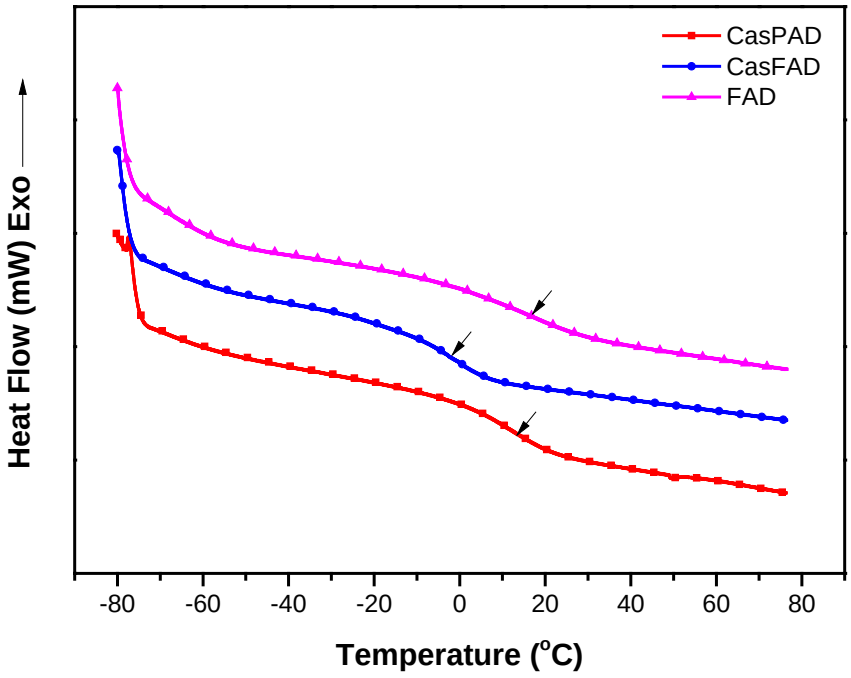

Figure 3-8 DSC scans of PUD films

Figure 3-9 depicts the temperature dependence of the storage modulus (E') and the loss factor (tan δ) of the PUD films. The storage moduli of all films were similar at temperatures below 0 °C. After a dramatic drop in the value of E', the materials entered into a rubbery stage from the glassy stage. A rubbery plateau was observed for CasPAD

and CasFAD, while FAD yielded at elevated temperatures. The glass transition temperatures (obtained from the maximum of the tan δ curve) and *E'* at room temperature are summarized in Table 3-3. The difference between T_gs obtained from DSC and DMA are caused by the different nature of the two measurements. DSC measures the heat capacity change from frozen to unfrozen chains, while DMA measures the change in mechanical response of polymer chains to heating [28]. All PUD films exhibited only one tan δ peak, indicating the homogeneous nature of the PUs. The hard segment content of CasFAD was substantially lower than that of CasPAD (36.4 % compared to 52.1 %). The higher hard segment content contributed to the stiffness of the network structure, directly influencing both storage modulus and T_g [29]. Comparing CasFAD and FAD, the OH number of the starting monomers directly influenced glass transition temperature and storage modulus. Higher OH numbers led to higher crosslinking densities so that less dangling chains acted as plasticizers in the network structure.

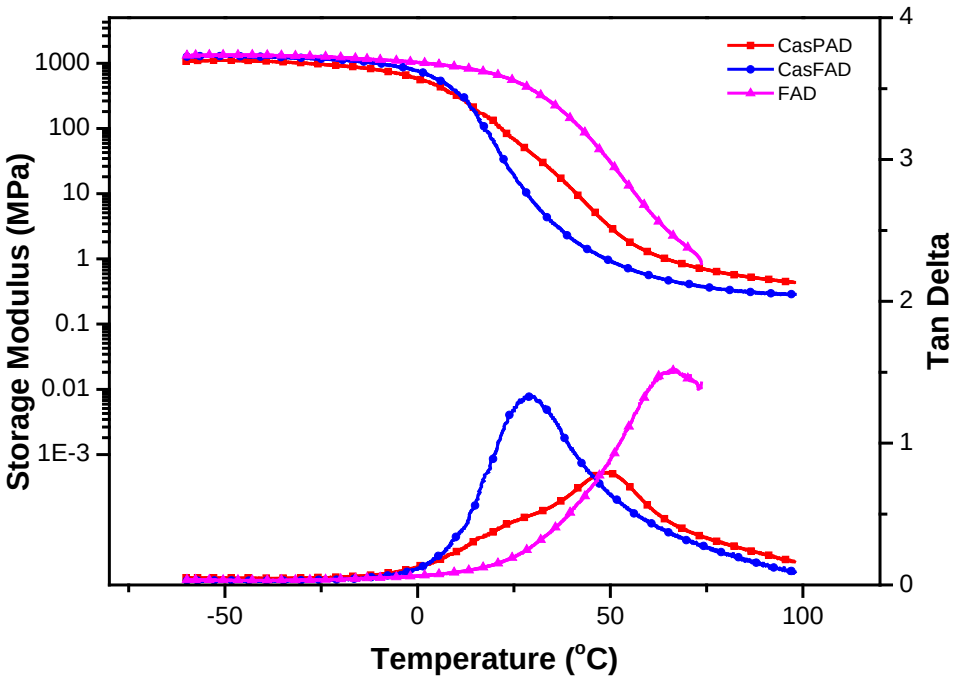

Figure 3-9 Storage modulus and loss factor of PU films as functions of temperature

The thermal degradation profiles for the obtained PUDs are plotted in Figure 3-10. In general, PUs exhibit three stages of thermal decomposition in air atmosphere [30]. The first weight loss domain was observed between 200 and 300 °C and assigned to the dissociation of the labile urethane bonds [31]. The dissociation of urethanes to isocyanates and alcohols, the formation of primary amines and olefins, and the formation of secondary amines were reported as three possible mechanisms by Wang *et al*. [20]. The weight percentage of IPDI in CasPAD and CasFAD, which determined the amount of urethane bonds, differed remarkably: CasPAD contained 27.3% IPDI, while CasFAD contained 23.7% IPDI. Consequently, CasFAD exhibited lower weight loss at 300 °C than CasPAD, and FAD underwent greater weight loss during the urethane bond decomposition stage than CasFAD. The second thermal degradation stage between 300

°C and 450 °C resulted from chain scission of the oil structure. The last stage, above 450 °C, was attributed to further thermo-oxidation of the PUs in air. The temperatures of 10% and 50% weight loss (T_{10} and T_{50}) are summarized in Table 3-3. CasFAD exhibited better thermal resistance than CasPAD because of its lower content of labile urethane bonds[30]. FAD showed better thermal resistance after urethane bond dissociation than CasFAD, attributed to higher crosslinking densities caused by higher OH numbers of the polyol component [5].

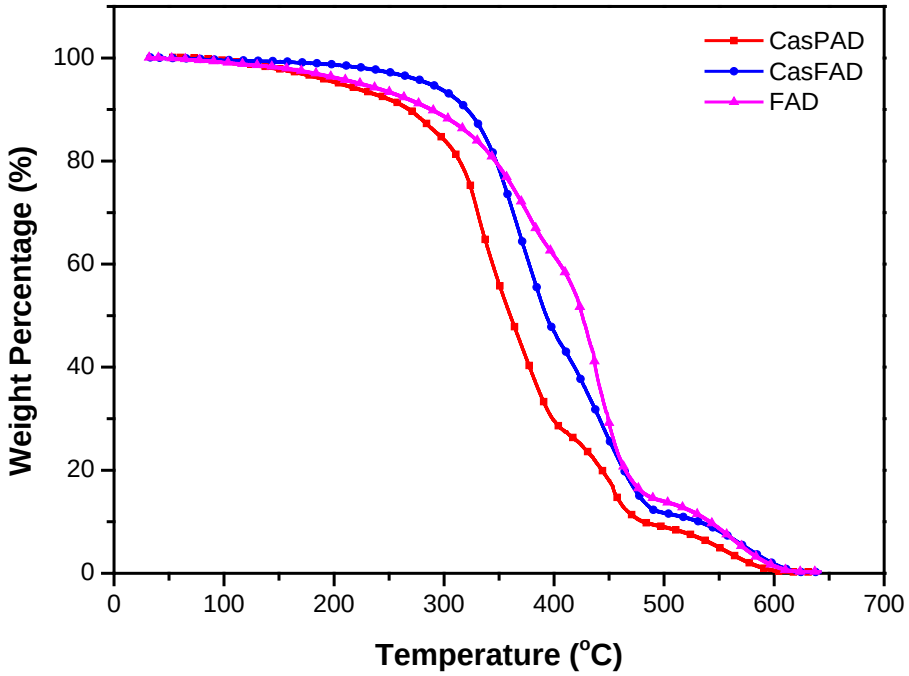

Figure 3-10 TGA curves of PU films

Table 3-3 Physical and thermal properties of the polyurethanes

	Hard segment content (wt %)	T_g (°C) DSC	T_g (°C) DMA	E' at room temperature (MPa)	T_{10} (°C)	T_{50} (°C)
CasPAD	52.1	12.9	49.1	68.3	305.2	383.5
CasFAD	36.4	5.9	29.4	19.0	302.5	379.1
FAD	49.3	17.6	65.7	539.3	301.32	376.6

Figure 3-11 shows tensile stress-strain curves for all PUD films. Young's moduli, tensile strength at break, elongation at break, and toughness are summarized in Table 3-4. CasFAD exhibited lower tensile strength, lower Young's modulus, but higher ductility than CasPAD, which met expectation because of the lower hard segment content in CasFAD. CasFAD and CasPAD did not differ significantly in toughness (14.31 MPa and 11.76 MPa, respectively), while the toughness of FAD was substantially lower. Because FAD had a relatively higher content of carboxylic acid, the mechanical properties may have been compromised [32]. In general, brittle materials exhibit low toughness, while ductile materials are tough [5].

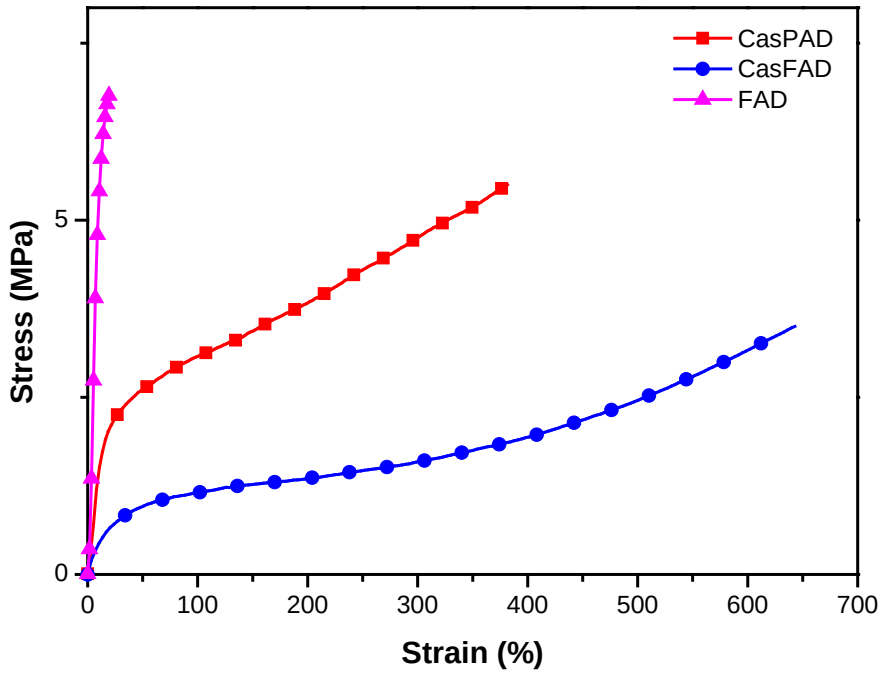

Figure 3-11 Stress-strain curves for PU films

Table 3-4 Mechanical properties of the polyols

	E (MPa)	σ_b (MPa)	ε_b (%)	Toughness (MPa)
CasPAD	13.6	5.5	381.7	14.31
CasFAD	2.3	3.5	642.9	11.76
FAD	77.4	6.8	19.3	0.83

3.5 Conclusion

In this work, ELO was ring-opened by glycol and HCl, followed by saponification to yield polyhydroxy fatty acid (FA). FA was successfully utilized to replace DMPA in castor oil-based anionic polyurethane dispersion system. The obtained CasFAD had an average particle size diameter of 35.2 nm, while the control sample CasPAD had an average particle size of 30.0 nm. It was shown that FA can serve as both polyol component and as ionic segment in the preparation of PUDs. The resulting FAD had an average particle size of 56.1 nm. CasFAD exhibited lower tensile strength and Young's modulus than CasPAD because of its lower hard segment content. Nonetheless, CasFAD and CasPAD were comparable in terms of toughness. The mechanical properties of FAD were compared with those of CasFAD. FAD was relatively brittle and less tough because of its high OH number and acid content. In general, vegetable oil-based polyhydroxy fatty acids were successfully incorporated into anionic PU systems as ionic segments.

3.6 Acknolwedgement

This work was sponsored by Kumho Petrochemical Co.

3.7 References

1. Shen L, Haufe J, Patel MK: **Product Overview and Market Projection of Emerging Bio-based Plastics**. 2009.

2. Xia Y, Larock RC: **Vegetable oil-based polymeric materials: synthesis, properties, and applications**. *Green Chem* 2010, **12**(11):1893-1909.

3. Noble KL: **Waterborne polyurethanes**. *Prog Org Coat* 1997, **32**(1-4):131-136.

4. Lu YS, Larock RC: **Soybean-Oil-Based Waterborne Polyurethane Dispersions: Effects of Polyol Functionality and Hard Segment Content on Properties**. *Biomacromolecules* 2008, **9**(11):3332-3340.

5. Xia Y, Larock RC: **Castor-Oil-Based Waterborne Polyurethane Dispersions Cured with an Aziridine-Based Crosslinker**. *Macromol Mater Eng* 2011, **296**(8):703-709.

6. Guo A, Demydov D, Zhang W, Petrovic ZS: **Polyols and polyurethanes from hydroformylation of soybean oil**. *J Polym Environ* 2002, **10**(1-2):49-52.

7. Kandanarachchi P, Guo A, Petrovic Z: **The hydroformylation of vegetable oils and model compounds by ligand modified rhodium catalysis**. *J Mol Catal a-Chem* 2002, **184**(1-2):65-71.

8. Guo A, Cho YJ, Petrovic ZS: **Structure and properties of halogenated and nonhalogenated soy-based polyols *multiple melting for polyols**. *J Polym Sci Pol Chem* 2000, **38**(21):3900-3910.

9. Miao SD, Zhang SP, Su ZG, Wang P: **Synthesis of bio-based polyurethanes from epoxidized soybean oil and isopropanolamine**. *J Appl Polym Sci* 2013, **127**(3):1929-1936.

10. Nikje MMA: **Epoxidized Soybean Oil Ring Opening Reaction under MW irradiation**. 2011.

11. Petrovic ZS, Zhang W, Javni I: **Structure and properties of polyurethanes prepared from triglyceride polyols by ozonolysis**. *Biomacromolecules* 2005, **6**(2):713-719.

12. Zhang CQ, Xia Y, Chen RQ, Huh S, Johnston PA, Kessler MR: **Soy-castor oil based polyols prepared using a solvent-free and catalyst-free method and polyurethanes therefrom**. *Green Chem* 2013, **15**(6):1477-1484.

13. Ahn YU, Lee SK, Lee SK, Jeong HM, Kim BK: **High performance UV curable polyurethane dispersions by incorporating multifunctional extender**. *Prog Org Coat* 2007, **60**(1):17-23.

14. Bai CY, Zhang XY, Dai JB: **Synthesis and characterization of a new UV cross-linkable waterborne siloxane-polyurethane dispersion**. *J Macromol Sci A* 2007, **44**(10-12):1203-1208.

15. Chattopadhyay DK, Raju KVSN: **Structural engineering of polyurethane coatings for high performance applications**. *Prog Polym Sci* 2007, **32**(3):352-418.

16. Chen PC, Wang SC, Hwang JZ, Yeh JT, Huang CY, Chen KN: **A New Self-polymerization of Acrylic Acid with a Mono-aziridine Containing Compound**. *J Chin Chem Soc-Taip* 2010, **57**(4B):901-908.

17. Lu YS, Larock RC: **Synthesis and Properties of Grafted Latices from a Soybean Oil-Based Waterborne Polyurethane and Acrylics**. *J Appl Polym Sci* 2011, **119**(6):3305-3314.

18. Madbouly SA, Otaigbe JU, Nanda AK, Wicks DA: **Rheological behavior of POSS/polyurethane-urea nanocomposite films prepared by homogeneous solution polymerization in aqueous dispersions**. *Macromolecules* 2007, **40**(14):4982-4991.

19. Xia Y, Larock RC: **Soybean Oil-Isosorbide-Based Waterborne Polyurethane-Urea Dispersions**. *Chemsuschem* 2011, **4**(3):386-391.

20. Wang CS, Yang LT, Ni BL, Shi G: **Polyurethane Networks from Different Soy-Based Polyols by the Ring Opening of Epoxidized Soybean Oil with Methanol, Glycol, and 1,2-Propanediol**. *J Appl Polym Sci* 2009, **114**(1):125-131.

21. Marechal Y: **Ir-Spectra of Carboxylic-Acids in the Gas-Phase - a Quantitative Reinvestigation**. *J Chem Phys* 1987, **87**(11):6344-6353.

22. Adhvaryu A, Erhan SZ: **Epoxidized soybean oil as a potential source of high-temperature lubricants**. *Ind Crop Prod* 2002, **15**(3):247-254.

23. Biswas A, Adhvaryu A, Gordon SH, Erhan SZ, Willett JL: **Synthesis of diethylamine-functionalized soybean oil**. *J Agr Food Chem* 2005, **53**(24):9485-9490.

24. Sharmin E, Ashraf SM, Ahmad S: **Synthesis, characterization, antibacterial and corrosion protective properties of epoxies, epoxy-polyols and epoxy-polyurethane coatings from linseed and Pongamia glabra seed oils**. *Int J Biol Macromol* 2007, **40**(5):407-422.

25. Park SH, Chung ID, Hartwig A, Kim BK: **Hydrolytic stability and physical properties of waterborne polyurethane based on hydrolytically stable polyol**. *Colloid Surface A* 2007, **305**(1-3):126-131.

26. Jang JY, Jhon YK, Cheong IW, Kim JH: **Effect of process variables on molecular weight and mechanical properties of water-based polyurethane dispersion**. *Colloid Surface A* 2002, **196**(2-3):135-143.

27. Pechar TW, Wilkes GL, Zhou B, Luo N: **Characterization of soy-based polyurethane networks prepared with different diisocyanates and their blends with petroleum-based polyols**. *J Appl Polym Sci* 2007, **106**(4):2350-2362.

28. Lu YS, Larock RC: **New hybrid latexes from a soybean oil-based waterborne polyurethane and acrylics via emulsion polymerization**. *Biomacromolecules* 2007, **8**(10):3108-3114.

29. Zlatanic A, Petrovic ZS, Dusek K: **Structure and properties of triolein-based polyurethane networks**. *Biomacromolecules* 2002, **3**(5):1048-1056.

30. Wang KP, Yang LT: **New Waterborne Polyurethane Dispersions from the Soybean-Oil-Based Polyols by Ring Opening of ESO with Glycol**. *New and Advanced Materials, Pts 1 and 2* 2011, **197-198**:1196-1200.

31. Trovati G, Ap Sanches E, Neto SC, Mascarenhas YP, Chierice GO: **Characterization of Polyurethane Resins by FTIR, TGA, and XRD**. *J Appl Polym Sci* 2010, **115**(1):263-268.

32. Gindin L, Konitsney R, McLafferty J, Roesler R: **Polyurethane dispersion prepared from a high acid functional polyester**. *US Patent 20050288431 A1* 2005.

CHAPTER 4: RAPID ROOM-TEMPERATURE POLYMERIZATION OF BIO-BASED MULTIAZIRIDINE-CONTAINING COMPOUND

A paper to be submitted to *ChemSusChem*

4.1 Abstract

2-methyl aziridines were successfully grafted onto acrylated epoxidized soybean oils via Michael addition under mild reaction conditions. The content of aziridinyl groups was titrated as 0.00413 mol/g. The multiaziridine-containing compound (AESO-AZ) was then subject to rapid room-temperature polymerization with isosorbide-based diacid, succinic acid and citric acid, respectively. Stoichiometric ratio between AESO-AZ and polyacid was followed. The thermo-mechanical properties of the acquired film products were investigated. Differential scanning calorimetry (DSC), dynamic mechanical analysis (DMA), thermogravimetric analysis (TGA), and tensile stress-strain tests were performed. The collected glass transition temperatures (T_g) of the samples suggested the increased functionality of carboxylic acid groups of polyacids could effectively increase T_g. In addition, the presence of rigid ring structures in polymer network was also proved to increase T_g. This work illustrates the feasibility of synthesizing bio-based multiaziridine-containing compound, which has been directly used as the monomer in rapid polymerization with bio-based polyacids at ambient temperature.

4.2 Introduction

Aziridine (AZ), a three-membered heterocycle with one amine group (-NH-), was first synthesized in 1888 [1]. Aziridine has been known as a reactive compound in nucleophilic ring-opening reactions. A considerable amount of research has involved multi-functional aziridines for the purpose of post-curing polymer systems containing free carboxylic acid groups. Xia *et al.* [2] have employed a triaziridine-based crosslinker CX-100 to post-cure castor oil-based anionic PU dispersions due to the presence of carboxylic groups in the system. The crosslinking density of the polymer system has been increased, leading to higher glass transition temperature (T_g) and higher Young's modulus. Besides the application as post-curing agents, Mono-aziridine compound and tri-aziridine compound have been reported by Chen *et al.* [3] to polymerize with acrylic acid. However, no mechanical properties were reported in their research papers. To the best of our knowledge, there is no precedent work about directly utilizing bio-based multiaziridine-based compound as the monomer to yield structural polymeric materials.

Most of the multiaziridine-based compounds are derived from petroleum-based molecules via Michael addition, which is known as the reaction of nucleophiles attacking active unsaturated groups [4]. The amine bridge (-NH-) in aziridine and 2-methyl aziridine has been respectively used to react with acrylics [5, 6]. It is worth noting that the acrylics used as the substrates for aziridine addition are mostly tri-functional molecules which are not bio-renewable [1, 2, 6, 7]. For the purpose of developing greener products, acrylated epoxidized soybean oil (AESO), which is a derivative product of soybean oil, has been considered due to its multifunctionality of acrylics. AESO is a renown green material in a number of applications, such as coatings, adhesives, etc [8].

The presence of acrylic group in AESO enables the reaction with aziridine/2-methyl aziridine. In this work, we proposed the synthesis of bio-based aziridine-containing compound (AESO-AZ) by reacting acrylated epoxidized soybean oil with excess 2-methyl aziridine. The structure of the obtained product was confirmed by proton nuclear magnetic resonance (^{1}H NMR). Gel permeation chromatography (GPC) and rheometry tests have been performed to determine the fundamental properties of AESO-AZ. The aziridine content was 0.00413 mol/g and was used to calculate the stoichiometric quantity of the poly-acids involved in later polymerization step.

Succinic acid, citric acid and isosorbide-based di-acid [9] were chosen to react with AESO-AZ, respectively. This reaction was a catalyst-free process and the polymerization took place rapidly at ambient temperature. The effect of the functionality and the chemical structure of the polyacids was examined by conducting differential scanning calorimetry (DSC), dynamic mechanical analysis (DMA), thermogravimetric analysis (TGA), and tensile tests for the polymeric materials. Based on the fact that the polyacids used are bio-based and AESO-AZ is partially bio-based, the resulting polymeric products possess significantly high bio-content. The concept of this work conforms to the global awareness of the importance of bio-renewable materials. The fast polymerization rate could also trigger the interest of industry to develop the valuable applications of this novel polymerization system.

4.3 Experimental

4.3.1 Materials

Soybean oil epoxidized acrylate, containing 4000 ppm monomethyl ether hydroquinone as inhibitor (AESO), dichloromethane (CH_2Cl_2), *N*,*N*-Dimethylformamide (DMF), succinic acid, citric acid, 2-Methylaziridine, 0.1 N perchloric acid concentrate ($HClO_4$), tetrabutylammonium iodide, 0.5% crystal violet solution, chloroform ($CHCl_3$), tetrahydrofuran (THF) were purchased from Sigma-Aldrich (Milwaukee, WI). Ethanol was purchased from Decon Laboratories Inc., King of Prussia, PA. All materials were used as received without further purification.

4.3.2 Preparation of AESO-AZ

20 g of AESO was dissolved in 30 mL dichloromethane and placed in a round-bottom flask. Dichloromethane solution (15 mL) of 2-methylaziridine (5 g) was added dropwise (1 drop/s) through an addition funnel in an ice bath. The reaction mixture was kept at ambient temperature for 18 h after addition. Dichloromethane and excess 2-methylaziridine were removed by roto-evaporation at 68 °C under reduced pressure. The obtained AESO-AZ was dried in oven overnight. The appearance of AESO-AZ was brown viscous liquid at room temperature. The reaction was sketched in Figure 4-1.

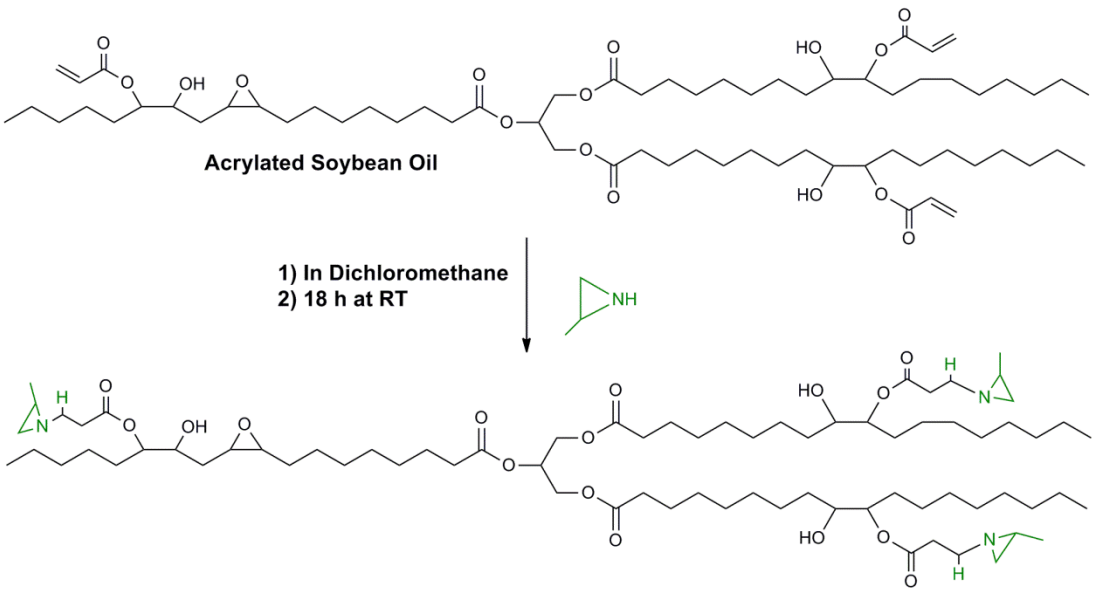

Figure 4-1 Synthesis of AESO-AZ

4.3.3 Polymerization of AESO-AZ with polyacids

Succinic acid, citric acid and isosorbide-based diacid were used to polymerize with AESO-AZ. The structures of the three polyacids were sketched in Figure 4-2. Isosorbide-based diacid was synthesized according to the protocol published elsewhere [9]. Basically, it was derived from the double esterification of isosorbide by succinic anhydride under solvent-free conditions. DMF solution of AESO-AZ (20%) was mixed with corresponding DMF solution of polyacid (20%) in vials for 10 min. The mixture was then poured into Teflon mold (5 inch x 5 inch) and dried at ambient temperature. The mold was placed in oven at 60 °C for 24 h. The obtained films were transparent, indicating the amorphous nature of the polymer network. Because for semi-crystalline or crystalline materials, the refraction indices differ from crystalline regime to another, the incident light cannot pass through them.

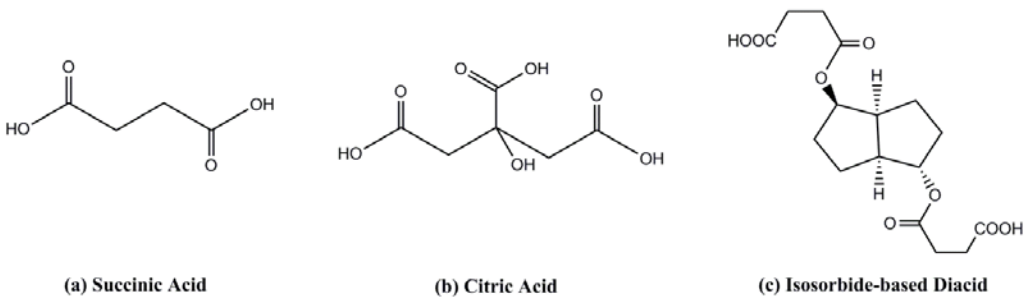

Figure 4-2 Structures of polyacids

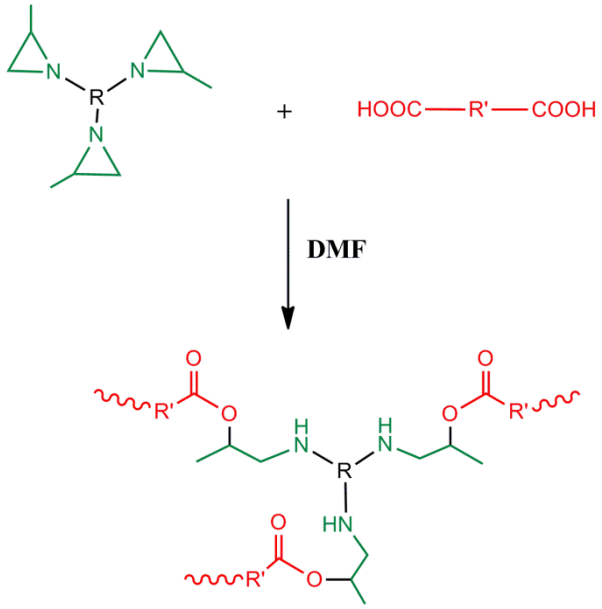

Figure 4-3 Polymerization of polyacids and AESO-AZ

4.3.4 Characterizations

The aziridine content of AESO-AZ was determined according to the titration method published by Jay [10]. Dissolve about 0.500 g of sample in 15 mL chloroform. Add 15.00 mL 10% chloroform solution of tetrabutylammonium iodide along with 2 to 3 drops of crystal violet indicator. Titrate with 0.1 N $HClO_4$. Blank sample was used to eliminate background effect. Since this titration method is also applicable to epoxy groups, AESO served as control sample due to the possible presence of residual epoxy

groups resulted from the manufacturing process (acrylation of epoxidized soybean oil). ^{1}H NMR and ^{13}C NMR spectra of the polyols were recorded on a Varian spectrometer (Palo Alto, CA) at 300 MHz in chloroform-*d*. The average molecular weight of AESO and AESO-AZ were determined by a Thermo Scientific Dionex Ultimate 3000 GPC (Sunnyvale, CA) equipped with a Shodex Refractive Index (RI) at room temperature. Tetrahydrofuran (THF) was used as eluent solvent and the delivery speed was 1.0 mL/min. The viscosity of AESO-AZ was measured by varying the shear rate from 10 s^{-1} to 1000 s^{-1} on an AR2000 Rheometer (TA Instrument).

Gel content was measured via Soxhlet extraction. A known weight (W_0) of pre-conditioned sample was placed into Soxhlet extractor with continuous THF extraction for 1 d. The remained sample was dried and weighed as W_1. Three replica were tested for each sample. The gel content was calculated as:

$$Gel\ Content\% = \frac{W_1}{W_0} \times 100\%$$

Differential scanning calorimetry (DSC) was performed on a TA Instrument Q20. Samples were heated to 100 °C in the first ramp in order to eliminate their heat histories. The samples were then cooled down to –50 °C and heated to 100 °C at a rate of 10 °C/min. The heat profile of the second heating ramp was recorded and the glass transition temperature was determined by the midpoint inflection method.

DMA Q800 of TA Instruments was implemented to record the dynamic thermal mechanical behavior of the samples. Film-tension mode of 1 Hz was used for testing rectangular samples with a dimension of 15 mm x 10 mm. The samples were kept

isothermally for 3 min at –80 °C followed by the temperature being raised to 120 °C at a programmed rate of 3 °C/min. *Tan δ* was calculated and plotted as the loss modulus over storage modulus and the glass transition temperatures (T_gs) were the positions of the peaks of *tan δ* profiles.

Thermogravimetric analysis (TGA) of the films was conducted on a TA Instrument Q50 (New Castle, DE). At a constant air flow rate of 60 mL/min, the samples were heated from ambient temperature to 650 °C. The decomposition profile was recorded as a function of temperature.

The tensile profiles of the samples were determined by an Instron universal testing machine (model 4502). Rectangular samples of 50 mm x 10 mm were subject to tension at a crosshead speed of 100 mm/min. At least three replicates were tested for each sample and all the reported values were the average. Toughness was calculated by integrating the area beneath the stress-strain curve.

4.4 Results and Discussion

4.4.1 Preparation and Properties of AESO-AZ

The preparation of AESO-AZ involved Michael addition of 2-methylaziridine to acrylic groups on AESO [1]. Excess amount of 2-methylaziridine was added and the unreacted residual was expected to be removed via roto-evaporation due to the low boiling point of 2-methylaziridine (b.p. 66-67 °C). FTIR spectra of AESO and ASEO-AZ were shown in Figure 4-4. The disappearance of the peak at 1635 cm^{-1} (blue box) indicated the complete consumption of acrylic groups. The peak at 3053 cm^{-1} was attributed to the C-H stretching on the aziridinyl ring. The peaks at 2930 cm^{-1} and 2850

cm^{-1} (C-H stretching in fatty acid chains) and at 1750 cm^{-1} (C=O stretching of ester groups) remained after the reaction, indicating the triglyceride structure of AESO was preserved.

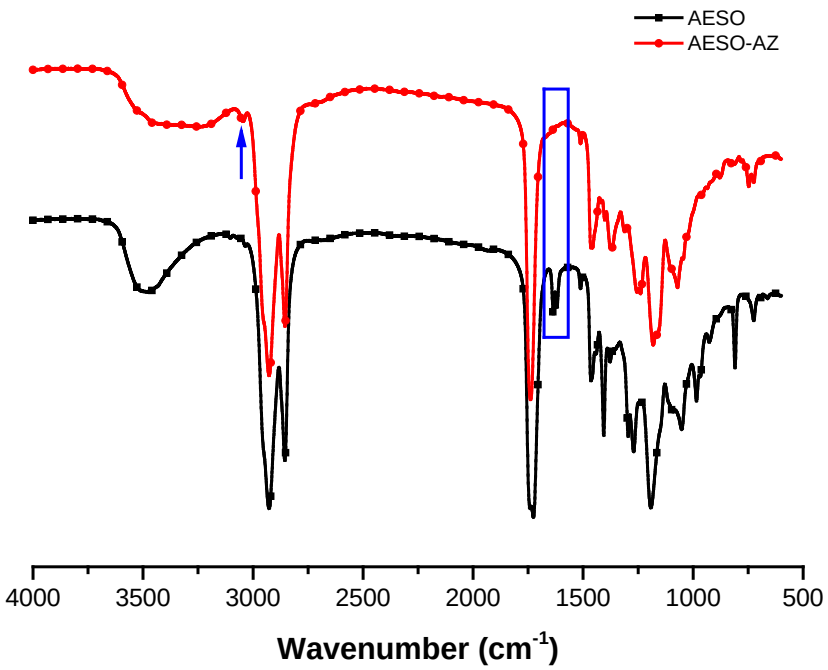

Figure 4-4 FTIR spectra of AESO and AESO-AZ

^{1}H-NMR spectra in Figure 4-5 also confirmed the completion of this reaction. Peak b,c,d, corresponding to the hydrogens on acrylic group, disappeared after the reaction which indicated the occurrence of Michael addition. Peak a, e and f, associated with the hydrogens labeled on the embedded structure, remained throughout the reaction. That could further confirm the preservation of the triglyceride structure of AESO. Peak h,i in AESO-AZ were attributed to the methylene groups ($-CH_2-$), given that the acrylics were saturated after Michael addition. Peak g appeared due to the linkage of 2-methylaziridine to the AESO. The three hydrogens on the ring structure could not be

clearly observed. Nonetheless, given that peak g existed and that the subsequent polymerization with polyacids could proceed, it could be concluded that the ring structure was not opened at this step.

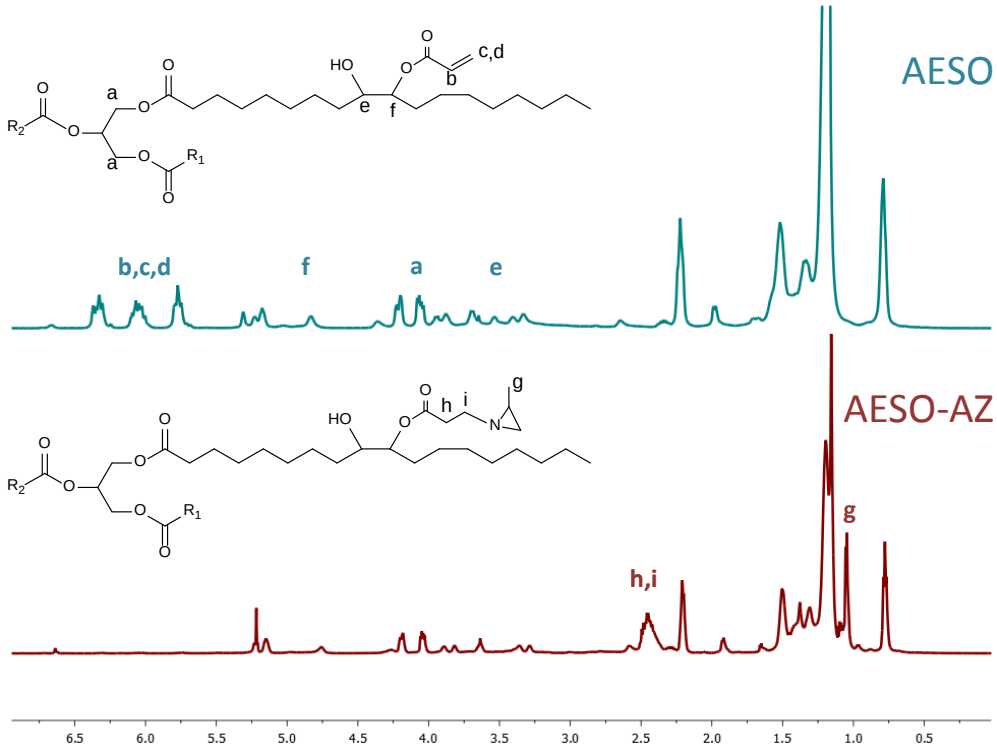

Figure 4-5 ^{1}H-NMR spectra of AESO and AESO-AZ

^{13}C-NMR spectra were obtained for AESO and AESO-AZ. In Figure 4-6, the disappearance of peak a,b and the appearance of peak c,d illustrated the fact that acrylics underwent Michael addition with –NH- of the 2-methylaziridine.

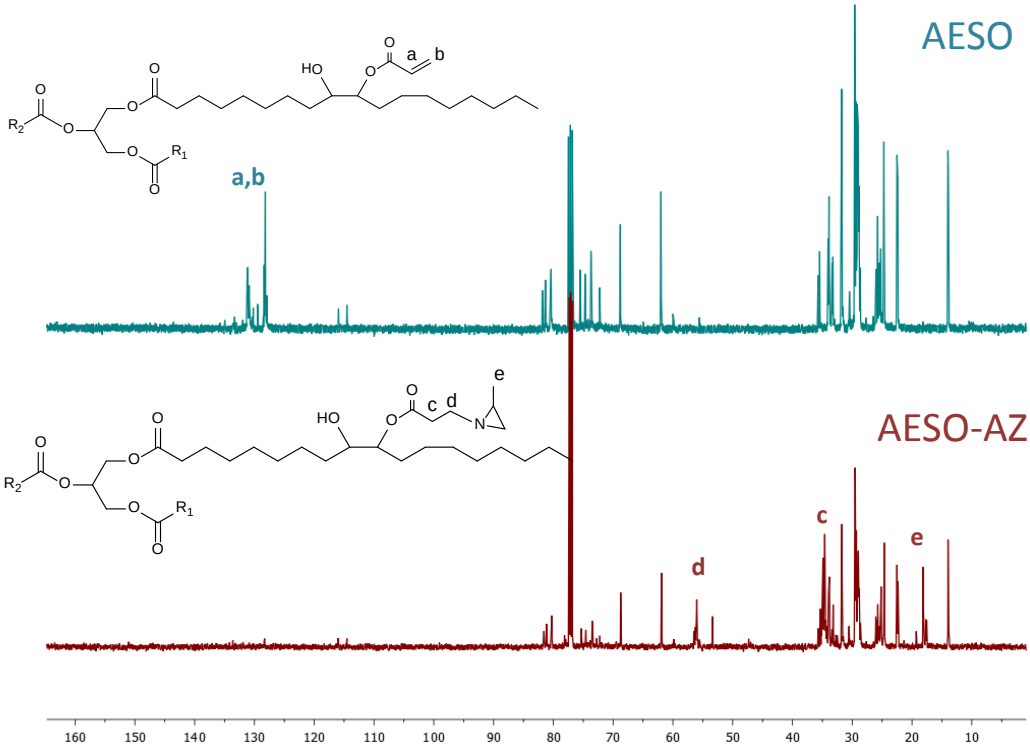

Figure 4-6 ^{13}C-NMR spectra of AESO and AESO-AZ

Viscosity at room temperature, M_n and M_w of AESO and AESO-AZ were measured and summarized in Table 4-1. There was no distinct difference in viscosity of the two specimens, demonstrating that the intermolecular interactions were not remarkably changed after the addition of 2-methylaziridine. The molecular weight of AESO-AZ was slightly higher than that of AESO due to the addition of 2-methylaziridine.

Table 4-1 Properties of AESO and AESO-AZ

	Viscosity (Pa·s)	M_n	M_w	PDI
AESO	27.3	1967	2165	1.10
AESO-AZ	29.9	2492	2665	1.07

Titration of the aziridine content was critical in determining the required amount of polyacids for polymerization step, because the molar ratio of aziridine and carboxylic acid was set as 1:1. The titration method for aziridine content also applies to epoxy content at the same time. Upon titration, AESO had a content of epoxy as 5.55×10^{-5} mol/g. Assuming there was no change of epoxy after Michael addition, the value of epoxy content remained and was subtracted from the overall value for AESO-AZ to get a net content of aziridine. AESO-AZ had a aziridine content of 0.00413 mol/g.

4.4.2 Polymer Properties

Differential scanning calorimetry (DSC) is widely used to determine the thermal transitions of polymeric materials. DSC thermograms of the samples were shown in Figure 4-7. Each sample exhibited only one T_g, indicating the homogeneity of the structure. Additionally, no melting peak was observed so that all the samples were considered amorphous. Notice that Succinic-AZ exhibited the lowest T_g as 12.0 °C. When succinic acid was replaced by citric acid or isosorbide-based diacid, the T_g increased to 20.3 °C and 20.8 °C, respectively. The increase in T_g of Citric-AZ was attributed to higher crosslinking density [11]. As the functionality of citric acid was 3 while that of succinic acid was 2, it was expected that more crosslinking sites were formed in the polymer network, which would result in the observed phenomenon. In terms of Iso-AZ, an increasing content of hard segments contributed to the increasing of T_g [12]. The rigid ring structure derived from isosorbide remained throughout the process and it could restrict the motion of the polymer chains. Herein, the increase of functionality of monomer and the addition of hard segment led to similar effects on T_g.

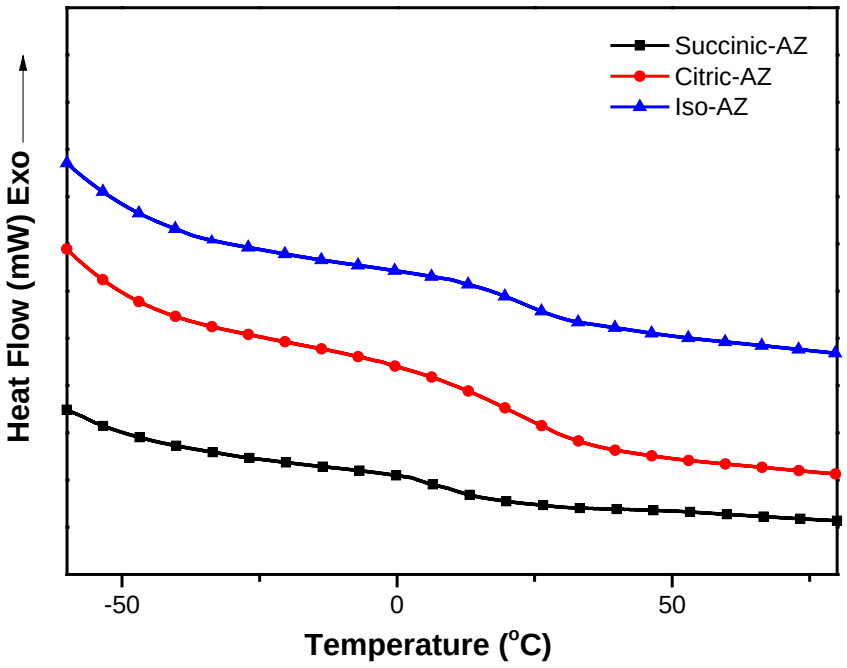

Figure 4-7 DSC curves of Succinic-AZ, Citric-AZ and Iso-AZ

In Figure 4-8, the storage modulus (*E′*) and the loss factor (*tan δ*) of the samples versus temperature were shown. At the low temperature regime, all samples were in a glassy state so that the storage modulus was relatively high due to the low mobility of the polymer chains. Plus, *E′* dropped slightly before the temperature reached the material's glass transition temperature at which the polymer chains were activated. The T_gs obtained from DMA were defined by the peak of *tan δ* and only one *tan δ* was observed for each material. T_gs of Succinic-AZ, Citric-AZ, Iso-AZ were 32.6 °C, 39.7 °C, 38.9 °C, respectively. Similar trend was observed from DSC data. The functionality of citric acid and rigid segment content of isosorbide-based diacid played important roles of the glass transition. It is worth mentioning that the discrepancy in T_g values obtained by DSC and by DMA was commonly observed, which is caused by the different measuring

mechanisms. DSC measured the heat capacity change from frozen to unfrozen chains, while DMA measured the change in mechanical response of the polymer chains to heating [13]. As the temperature passed glass transition regime, all samples entered into the rubbery state and E' exhibited less dependence on temperature so that a rubbery plateau was observed which was a strong evidence of the presence of crosslinked network [14]. The value of E' at T_g + 50 °C could be used in determination of crosslinking density (v_e) [15]:

$$E' = 3v_eRT$$

where E' is the rubbery storage modulus, typically at T_g + 50 °C, R is the universal gas constant, and T is the absolute temperature. The calculated crosslinking density of Succinic-AZ, Citric-AZ, Iso-AZ were 287.4 mol/m^3, 468.5 mol/m^3, 107.4 mol/m^3, respectively, see Table 4-2. Further, the height of *tan δ* decreased with increasing crosslinking density, matching the calculated results [2, 16]. Citric-AZ has higher crosslinking density than Succinic-AZ, because citric acid has a functionality of 3 while succinic only has 2 carboxylic acid groups per molecule. The higher functionality created more crosslinking sites so that the polymer network was denser. Given that isosorbide-based diacid has the same functionality as succinic acid, Iso-AZ was noticeably less crosslinked than Succinic-AZ. It could be attributed to the presence of rigid ring which diluted the polymer network. Additionally, the rigid ring might restrict the conformation of the isosorbide-based diacid which could have negative impact on the compactness of the network.

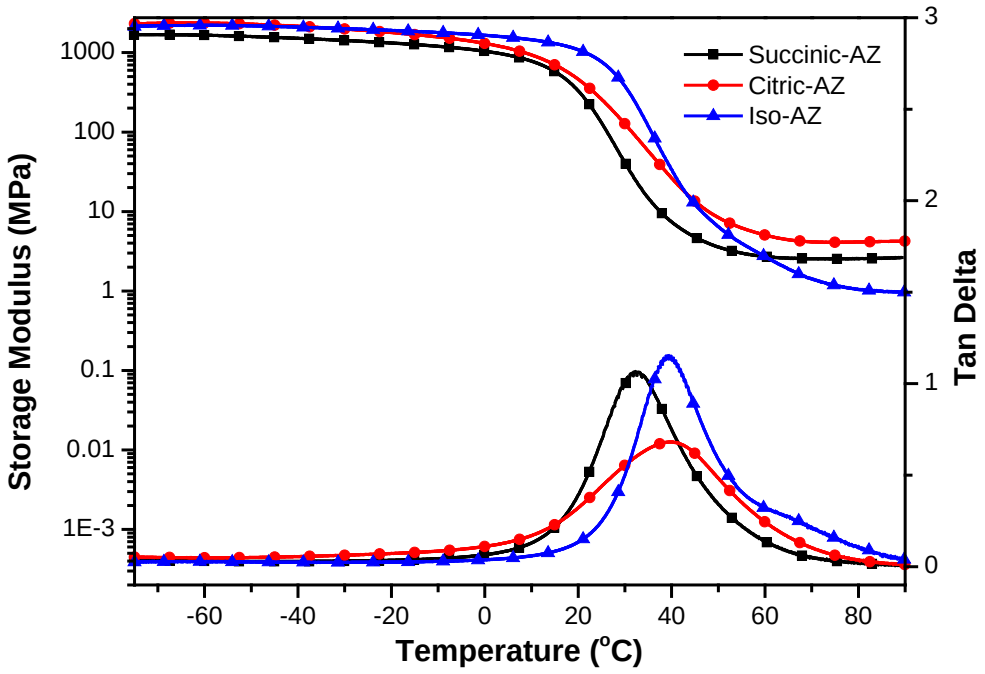

Figure 4-8 Storage modulus and loss factor of Succinic-AZ, Citric-AZ and Iso-AZ as functions of temperature

Gel content was examined and summarized in Table 4-2. The gel content of all the samples was close and higher than 90%. These data indicated the presence of the highly crosslinked polymer network for each sample. The success of the polymerization was confirmed by the thermosetting behavior of the samples.

TGA was conducted to investigate the thermal resistance of the samples, see Figure 4-9. As a summary, all samples underwent three stages of thermal decomposition in air atmosphere. The first weight loss domain spanned from 100 °C to 350 °C is assigned to the dissociation of the labile bonds such as ester groups and secondary amine groups. Succinic-AZ and Citric-AZ exhibited similar decomposition profile, because they derived from similar small aliphatic polyacids except for the difference in functionality. The onset of decomposition of Iso-AZ happened at lower temperature. The main reason

could probably be attributed to the instability of isosorbide-based diacid. It was found isosorbide-based diacid started ester group dissociation at temperature slightly over 100 °C. The second thermal degradation stage between 350 °C and 450 °C is attributed to chain scission in the soybean oil structure [16]. The last stage, above 450 °C, is derived from further thermo-oxidation of the samples due to the presence of oxygen in air atmosphere. T_{10} and T_{50}, representing the temperature of 10% weight loss and 50% weight loss respectively, are summarized in Table 4-2. Iso-AZ exhibited the lowest T_{10}, due to the low thermal resistance of the ester bond attached to the isosorbide ring. All samples had close T_{50}, which is actually the temperature regime of chain scission of triglyceride structure.

Table 4-2 Summary of physical and thermal properties

	Gel Content (%)	T_g (^oC) DSC	T_g (^oC) DMA	ν_e (mol/m^3)	T_{10} (^oC)	T_{50} (^oC)
Succinic-AZ	94.3	12.0	32.6	287.4	301.8	402.9
Citric-AZ	93.8	20.3	39.7	468.5	293.1	400.6
Iso-AZ	90.9	20.8	38.9	107.4	253.3	405.6

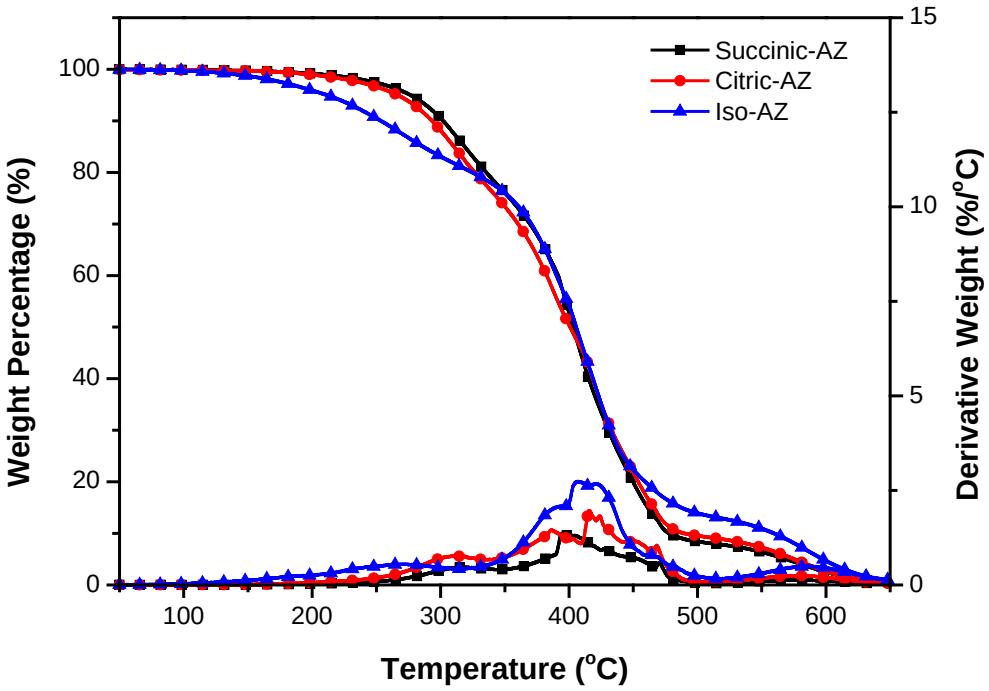

Figure 4-9 TGA curves and their derivative curves for Succinic-AZ, Citric-AZ and Iso-AZ

Tensile profiles of all samples were plotted in Figure 4-10. Young's moduli, tensile strength at break, elongation at break and toughness are summarized in Table 4-3. Citric-AZ and Iso-AZ were stiffer and stronger compared to Succinic-AZ. The relatively higher crosslinking density of Citric-AZ provided the better resistance to deformation and thus, resulted in higher Young's Modulus than that of Succinic-AZ. Though Iso-AZ was of lowest crosslinking density, the presence of rigid ring compensated for its negative effect from crosslinking density. The ductility of Succinic-AZ was the highest among all samples, which was generally a common phenomenon that weaker materials exhibit better ductility [2]. The toughness of all samples was comparable with each other, indicating the energy absorbed upon tension was similar.

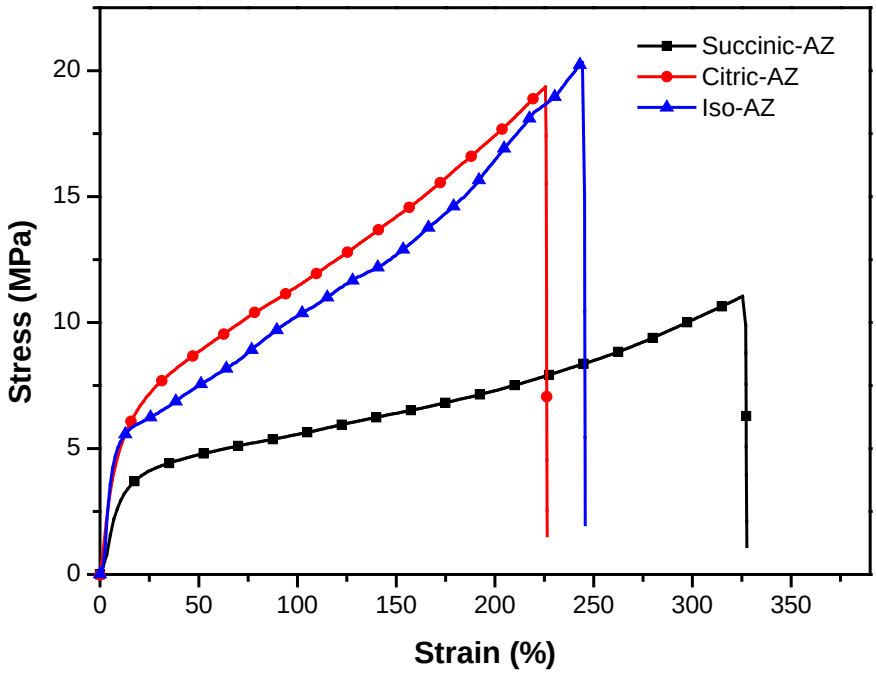

Figure 4-10 Stress-strain curves for Succinic-AZ, Citric-AZ and Iso-AZ

Table 4-3 Summary of mechanical properties

	E (MPa)	σ_b (MPa)	ε_b (%)	Toughness (MPa)
Succinic-AZ	35.6	11.0	327.3	22.2
Citric-AZ	61.0	19.4	225.9	27.2
Iso-AZ	84.4	20.3	244.3	28.6

4.5 Conclusion

2-methylaziridine was subject to Michael addition to acrylated epoxidized soybean oil. The reaction was confirmed by FTIR, ^{1}H-NMR and ^{13}C-NMR. The consumption of acrylic group indicated the completion of nucleophilic reaction. Polymeric materials were successfully acquired by solution polymerization at room temperature. The process took place rapidly and the films were obtained evaporating the solvents. Generally, glass transition temperatures of Citric-AZ and Iso-AZ were higher than that of Succinic-AZ. Citric acid has a functionality of 3 while succinic acid has a functionality of 2. High functionality results in higher crosslinking density, which contributes to the higher T_g. Though isosorbide-based diacid has the same functionality as succinic acid, the presence of rigid ring derived from isosorbide has an increasing effect on T_g. Citric-AZ and Iso-AZ possess higher Young's Moduli and higher tensile strength than Succinic-AZ. Nonetheless, Succinic-AZ is the most ductile sample, which is resulted from the highest mobility of the polymer chains.

4.6 References

1. Chen PC, Wang SC, Huang CY, Yeh JT, Chen KN: **New crosslinked polymer from a rapid polymerization of acrylic acid with triaziridine-containing compound**. *J Appl Polym Sci* 2007, **104**(2):809-815.

2. Xia Y, Larock RC: **Castor-Oil-Based Waterborne Polyurethane Dispersions Cured with an Aziridine-Based Crosslinker**. *Macromol Mater Eng* 2011, **296**(8):703-709.

3. Chen PC, Wang SC, Hwang JZ, Yeh JT, Huang CY, Chen KN: **A New Self-polymerization of Acrylic Acid with a Mono-aziridine Containing Compound**. *J Chin Chem Soc-Taip* 2010, **57**(4B):901-908.

4. Tillet G, Boutevin B, Ameduri B: **Chemical reactions of polymer crosslinking and post-crosslinking at room and medium temperature**. *Prog Polym Sci* 2011, **36**(2):191-217.

5. Lai JZ, Ling HJ, Chen GN, Yeh JT, Chen KN: **Polymer hybrids from self-emulsified PU anionomer and water-reducible acrylate copolymer via a postcuring reaction**. *J Appl Polym Sci* 2003, **90**(13):3578-3587.

6. Czech Z: **New generation of crosslinking agents based on multifunctional methylaziridines**. *Int J Adhes Adhes* 2007, **27**(1):49-58.

7. Liu PG, Zhang QF, He LH, Xie QJ, Ding HY: **Synthesis and Properties of Poly(Urethane-Imide) Diacid/Epoxy Composites Cured with an Aziridine System**. *J Appl Polym Sci* 2009, **113**(4):2628-2637.

8. Basturk E, Inan T, Gungor A: **Flame retardant UV-curable acrylated epoxidized soybean oil based organic-inorganic hybrid coating**. *Prog Org Coat* 2013, **76**(6):985-992.

9. Zenner MD, Xia Y, Chen JS, Kessler MR: **Polyurethanes from Isosorbide-Based Diisocyanates**. *Chemsuschem* 2013, **6**(7):1182-1185.

10. Jay RR: **Direct Titration of Epoxy Compounds + Aziridines**. *Anal Chem* 1964, **36**(3):667-&.

11. Stutz H, Illers KH, Mertes J: **A Generalized Theory for the Glass-Transition Temperature of Cross-Linked and Uncrosslinked Polymers**. *J Polym Sci Pol Phys* 1990, **28**(9):1483-1498.

12. Zlatanic A, Petrovic ZS, Dusek K: **Structure and properties of triolein-based polyurethane networks**. *Biomacromolecules* 2002, **3**(5):1048-1056.

13. Lu YS, Larock RC: **New hybrid latexes from a soybean oil-based waterborne polyurethane and acrylics via emulsion polymerization**. *Biomacromolecules* 2007, **8**(10):3108-3114.

14. Lu YS, Larock RC: **Soybean-Oil-Based Waterborne Polyurethane Dispersions: Effects of Polyol Functionality and Hard Segment Content on Properties**. *Biomacromolecules* 2008, **9**(11):3332-3340.

15. Andjelkovic DD, Valverde M, Henna P, Li FK, Larock RC: **Novel thermosets prepared by cationic copolymerization of various vegetable oils - synthesis and their structure-property relationships**. *Polymer* 2005, **46**(23):9674-9685.

16. Zhang CQ, Xia Y, Chen RQ, Huh S, Johnston PA, Kessler MR: **Soy-castor oil based polyols prepared using a solvent-free and catalyst-free method and polyurethanes therefrom**. *Green Chem* 2013, **15**(6):1477-1484.

CHAPTER 5: POLYOLS FROM HEAT-BODIED SOYBEAN OIL VIA OZONOLYSIS AND POLYURETHANES THEREFROM

A paper to be submitted to *Journal of Applied Polymer Science*

5.1 Abstract

Bio-based polyols have been successfully prepared from heat-bodied soybean oil followed by ozonolysis. The effects of the heat-bodying time to the properties of the polyols have been systematically studied. Bisallylic structure present in linolenic and linoleic fatty acids of soybean oil transformed into conjugated structure at elevated temperature, facilitating intra- or inter- molecular Diels Alder cyclization. Polymerization of soybean oils would decrease the amount of carbon-carbon double bonds as heat-bodying time increases. Consequently, OH number of the polyols via subsequent ozonolysis/reduction drops from 186.0 mg KOH/g to 94.3 mg KOH/g, which affects the crosslinking density of polyurethanes thereafter. PUs were prepared from MDI and bio-polyols and characterized by differential scanning calorimetry (DSC), dynamic mechanical analysis (DMA), thermogravimetric analysis (TGA) and tensile stress-strain test. The mechanical and thermal properties of PUs from bodied soybean oils were compared with those of PU from ozonated unpolymerized soybean oil. The results reveal that mechanical properties such as elongation at break and toughness are improved for PU from bodied soybean oils. It was also found that as heat-bodying time reaches 3 h, which results in noticeably low OH number of polyols thereafter, prominent deterioration

of mechanical properties of PUs is observed. This work provides a viable way of utilizing soybean oil for the preparation of polyols with high functionality and primary hydroxyl groups, which is also applicable to the usage of other vegetable oils containing respectable amount of linoleic or linolenic fatty acid arms.

5.2 Introduction

Polyurethanes (PUs), which contain recurring urethane linkages in the main chain, have been widely developed into a variety of applications, such as coatings, adhesives, sealants, foams, elastomers, etc. Conventionally, polyurethane is synthesized via isocyanate route, which is essentially a reaction between a polyol and an isocyanate. Both components involved in industrial manufacturing are typically derived from petroleum-based products. However, the depletion of crude oil and the accompanied environment issues have triggered global awareness of the importance of bio-renewable alternatives in future plastic industry. Recent studies on bio-based isocyanates have been focusing on non-phosgene route while phosgene route, known as treating amines with phosgene, is hazardous and requires special precautions. By introducing acyl azide onto bio-based carrier, thermal degradation of the intermediate would yield isocyanate via Curtius rearrangement [1-3]. On the other hand, bio-based polyols have been extensively investigated in the past few decades and subject to partial substitution of petroleum-based starting materials in industrial productions [4].

Vegetable oil is one of the most promising options due to its readily availability, relatively low cost, environmental sustainability and low eco-toxicity. Vegetable oils are mainly triglycerides, constituted by glycerol with three fatty acid chains. There are a

variety of fatty acids: palmitic (C16:0), stearic (C18:0), oleic (C18:1), linoleic (C18:2), linolenic (C18:3), ricinoleic (C16:1), etc. The unsaturated bonds and hydroxyl groups present in the fatty acids open the opportunities for various chemical modifications to promote the reactivity of vegetable oil molecules. Epoxidation of carbon-carbon double bonds followed by ring-opening is one of the most common routes to generate hydroxyl groups. Alcohols [5, 6], amines [7, 8], carboxylic acids [9], halogenated acids [10, 11], etc. are typically used in the subsequent ring-opening step. Hydroformylation, though proceeded under harsh conditions, yields relatively reactive primary hydroxyl groups in two steps. Aldehydes are produced in the first step in the presence of CO and H_2 along with catalysts, which are then reduced into hydroxyl groups [12, 13].

Ozonolysis has also been reported as an efficient technique to yield primary hydroxyl groups at double bond sites [14-16]. With the presence of methanol in the mixture of solvent, the double bonds could be cleaved to form hydroperoxides and aldehydes, which then are subject to reduction at a relatively fast rate [16]. The reducing agent used is sodium borohydride, a mild chemical that is non-reactive to carboxyl group so that the triglyceride structure of vegetable oil can be preserved. Low-molecular-weight mono- and di-ols, derived from the cleavage of the fatty acid chains, can be removed by distillation at high temperature under reduced pressure.

Heat-bodying of vegetable oil has been claimed to obtain a large and highly branched molecule. By coupling heat-bodying and ozonolysis techniques, we expected to achieve polyols with high functionality as well as high reactivity due to primary hydroxyl groups generated by ozonolysis. In this work, soybean oil is chosen as starting material for heat-bodying followed by ozonolysis/reduction. United States is currently the top

producer of soybean oil worldwide [17]. The abundance of the resource ensures the cost advantage for research and development of related products from SBO. The composition of SBO is shown in Table 5-1.

Table 5-1 Composition of Soybean Oil

Fatty Acid	Weight Percent (%)
Palmitic (C16:0)	12.0
Stearic (C18:0)	5.0
Oleic (C18:1)	25.0
Linoleic (C18:2)	52.0
Linolenic (C18:3)	6.0

It could be seen that ~83% of the fatty acids contain at least one carbon-carbon bond in the structure of SBO, which leads to double content per triglyceride as high as ~4.4. Also, high content of linoleic and linolenic acid also makes Diels Alder cyclization possible. SBO was subject to heat-bodying for different length of time and ozonolysis to prepare polyols, which were characterized by Proton nuclear magnetic resonance (^{1}H NMR), Fourier transform infrared spectroscopy (FTIR), gel permeation chromatography (GPC) and rheometry. Mechanical and thermal properties of polyurethanes from bio-based polyols were also systematically investigated and discussed.

5.3 Experimental

5.3.1 Materials

Soybean oil (approximately 4.4 degrees of unsaturation per triglyceride) was purchased from Walmart. Magnesium sulfate ($MgSO_4$), sodium chloride, methanol, methylene chloride and methyl ethyl ketone (MEK) were purchased from Fisher

Scientific Company (Fair Lawn, NJ). Dibutyltin dilaurate (DBTDL), 4,4'-methylenebis(phenyl isocyanate) (MDI), sodium borohydride were obtained from Sigma-Aldrich (Milwaukee, WI). All materials were used as received without further purification.

5.3.2 Polymerziation of soybean oil

Soybean oil (100mL-300mL) was placed in a three-necked reaction flask equipped with nitrogen inlet, thermometer and mechanical stirrer. The reaction vessel was partially buried in sand bath and the polymerization was carried out at 330°C±5°C for desired time. It has been reported that intermolecular oligomerization could occur at elevated temperature via Diels Alder reaction for vegetable oils containing linoleic, linolenic, licanic fatty acid structures[17, 18]. The obtained bodied oil samples were named as HBSO-1hr, HBSO-2hr, HBSO-3hr, with respect to the polymerization time. As the polymerization time increases, the color of oil changes from light yellow to dark brown as the polymerization time increases.

5.3.3 Preparation of polyols from heat-bodied soybean oils via ozonolysis

Polyols were prepared by ozonation followed by reduction of bodied oils and soybean oil. Oils were dissolved in the mixture of methanol and methylene chloride (45/55 w/w) and poured in a three-necked flask equipped with a thermometer, an ozone inlet and a solvent trap. Ozone was bubbled to the mixture at 7 cu. ft./min and the reaction temperature was controlled in between -40°C and -20°C. Ozonolysis was finished as the trapped solvent became blue. Over-ozonlysis might further oxidize intermediates to carboxylic acids, which could not be reduced with sodium borohydride

in the following step. Mechanism was illustrated elsewhere [16]. The formation of carboxylic acids would lead to higher acid number and lower hydroxyl number of final products.

Prior to reduction, the mixture was purged with N_2 to remove peroxides. Then, sodium borohydride ($n_{\text{sodium borohydride}} : n_{\text{carbon double bond}} = 1 : 1.2$) was added slowly and the reaction was allowed for 15 min after addition was finished. The mixture temperature was maintained below 10°C throughout this process.

The obtained mixture was washed with brine solution three times. Then, the organic layer was dried over anhydrous magnesium sulfate. Solvent and short chains were removed by roto-evaporation at 120°C. The polyols were identified as SBOP, HBSOP-1hr, HBSOP-2hr and HBSOP-3hr. Scheme 1 illustrates the synthesis route.

5.3.4 Preparation of polyurethanes

Due to the presence of primary hydroxyls and large size of the polyols, the mixture with MDI gels fast at room temperature. In order to obtain uniform and poreless PU film, the polyols, MDI (molar ratio of OH and NCO was 1 : 1.02) were mixed in MEK with a droplet of DBTDL and allowed for reaction for 3 hours at 60°C. Then, the solution was poured into a teflon mold to produce a 80×80 mm thin film, which was dried overnight at 80 °C. Finally, the PU films were cut into specific dimensions for thermo-mechanical testing.

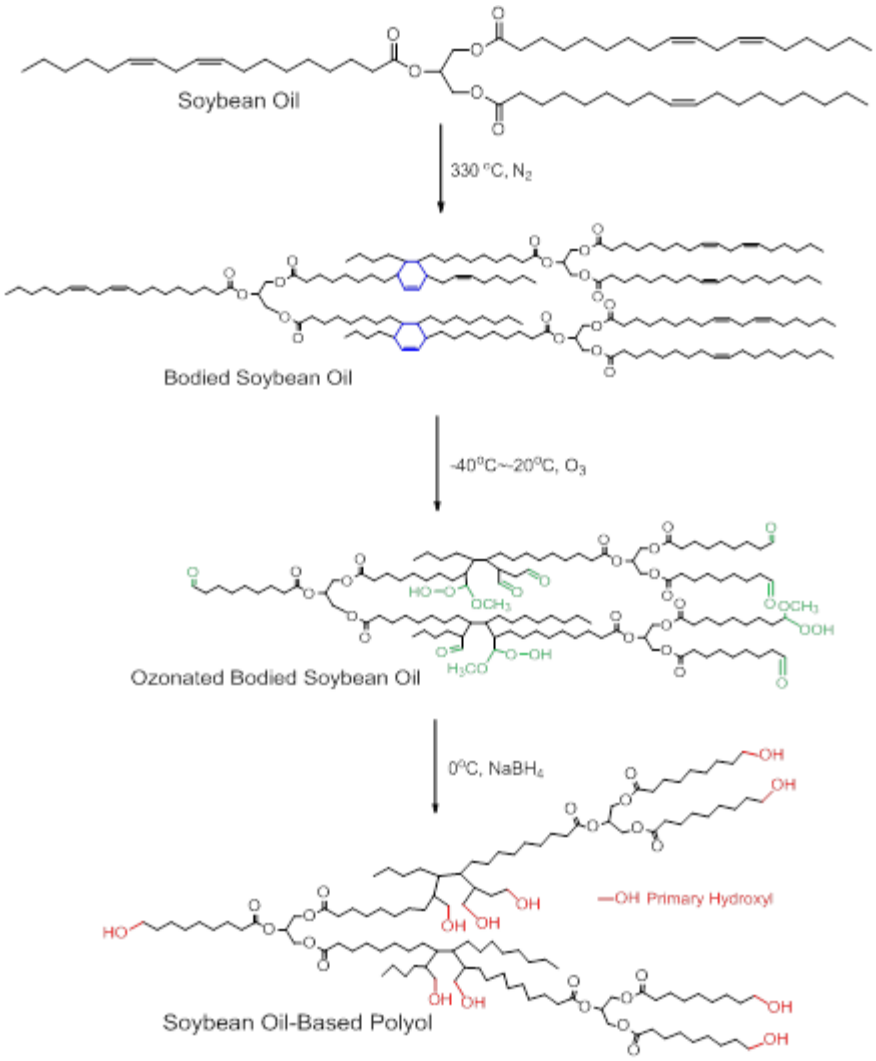

Fig 5-1 Representation of synthesis route

5.3.5 Characterizations

A Varian spectrometer (Palo Alto, CA) at 300 MHz was used to record the ^{1}H NMR spectroscopic analyses of the bodied oils and their polyols. Chloroform-*d* was used as sample solvents. IR characterization was performed with a Bruker IFS66V FT-IR spectrometer. The spectra were recorded with a resolution of $4cm^{-1}$ and the scan range was $4000cm^{-1}$ to $400cm^{-1}$. Hydroxyl number of polyols was determined using Unilever method. The acid number of the polyols was determined by AOCS Official Method Te

1a-64. The average molecular weight was measured by a Thermo Scientific Dionex Ultimate 3000 GPC (Sunnyvale, CA) equipped with a Shodex Refractive Index (RI). The eluent solvent used was tetrahydrofuran with two Agilent PLgel 3µm 100Å 300 x 7.5mm (p/n PL1110-6320) and one Mesopore 300 x 7.5mm (p/n PL1113-6325). The flow rate of THF was 1.0 mL/min and the temperature was kept at 25 °C. Viscosity was measured using an AR2000 (TA Instrument). Testing temperature was fixed at RT and shear rate was set to vary from 10 s^{-1} to 1000 s^{-1}.

Thermogravimetric analysis (TGA) of the films was carried out on a TA Instrument Q50 (New Castle, DE). The samples were heated from room temperature to 650 °C at a heating rate of 20 °C min^{-1} in air. The air flow rate was 60 mL/min. Generally, 10 mg samples were used for the TGA.

Differential scanning calorimetry (DSC) was conducted on a TA Instrument Q2000. The samples, weighed generally 10mg, were subject to heating, cooling and heating cycle in the range of -50 °C to 120 °C at a programmed ramp rate of 10 °C min^{-1}. The second heating ramp was recorded and glass transition temperature was determined by the midpoint inflection method.

The tensile properties of the PU films were determined with an Instron universal testing machine (model 4502) with a crosshead speed of 100 mm/min. Samples were prepared in rectangular shape of 50 mm ×10 mm (length × width). Average values of tensile strength at break, elongation at break were obtained from at least three replicates of each sample.

5.4 Results and discussion

5.4.1 Preparation and properties of heat-bodied soybean oil

Soybean oils were subject to self-polymerization at 330°C for 1 h, 2 h, 3 h, respectively. In terms of the common structure of soybean oil, it contains approximately 52.0% linoleic acid (C18:2) and 6.0% linolenic acid (C18:3), in which the carbon-carbon double bonds would migrate and form conjugated configurations at elevated temperature, enabling intra- or inter-molecular Diels-Alder reaction due to the high content of carbon-carbon double bond per triglyceride [19]. Detailed mechanism was reported by Erhan and his coworkers [20].

^{1}H-NMR spectra of Soybean oil and bodied soybean oils are shown in Figure 5-2. A representative structure of bodied soybean oil is embedded to illustrate the assignments of the peaks. It is worth noting that peak 1 and 7, at 5.2-5.5 ppm, and peak 8, at 2.7-2.8 ppm, decreased with increasing heat-bodying time. As shown in Scheme 1, every three carbon-carbon double bonds were incorporated into one cyclic structure with one left. As a result, peak 1 and 7, which belong to the overlap of –CH=CH– and –CCH_2C– (methylene of backbone), diminished. Additionally, carbon-carbon double bonds in linoleic and linolenic acids re-arrange into conjugated configuration in order to trigger Diels-Alder reaction, which causes the decrement of peak 8, corresponding to bisallylic structure.

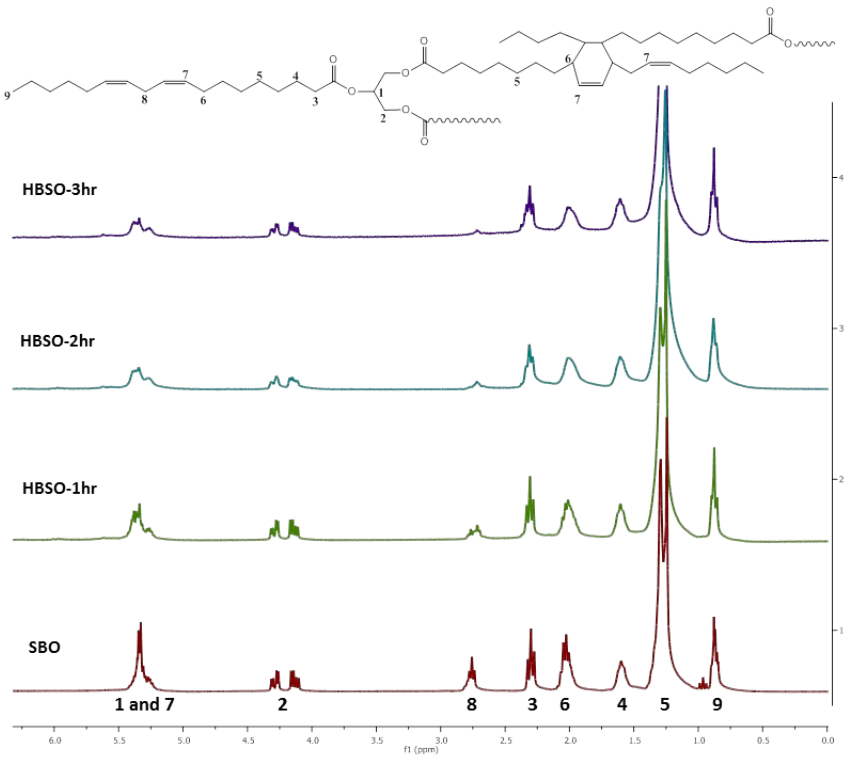

Figure 5-2 [1]HNMR spectra of soybean oil and heat-bodied soybean oils

Other properties of heat-bodied oils are summarized in Table 5-2. Viscosity increases along with increasing molecular weight, corresponding to increasing molecular weight. Gelation time for soybean oil is approximately 6 hours. Wider distribution of molecular weight is observed as heat-bodying time increases, shown in Figure 5-3. At the heat-bodying time of zero, a sharp peak is observed, indicating the uniformity of the molecular weight distribution. With an increase of heat-bodying time, shoulders to the side of shorter retention time appear and become prominent, which indicates the onset of polymerization of oil molecules.

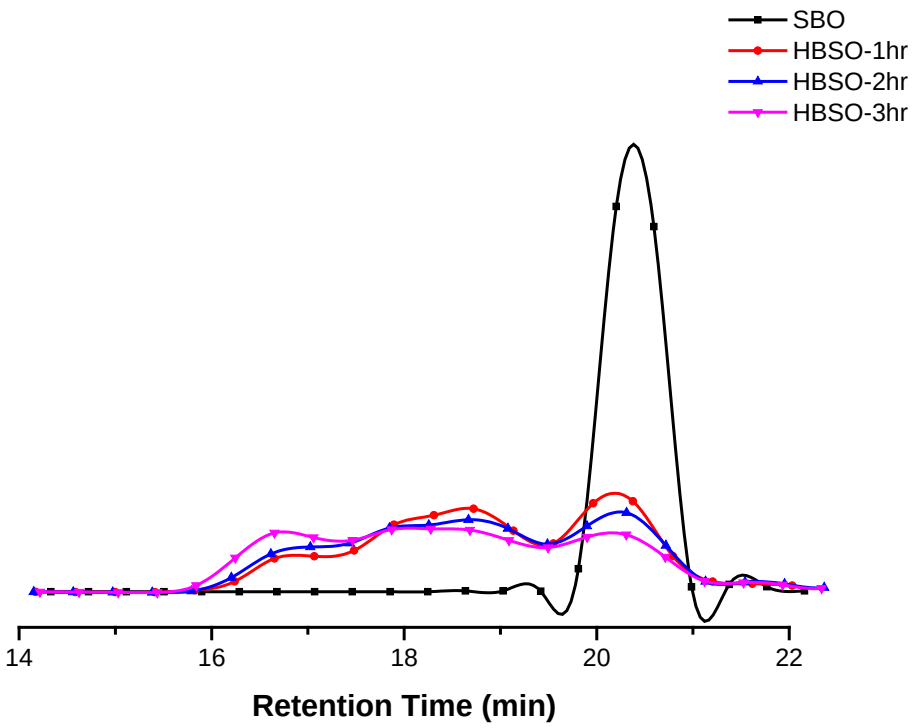

Figure 5-3 GPC curves of soybean oil and heat-bodied soybean oils

Table 5-2 Properties of soybean oil and heat-bodied soybean oils

Sample	Viscosity (Pa•s) at 25^{o}C	Mn	Mw	PDI
SBO	0.024	1319	1345	1.02
HBSO-1hr	0.072	1689	2692	1.59
HBSO-2hr	0.52	1815	2764	1.52
HBSO-3hr	1.27	1880	3125	1.66

5.4.2 Preparation and properties of polyols

The FTIR spectra of the polyols are compared with that of soybean oil, as shown in Figure 5-4. A new broad band in the range of 3600-3100 cm^{-1} appears for all the polyols, indicating the prsence of hydroxyl groups. The disappearance of the peak at

3008 cm^{-1}, attributed to CH stretching in –CH=CH– structure, proves the completion of ozonolysis as all the double bonds were oxidized and transformed [16].

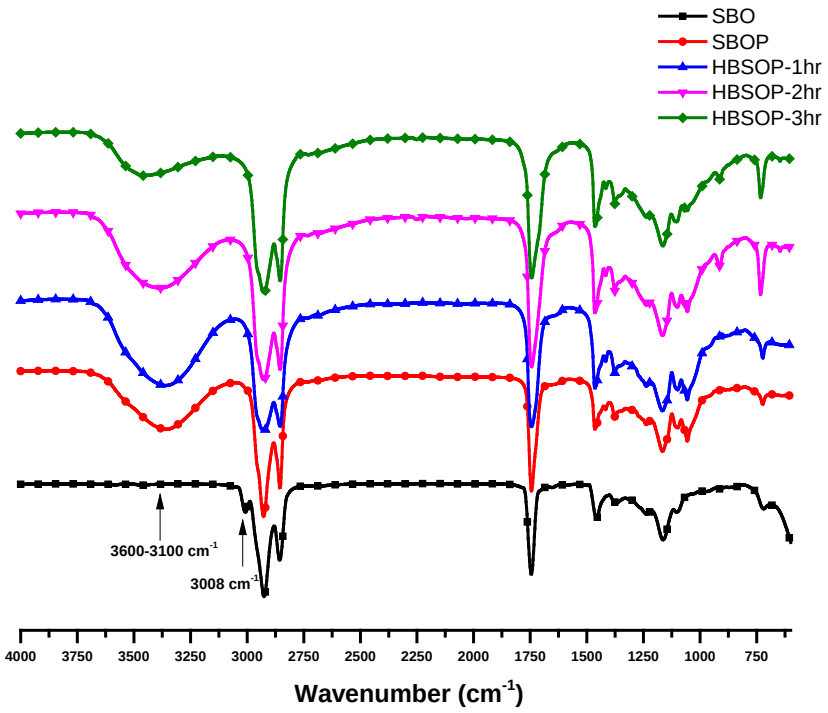

Figure 5-4 FTIR spectra of soybean oil and polyols

^{1}H-NMR spectra of the polyols are very similar. In Figure 5-5, peak 1 belongs to –CH_2– in the backbone glycerol while peak 2 is assigned to the hydrogen on the carbon attached to hydroxyl group, indicating the presence of hydroxyl groups [9]. By integrating and normalizing the intensity of peak 1 as 1.00, the intensities of peak 2 are 1.01 for SBOP; 0.95 for HBSOP-1hr; 0.90 for HBSOP-2hr; 0.82 for HBSOP-3hr. The declining trend is in accordance with the values of OH number for the polyols. Further, peaks at 2.7-2.8 ppm (bisallylic structure) and at 2.0 ppm (carbon-carbon double bond) disappear for all the polyols as all the double bonds were cleaved during ozonolysis/reduction.

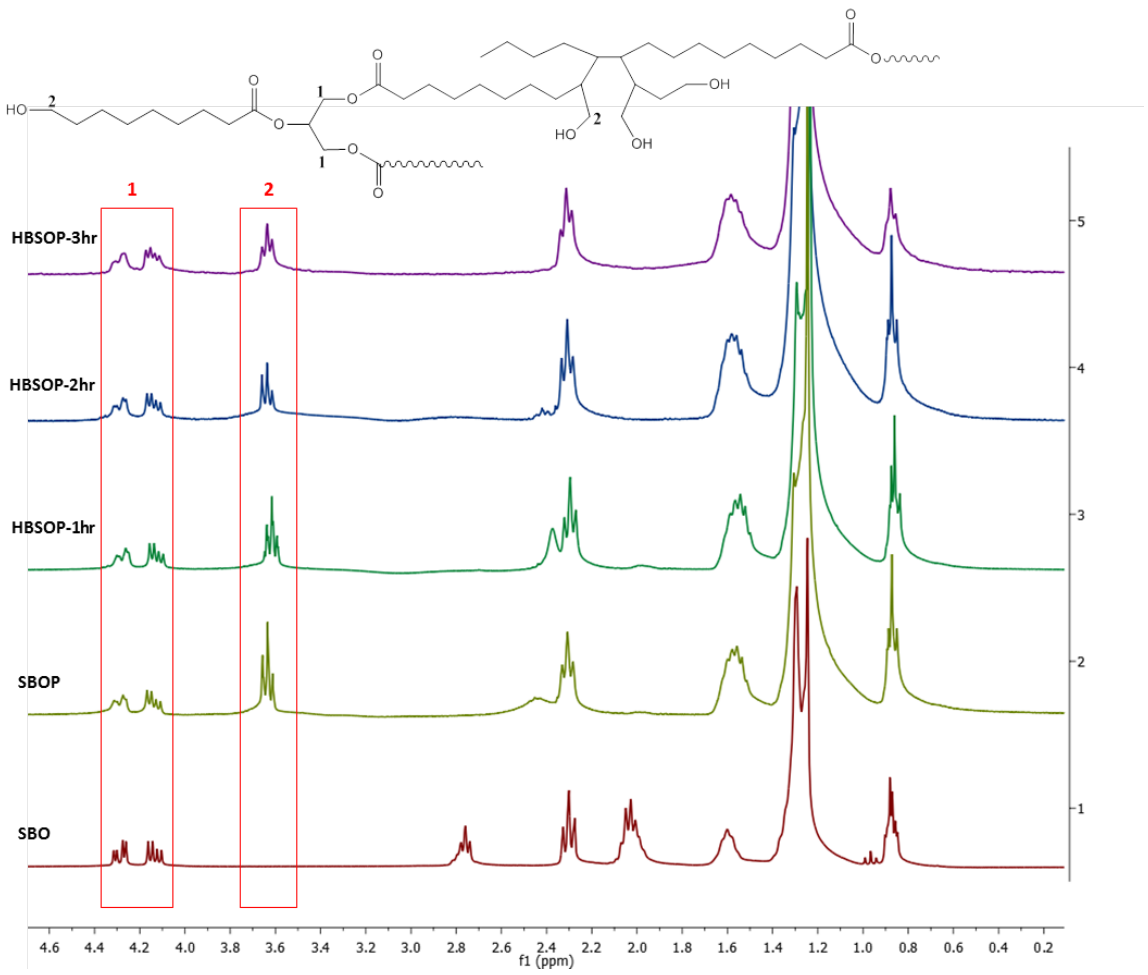

Figure 5-5 [1]HNMR spectra of soybean oil and polyols

Hydroxyl number, acid number, viscosity and molecular weight have been generalized in Table 5-3. The acidity of the polyols mainly derives from the formation of carboxylic acids, which cannot be reduced by mild reducing agent sodium borohydride [14, 21]. Hydroxyl number exhibits a decreasing trend with increasing heat-bodying time. It could be understood as more carbon-carbon double bonds were consumed in the cyclization along with increasing heat polymerization time.

Table 5-3 Properties of polyols

Polyol	OH number (mg KOH/g)	Acid number (mg KOH/g)	Viscosity (Pa•s) at 25°C	M_n	M_w	PDI
SBOP	220.4	3.4	0.11	701	794	1.13
HBSOP-1hr	186.0	4.2	0.24	1405	1701	1.22
HBSOP-2hr	122.6	2.9	0.53	1555	2275	1.46
HBSOP-3hr	94.3	2.1	1.48	1654	2467	1.49

5.4.3 Polyurethane properties

Differential Scanning Calorimetry (DSC) thermograms of the polyurethane films are shown in Figure 5-6 and data are presented in Table 5-4. Interestingly, each curve exhibits two T_gs, corresponding to hard segments and soft segments in the obtained PUs, respectively. The higher T_g is assigned to hard segments and its value is independent of hard segment content, which could be explained by the incorporation of same hard segment source, MDI, in the polymer network [22, 23]. Consequently, the chain relaxation temperature for hard segments appears to be almost identical for all the samples. However, T_g value for soft segments decreases from 6.63 °C to -2.84 °C as OH number of the polyols drops from 220.4 mg KOH/g to 94.3 mg KOH/g. Lower OH number would lead to less urethane linkages between soft segments and hard segments and therefore, lower crosslinking density, which would further result in lower T_g [24, 25]. In addition, neither melting nor re-crystallization transitions are observed in the heating run, indicating the amorphous nature of all the PUs.

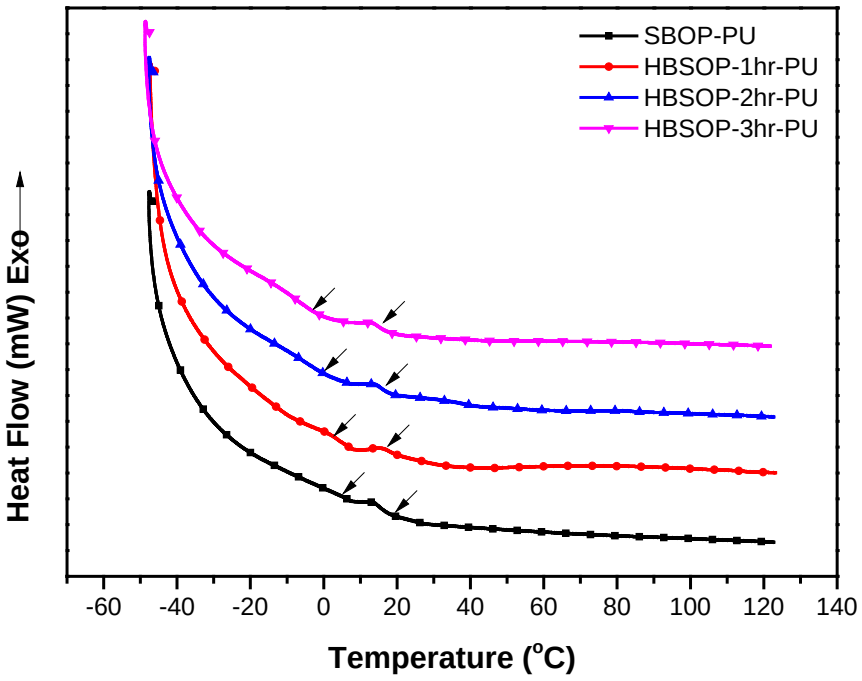

Figure 5-6 DSC scans of PU films

TGA curves for all of the PUs are shown in Figure 5-7. Basically, weight loss observed in the range from 200 °C to 300 °C is associated with the dissociation of the labile urethane bonds. Three mechanisms have been reported, which are dissociation of urethanes to isocyanates and alcohols, formation of primary amines and olefins and formation of secondary amines [5]. The second decomposition stage between 300 °C and 450 °C is attributed to chain scission in soybean oil structure. The last stage above 450 °C results from further thermo-oxidation of the PUs in air. T_{10} and T_{50} are recorded in Table 5-4, which correspond to the temperature at which 10% and 50% of the weight is lost, respectively. For PUs from polyols with different OH numbers, the weight loss at the end of the first stage increases with increasing OH number. Given that the ratio of OH and NCO was kept constant, higher content of MDI was incorporated in the polymerization in

order to compensate for higher OH number. As a result, more urethane linkages were formed, causing greater weight loss in the first stage. At 300 °C, the weight loss of PUs changes from 46.5% to 27.3% as OH number of polyols for these PUs varies from 220.4 mg KOH/g to 94.3 mg KOH/g. On the other hand, T_{10} and T_{50} could also reflect this trend [26].

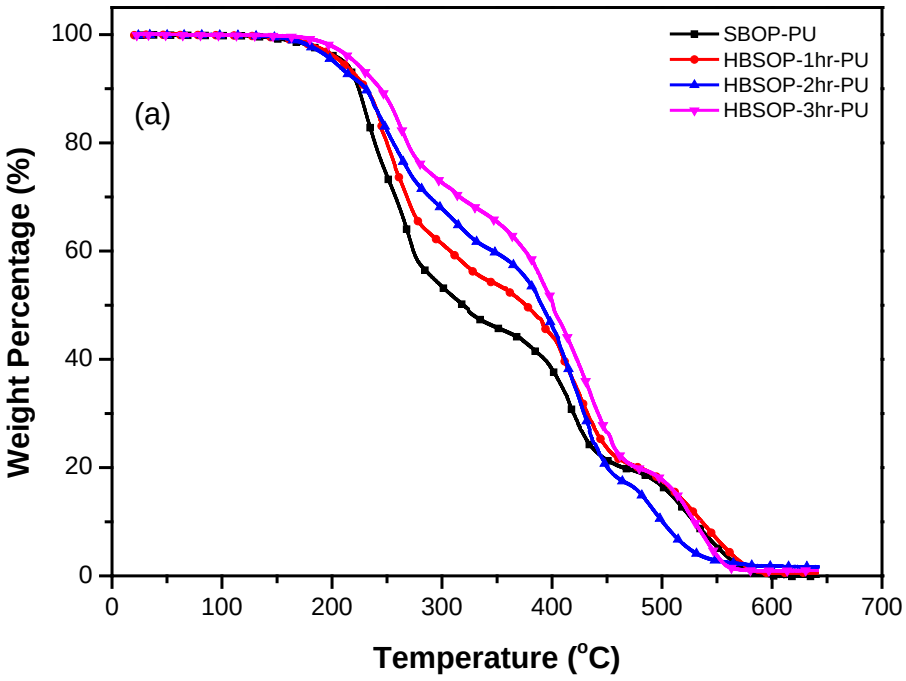

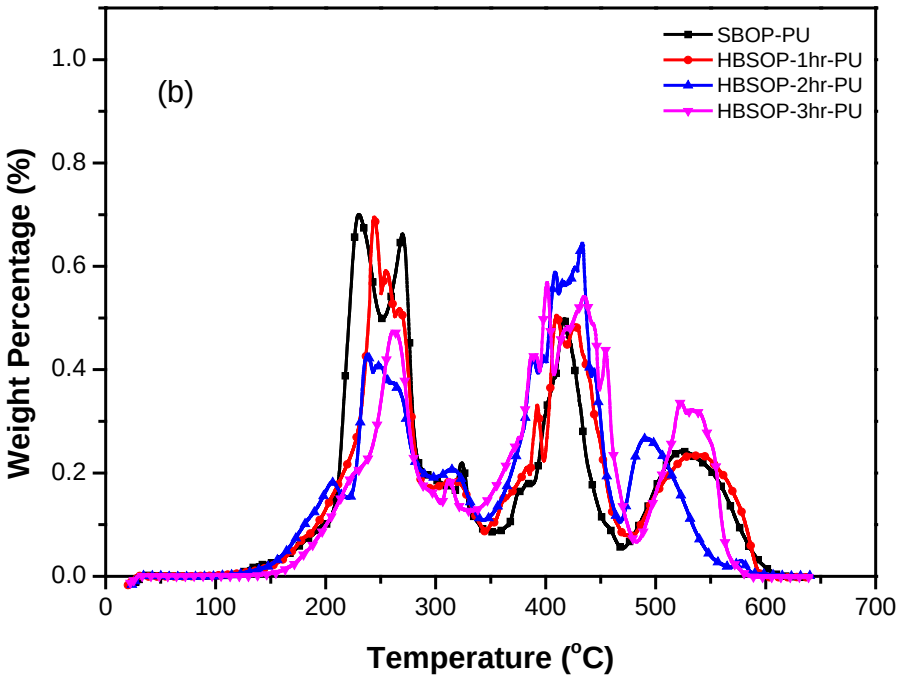

Figure 5-7 TGA curves (a) and their derivative curves (b) for PU films

In general, tensile properties of strained PU materials are predominantly dependent on the concentration of the hard segments and intermolecular bonding within the hard domains [26]. As for urethane linkages, -NH- serves as proton donor while C=O acts like proton acceptor. The high concentration of urethane linkages would promote intermolecular hydrogen bonding so as to contribute to tensile modulus [27]. As shown in Table 5-4, the substantial decrease in Young's modulus from SBOP-PU to HBSOP-2hr-PU could be attributed to the prominent decrease of hard segment content, which results in poorer interconnectivity of hard domains [28]. HBSOP-1hr-PU, HBSOP-2hr-PU and HBSOP-3hr-PU exhibit yielding behavior before plastic deformation, although HBSOP-3hr-PU was unable to withstand further strain beyond yield point. Before yielding, elastic deformation was observed and Young's moduli were recorded as the slope of the linear

domain of the curves. PU films started to deform plastically beyond yielding point and strain-softening was observed. The reason for that was unknown. In terms of SBOP-PU, there was no plastic deformation plateau, which could be ascribed to the high content of hard segments and lack of dangling chain acting as plasticizer. The brittleness of SBOP-PU results in lower toughness than HBSOP-1hr-PU and HBSOP-2hr-PU, even though the tensile strength is predominantly higher.

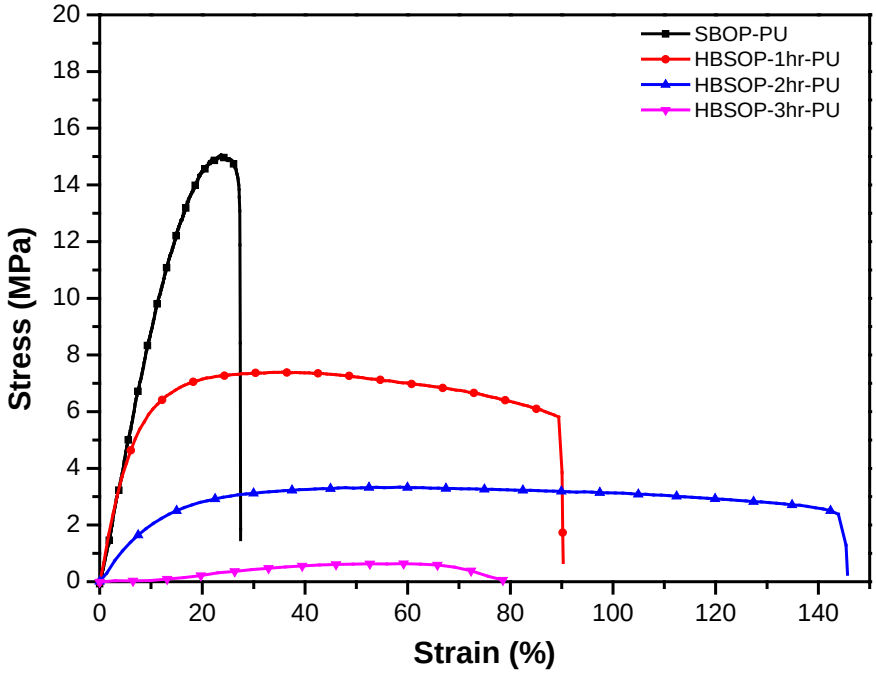

Figure 5-8 Stress-strain curves for PU films

Table 5-4 Thermal and mechanical properties of PU films

	Hard segment (%)	T_g (^oC)	T_{10} (^oC)	T_{50} (^oC)	E (MPa)	σ_b (MPa)	ε_b (%)
SBOP-PU	33.4	6.6/15.4	224.3	319.9	78.7	14.5	27.2
HBSOP-1hr-PU	29.7	3.8/15.6	231.1	376.6	72.6	6.1	90.3
HBSOP-2hr-PU	21.8	1.2/15.5	230.8	390.7	20.8	2.8	142.3
HBSOP-3hr-PU	17.7	-2.8/15.3	244.0	400.9	-	0.8	69.1

5.5 Conclusion

The effect of heat-bodying time on the properties of resulting polyols via ozonolysis has been investigated. A positive relationship between molecular weight and heat-bodying time of soybean oil was observed in this work. Viscosities of heat-bodied soybean oils also positively correlate to their molecular weight. The content of carbon-carbon double bonds decreases prominently with increasing heat-bodying time so that ozonolysis treatment afterwards would generate polyols with noticeably different hydroxyl numbers, ranging from 220.4 mg KOH/g to 94.3 mg KOH/g, which has significant impact on the PUs thereafter. The thermal and mechanical properties of these have been systematically studied. In general, PUs exhibit a declining trend of Young's modulus and tensile strength at break with increasing heat-bodying time. However, heat-bodying plays an important role in promoting bio-content and in improving toughness and ductility of resulting PU films, which can be attributed to the oligomerization of soybean oil molecules. Weight loss of the first thermal degradation stage conforms to the

trend of the content of urethane linkages within PU films. The synthesis of polyols from heat-bodying of vegetable oil followed by ozonolysis can produce polyols with primary hydroxyl groups with high reactivity, which could find valuable uses in polyurethane applications.

5.6 Acknowledgement

This work was sponsored by Kumho Petrochemical Co.

5.7 References

1. Hojabri L, Kong XH, Narine SS: **Novel Long Chain Unsaturated Diisocyanate from Fatty Acid: Synthesis, Characterization, and Application in Bio-Based Polyurethane**. *J Polym Sci Pol Chem* 2010, **48**(15):3302-3310.

2. More AS, Lebarbe T, Maisonneuve L, Gadenne B, Alfos C, Cramail H: **Novel fatty acid based di-isocyanates towards the synthesis of thermoplastic polyurethanes**. *Eur Polym J* 2013, **49**(4):823-833.

3. Zenner MD, Xia Y, Chen JS, Kessler MR: **Polyurethanes from Isosorbide-Based Diisocyanates**. *Chemsuschem* 2013, **6**(7):1182-1185.

4. Shen L, Haufe J, Patel MK: **Product Overview and Market Projection of Emerging Bio-based Plastics**. 2009.

5. Wang CS, Yang LT, Ni BL, Shi G: **Polyurethane Networks from Different Soy-Based Polyols by the Ring Opening of Epoxidized Soybean Oil with Methanol, Glycol, and 1,2-Propanediol**. *J Appl Polym Sci* 2009, **114**(1):125-131.

6. Dai HH, Yang LT, Lin B, Wang CS, Shi G: **Synthesis and Characterization of the Different Soy-Based Polyols by Ring Opening of Epoxidized Soybean Oil with Methanol, 1,2-Ethanediol and 1,2-Propanediol**. *J Am Oil Chem Soc* 2009, **86**(3):261-267.

7. Yang LT, Zhao CS, Dai CL, Fu LY, Lin SQ: **Thermal and Mechanical Properties of Polyurethane Rigid Foam Based on Epoxidized Soybean Oil**. *J Polym Environ* 2012, **20**(1):230-236.

8. Biswas A, Adhvaryu A, Gordon SH, Erhan SZ, Willett JL: **Synthesis of diethylamine-functionalized soybean oil**. *J Agr Food Chem* 2005, **53**(24):9485-9490.

9. Zhang CQ, Xia Y, Chen RQ, Huh S, Johnston PA, Kessler MR: **Soy-castor oil based polyols prepared using a solvent-free and catalyst-free method and polyurethanes therefrom**. *Green Chem* 2013, **15**(6):1477-1484.

10. Guo A, Cho YJ, Petrovic ZS: **Structure and properties of halogenated and nonhalogenated soy-based polyols *multiple melting for polyols**. *J Polym Sci Pol Chem* 2000, **38**(21):3900-3910.

11. Miao SD, Zhang SP, Su ZG, Wang P: **Synthesis of bio-based polyurethanes from epoxidized soybean oil and isopropanolamine**. *J Appl Polym Sci* 2013, **127**(3):1929-1936.

12. Petrovic Z, Kandanarachchi P: **Recovery and reuse of rhodium catalyst in the hydroformylation of vegetable oils.** *Abstr Pap Am Chem S* 2002, **223**:B235-B235.

13. Kandanarachchi P, Guo A, Petrovic Z: **The hydroformylation of vegetable oils and model compounds by ligand modified rhodium catalysis**. *J Mol Catal a-Chem* 2002, **184**(1-2):65-71.

14. Petrovic ZS, Zhang W, Javni I: **Structure and properties of polyurethanes prepared from triglyceride polyols by ozonolysis**. *Biomacromolecules* 2005, **6**(2):713-719.

15. Petrovic ZS, Milic J, Xu YJ, Cvetkovic I: **A Chemical Route to High Molecular Weight Vegetable Oil-Based Polyhydroxyalkanoate**. *Macromolecules* 2010, **43**(9):4120-4125.

16. Cvetkovic I, Milic J, Ionescu M, Petrovic ZS: **Preparation of 9-Hydroxynonanoic Acid Methyl Ester by Ozonolysis of Vegetable Oils and Its Polycondensation**. *Hem Ind* 2008, **62**(6):319-328.

17. Petrovic ZS: **Polyurethanes from vegetable oils**. *Polym Rev* 2008, **48**(1):109-155.

18. Erhan SZ, Bagby MO: **Polymerization of Vegetable-Oils and Their Uses in Printing Inks**. *J Am Oil Chem Soc* 1994, **71**(11):1223-1226.

19. Kiatsimkul PP, Suppes GJ, Sutterlin WR: **Production of new soy-based polyols by enzyme hydrolysis of bodied soybean oil**. *Ind Crop Prod* 2007, **25**(2):202-209.

20. Erhan SZ, Bagby MO: **Lithographic and Letterpress Ink Vehicles from Vegetable-Oils**. *J Am Oil Chem Soc* 1991, **68**(9):635-638.

21. Rebrovic L: **The Peroxidic Species Generated by Ozonolysis of Oleic-Acid or Methyl Oleate in a Carboxylic-Acid Medium**. *J Am Oil Chem Soc* 1992, **69**(2):159-165.

22. Yoon SC, Ratner BD: **Surface and Bulk Structure of Segmented Poly(Ether Urethanes) with Perfluoro Chain Extenders .2. Ftir, Dsc, and X-Ray Photoelectron Spectroscopic Studies**. *Macromolecules* 1988, **21**(8):2392-2400.

23. Bengtson B, Feger C, Macknight WJ, Schneider NS: **Thermal and Mechanical-Properties of Solution Polymerized Segmented Polyurethanes with Butadiene Soft Segments**. *Polymer* 1985, **26**(6):895-900.

24. Guo A, Demydov D, Zhang W, Petrovic ZS: **Polyols and polyurethanes from hydroformylation of soybean oil**. *J Polym Environ* 2002, **10**(1-2):49-52.

25. Kurimoto Y, Takeda M, Doi S, Tamura Y, Ono H: **Network structures and thermal properties of polyurethane films prepared from liquefied wood**. *Bioresource Technol* 2001, **77**(1):33-40.

26. Lu YS, Larock RC: **Soybean-Oil-Based Waterborne Polyurethane Dispersions: Effects of Polyol Functionality and Hard Segment Content on Properties**. *Biomacromolecules* 2008, **9**(11):3332-3340.

27. Pechar TW, Wilkes GL, Zhou B, Luo N: **Characterization of soy-based polyurethane networks prepared with different diisocyanates and their blends with petroleum-based polyols**. *J Appl Polym Sci* 2007, **106**(4):2350-2362.

28. Miller JA, Lin SB, Hwang KKS, Wu KS, Gibson PE, Cooper SL: **Properties of Polyether Polyurethane Block Copolymers - Effects of Hard Segment Length Distribution**. *Macromolecules* 1985, **18**(1):32-44.

CHAPTER 6: GENERAL CONCLUSIONS

6.1 General discussion

In chapter 2, a series of polyhydroxy fatty acids obtained from ESBO/ELO ring-opened by methanol/glycol were used to produce polyols using a solvent-free method. The fatty acids were reacted with ESBO at a ratio of carboxylic acid to epoxy groups of 0.5:1. The resulting polyols exhibited increasing OH numbers with increasing OH numbers of the fatty acids. PU films prepared from these polyols exhibited significant differences in thermal and mechanical properties. With increasing OH number, crosslinking density was significantly increased, resulting in PU networks with fewer free motions available to the chains. This allowed for the tailoring of the properties of the resulting PUs, ranging from rigid and brittle to soft and ductile. The choice of epoxidized vegetable oil as starting material clearly determined the OH number of the resulting polyols because of the different functionalities of the respective epoxy groups. Being able to use the OH number of the polyol to influence the properties of PUs provides a pathway for the design of materials with desired thermo-mechanical properties.

In chapter 3, the idea came from chapter that the structure of the polyhydroxy fatty acid was similar to DMPA which was widely used in anionic PU waterborne dispersions. ELO was ring-opened by glycol and HCl, followed by saponification to yield polyhydroxy fatty acid (FA). FA was successfully utilized to replace DMPA in castor oil-based anionic polyurethane dispersion system. The obtained CasFAD had an average

particle size diameter of 35.2 nm, while the control sample CasPAD had an average particle size of 30.0 nm. It was shown that FA can serve as both polyol component and as ionic segment in the preparation of PUDs. The resulting FAD had an average particle size of 56.1 nm. CasFAD exhibited lower tensile strength and Young's modulus than CasPAD because of its lower hard segment content. Nonetheless, CasFAD and CasPAD were comparable in terms of toughness. The mechanical properties of FAD were compared with those of CasFAD. FAD was relatively brittle and less tough because of its high OH number and acid content. In general, vegetable oil-based polyhydroxy fatty acids were successfully incorporated into anionic PU systems as ionic segments.

In Chapter 4, 2-methylaziridine was subject to Michael addition to acrylated epoxidized soybean oil. The reaction was confirmed by FTIR, ^{1}H-NMR and ^{13}C-NMR. The consumption of acrylic group indicated the completion of nucleophilic reaction. Initially, aziridine-containing compound was designed to post-cure anionic waterborne polyurethane dispersion synthesized in the work of chapter 3. However, the post-curing did not have enhancing impact on the final dried PU films, mostly due to the insolubility of aziridine-containing compound in water as well as the presence of dangling chains. Polymeric materials were successfully acquired by solution polymerization at room temperature. The process took place rapidly and the films were obtained by evaporating the solvents. Generally, glass transition temperatures of Citric-AZ and Iso-AZ were higher than that of Succinic-AZ. Citric acid has a functionality of 3 while succinic acid has a functionality of 2. High functionality results in higher crosslinking density, which contributes to the higher T_g. Though isosorbide-based diacid has the same functionality as succinic acid, the presence of rigid ring derived from isosorbide has an increasing effect

on T_g. Citric-AZ and Iso-AZ possess higher Young's Moduli and higher tensile strength based on similar facts. Succinic-AZ is the most ductile sample, which is resulted from the highest mobility of the polymer chains.

In chapter 5, soybean oil was further investigated in self-polymerization. The effect of heat-bodying time on the properties of resulting polyols via ozonolysis has been investigated. A positive relationship between molecular weight and heat-bodying time of soybean oil was observed in this work. Viscosities of heat-bodied soybean oils also positively correlate to their molecular weight. The content of carbon-carbon double bonds decreases prominently with increasing heat-bodying time so that ozonolysis treatment afterwards would generate polyols with noticeably different hydroxyl numbers, ranging from 220.4 mg KOH/g to 94.3 mg KOH/g, which has significant impact on the PUs thereafter. The thermal and mechanical properties of these have been systematically studied. In general, PUs exhibit a declining trend of Young's modulus and tensile strength at break with increasing heat-bodying time. However, heat-bodying plays an important role in promoting bio-content and in improving toughness and ductility of resulting PU films, which could be attributed to the oligomerization of soybean oil molecules. Weight loss of the first thermal degradation stage conforms to the trend of the content of urethane linkages within PU films. The synthesis of polyols from heat-bodying of vegetable oil followed by ozonolysis could produce polyols with primary hydroxyl groups with high reactivity, which could find valuable use in polyurethane applications.

In general, research work has covered the exploitation of vegetable oil in various applications. Epoxidized vegetable oil has been subject to ring-opening, saponification, Michael addition with aziridines. Vegetable oil can also be thermally polymerized so that

the molecular weight can be increased and after ozonolysis, the OH functionality of polyol can exceed 3, which can ensure the thermosetting nature of the PU product. Monomer molecular weight, chemical structure and functionality play important roles in determining the properties of the polymeric materials. The research has focused on the product development from bio-renewable resource. The innovation, analyses and conclusions can serve as inspiration in green industry.

6.2 Recommendations for future research

Besides the work described and discussed above, it would be beneficial to expand current projects.

Since a novel type of anionic waterborne PUD from polyhydroxy fatty acid as ionic segment has been successfully acquired in chapter 3, it is worth fundamental investigation of the rheological properties. The systematic study would provide useful guide of synthesis, processing and modeling for later applications. Moreover, the new PUD system is distinct as polyol and ionic segment are both bio-based in our PUD system. The bio-based ionic segment lead to the alterations in particle size, position of ionic group and hydrophobicity of chains which could have significant impact on the rheological behavior.

In chapter 5, polyols with primary hydroxyl groups were synthesized. The relatively higher reactivity of primary hydroxyls, in comparison with secondary hydroxyls and phenol groups, can be potentially suitable in PU foam production. The bio-based polyol can be blended with petroleum-based polyol (polyester-based polyol, polyether-based polyol) at different ratios so that the properties variations can be studied

with respect to the ratios. Both open-cell and close-cell foams can be produced if appropriate catalyst, surfactant and foaming agent are chosen.